MAGNETIC SEARCH SYSTEM

(PHASE I REPORT)

Report No. UNH MP-TR-SG-84-9

Under Contract #NA81AA-D-00035

Prepared for:

Office of Sea Grant
6010 Executive Blvd.
Rockville, MD 20852

Prepared by:

Marine Systems Engineering Laboratory
University of New Hampshire
Durham, NH 03824

and

Shenandoah Systems Company
800 Follin Lane
Vienna, VA 22180

September 1984

TABLE OF CONTENTS

MAGNETIC SEARCH SYSTEM

TABLE OF CONTENTS (continued)

TABLE OF CONTENTS (continued)

TABLE OF CONTENTS (continued)

LIST OF ILLUSTRATIONS

LIST OF ILLUSTRATIONS (continued)

LIST OF TABLES

CHAPTER 1

INTRODUCTION

1.0 Introduction

The Magnetic Search System (MSS) is virtually the only effective means of detecting and localizing buried ferrous objects such as pipelines, wrecks, mines, etc. It is also effective in the confirmation of the ferrous content of objects located by sonar. In spite of the importance of the magnetometer, as a search and classification sensor, it has not received the research and development emphasis accorded other sensor systems. An objective of this study program to improve MSS performance through the application of intelligent system concepts and the use of modern microprocessors. This document addresses the initial phase of this program, an in-depth analysis of the system currently in use by the Explosive Ordnance Disposal Technology Center (EODTC).

1.1 Origins of the EOD MSS

The present system employed by the EODTC stems directly form the Suez Canal MSS deployment of 1973. The 1973 system consisted of one reference magnetometer towed just below the surface and four sensor magnetometers towed at 5 feet above the sea bed (Figures 1-1 and 1-2). The system could be used in one of two modes either as four separate magnetometers or as a ganged gradiometer. In the first mode, the reference magnetometer was used only at the commencement of the search to input a reference signal into the frequency synthesizer. In the gradiometer mode, the reference magnetometer was used continuously, its signal being mixed with the incoming near bottom sensor signals. The NCSL Magnetic processors took the resulting difference frequency and processed it to provide a dc voltage directly proportional to the difference in the total magnetic field as seen by the reference sensor and each of the bottom search sensors.

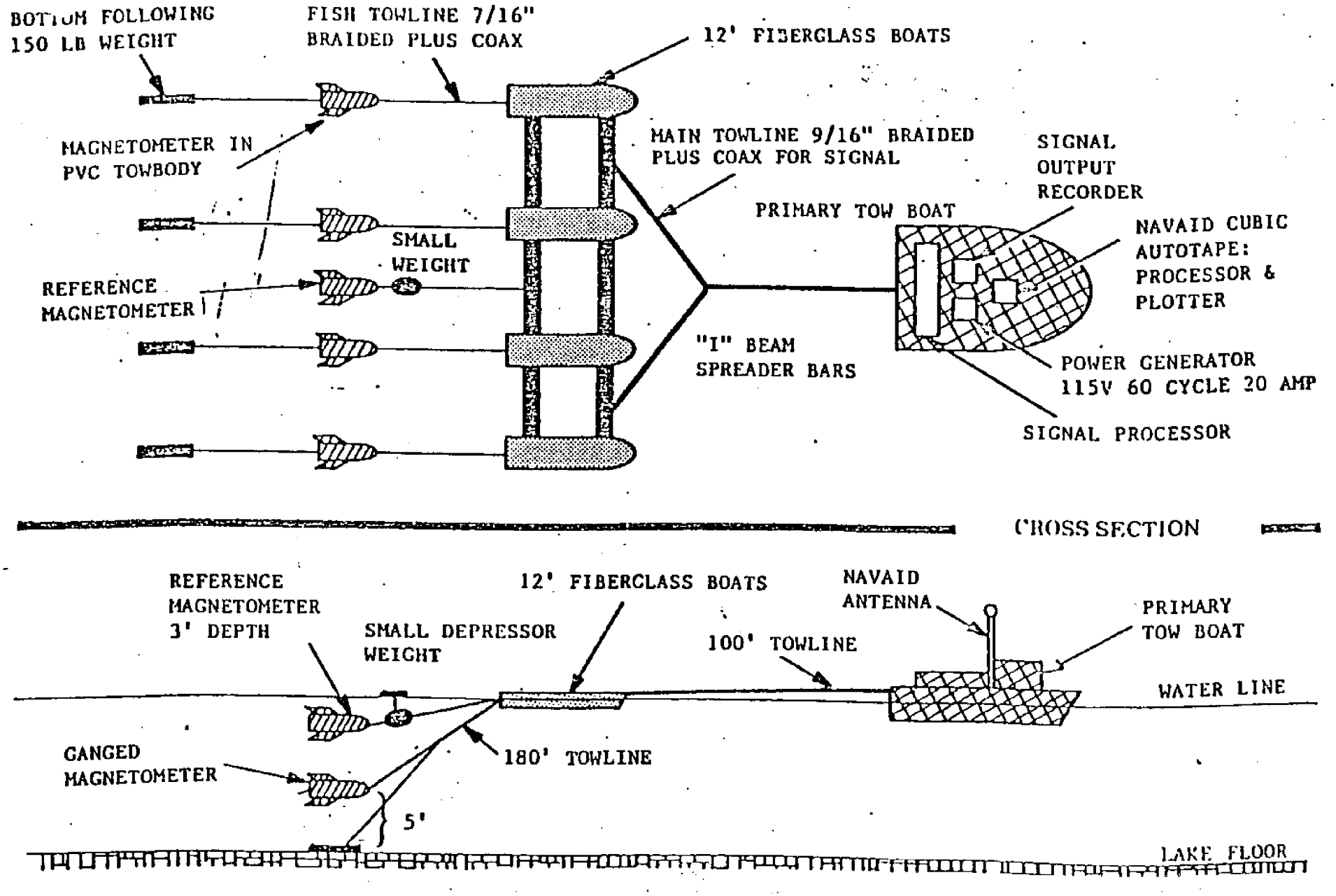

Figure 1-1 GANGED MAGNETIC SENSOR SYSTEM

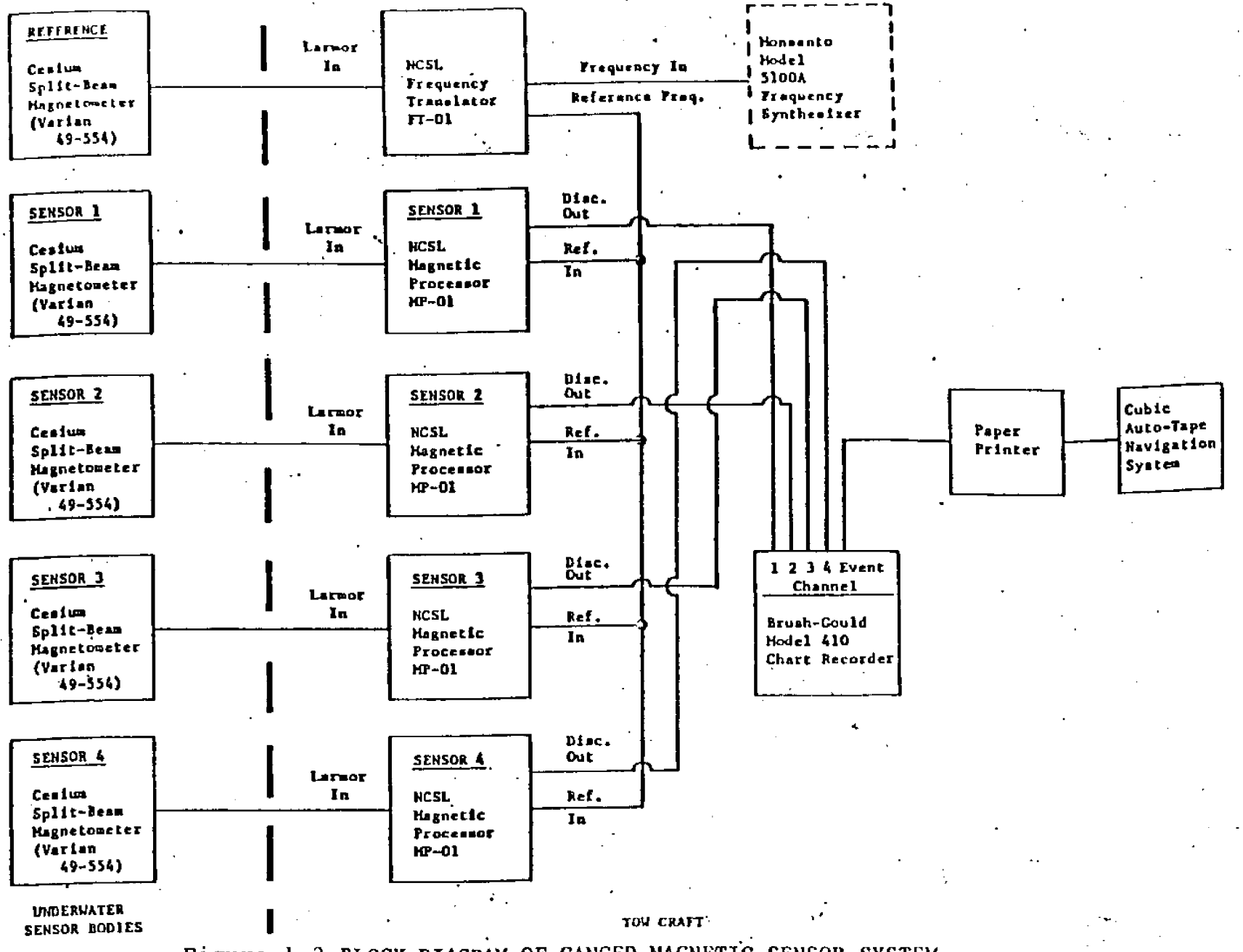

Figure 1-2 BLOCK DIAGRAM OF GANGED MAGNETIC SENSOR SYSTEM

The system utilized during Suez operations was assembled on a priority basis using available components. The Cesium Vapor magnetometer used in the system was available only from Varian. The signal processing equipment was developed at the Naval Coastal Systems Laboratory (NCSL) (now the Naval Coastal System Center) and was essentially an analog system. In spite of the short time available and entirely manual data analysis approach, the system did function as expected and accomplished its objective. It was capable of detecting and approximately locating a wide range of ordnance items from artillery shells to bombs and mines. It was slow, cumbersome and manpower intensive.

The components developed by NCSL performed as intended under difficult operational conditions. While the "Suez" system utilized a totally analog instrumentation approach, it apparently was accurate and stable. The Frequency Translator (FT-01) and the Magnetic Processor (MP-01) are both directly useable in the digital processing system that is discussed at a later point in this report. Both units require careful integration into an improved system to avoid some problems observed during normal search operations.

Although the Suez system provided a degree of success, the operational problems encountered were significant. These problems were mainly due to (1) the accuracy of sensor location, (2) the maintenance of an accurate search course, (3) the sheer volume of data and how to analyze it, and (4) the re-location and marking of the objects detected. A major problem not mentioned in the NCSL report and the reason why the EODTC now only deploys a single sensor system was a question of logistics. The deployment and recovery of the five magnetometer system was an operator's nightmare. The operational utility of a single magnetometer system and its capability to resolve spatial and temporal inconsistencies in search operations is the aim of this research effort.

1.2 The Present EODTC System

The system currently in use by EODTC consists of a Controllable Depth Depressor (CDD) whose function is to tow a magnetometer at a controlled altitude through the water. The magnetometer is housed in a torpedo shaped waterproof housing which has slightly positive buoyancy. The magnetometer unit trails the CDD by about 45 feet to eliminate the possibility of being affected by any magnetic influence emitting from the CDD and to keep it clear of the turbulence caused by the CDD (Figure 1-3).

The CDD was designed to fly at a constant height above the sea bed using data received from an acoustic altimeter in the CDD. As an alternative, the CDD can be controlled to maintain a constant depth. The CDD is hydrodynamically controlled from a control unit on the tow craft that is designed to supply power and command signals to both the CDD and the magnetometer. The control unit also routes depth, altitude, slant range and gamma reading to the data processing and recording portion of the system. Slant range is measured by an acoustic transponder with an interrogater at the surface and a receiver in the nose of the CDD. The time delay between transmission and reception is used to calculate slant range.

The electronics package in the CDD tow body was originally designed to accept the gamma (Larmor frequency) signal from the magnetometer, use it to modulate a carrier and then transmit it to the control box to be demodulated and processed. The resulting output signal was contaminated with external noise to the point that it could no longer be used to detect small anomalies. Therefore, the EODTC restored the system to its original configuration, transmitting the raw magnetometer output signal to the surface control box without

Figure 1-3 Present MSS Configuration.

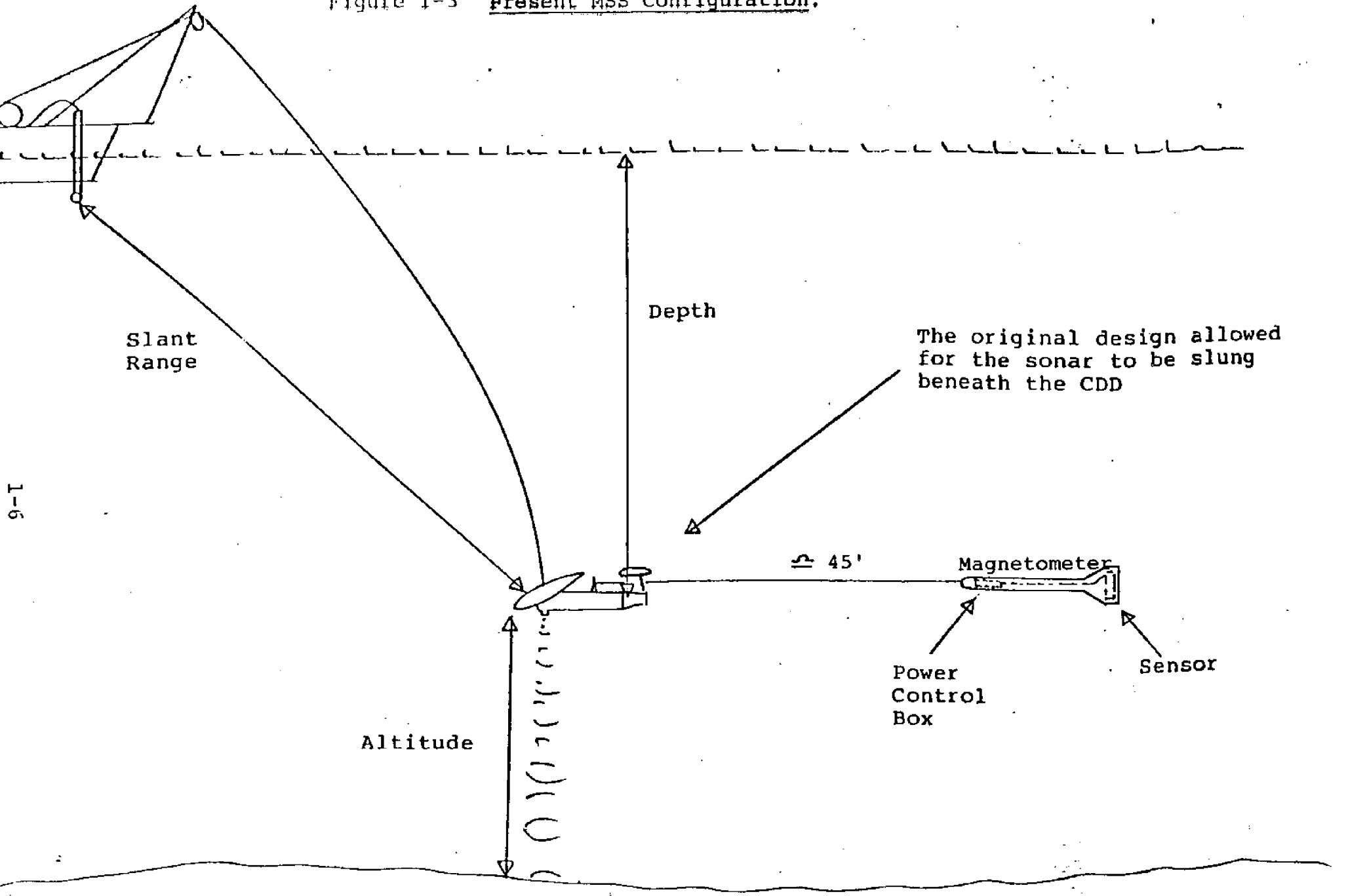

Figure 1-4 Present MSS Configuration

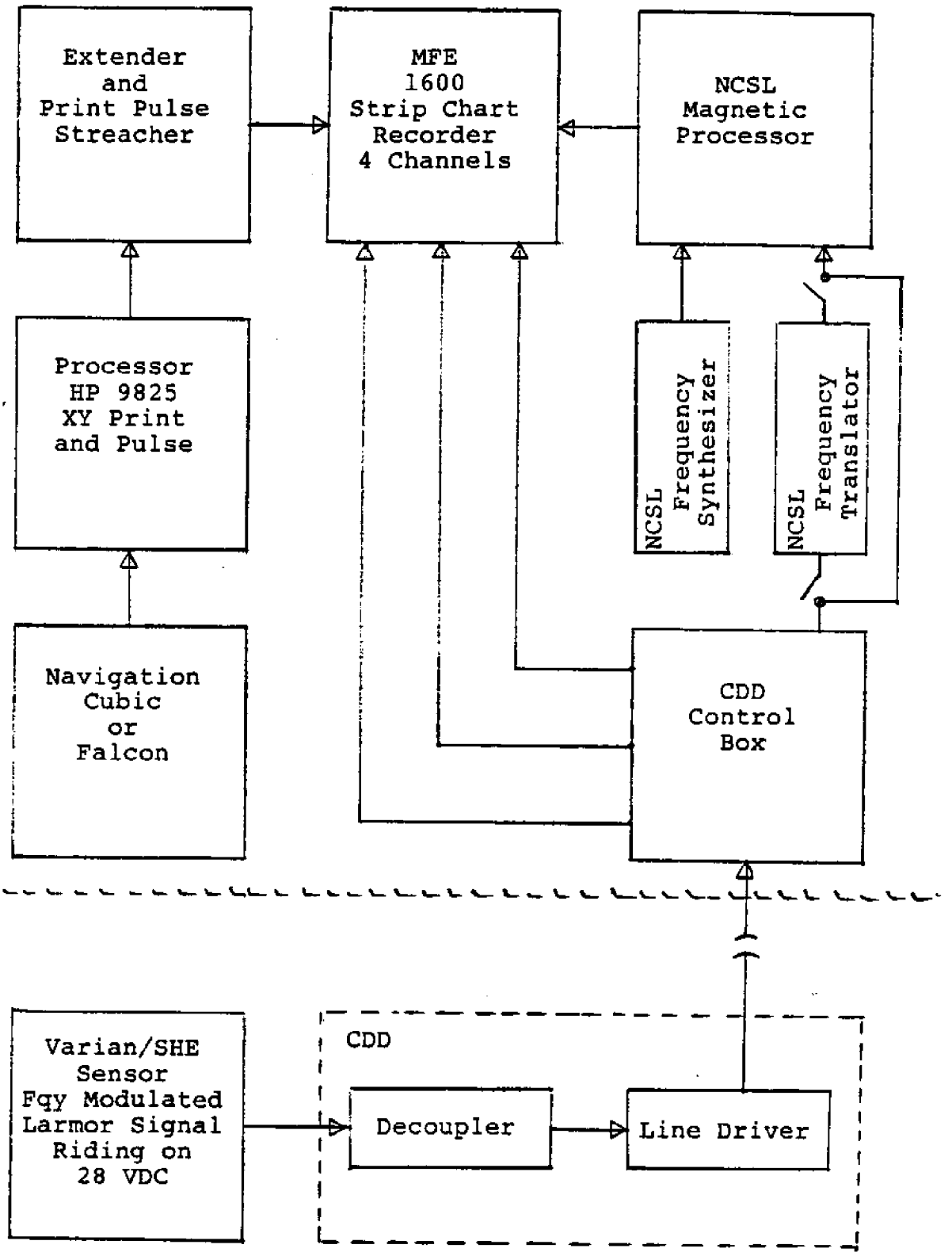

the modulation/demodulation taking place. The Larmor signal is now directly inputed to the magnetometer processor developed by NCSL for the Suez configuration. The geographic location of the gamma readings (indicated anomalies) are calculated from printed data and event marks at the edge of the strip chart from the MFE-1600 recorder. The operator annotates this event mark with the numerical designation of the XY position printed by the HP 9825 calculator.

1.3 Procedures Utilized in the Quick Look Analyses

There were four distinct elements in this quick look analysis. The first was an analytical review of the EODTC Magnetic Search System as it is currently configured and as it has evolved from the ganged magnetometer system deployed during the Suez Canal clean-up operation. This review was both to familiarize the study team with the system and to determine the expected performance characteristics and operational problems during typical search operations. While there may be a few remaining uncertainties, the objectives of this analytical review were achieved.

The second element of the study was to take the system out, operate it and acquire data that could be utilized in laboratory tests of a computerized MSS data acquisition and analysis scheme. These sea trials took place on 17 and 18 April in the Test Area. Arranged on an ad hoc basis, there were some initial MSS equipment and test instrumentation problems. However a quantity of digitized search data was acquired and full parallel analog recorded data was also obtained. Even more important, a number of the systemic problems in the EODTC system repeatedly occurred during these trials. This information will aid in defining some of the improvements that will enhance the operational effectiveness of the basic system. The EODTC personnel who crewed the system during these trials are well aware of these operational

problems, some of which can be partially resolved without significant modification to current hardware or data reduction procedures. A substantial portion of this report addresses these problems and the teams initial recommendations.

The third element of the study was to reduce the data, both analog and digital, and attempt to correlate measured data to expected anomaly signatures of ferrous objects of interest known to be in the test area. This effort constituted the bulk of the study. It also helped quantize the nature and extent of the problems in utilizing the MSS Some of these problems trace to equipment malfunctions or particular limitations in the magnetometer, the tow system or the problems in locating tow body position relative to the radio positioning system on the tow vessel. In general, the study team has been able to sort out these problems and their interaction and is making specific recommendations. The correlation between measured data and expected signature patterns (anomaly maps) from both a theoretical dipole concept and measured data (Reference 1) indicated that the single magnetometer system is capable of mapping anomaly contours useable for target location and magnetic moment approximation. Problems with tow body location (positioning) and intermittent sensor output make this a difficult task at present. However, realistic improvements to the equipment and analysis procedures should significantly improve system performance. A computer algorithm to locate and estimate the magnetic moment of a dipole anomaly is derived and tested.

The last element of the study, which is only partially addressed in this first study report, was to examine the potential improvements to the system. These concentrated upon digitization of the magnetometer output, digital filtering and computer correlation of anomaly contours. While most of this report looks at post exercise re-construction, the concept could be accomplished in real-time during search

operations. A real-time capability may require a more capable microcomputer than that utilized in the current system (HP 9825).

1.4 Objectives of the MSS Improvement Program

The long term objective of the overall MSS Improvement Program is to substantially increase the search rate, resolution (object size and location) and timeliness of MSS operations. Ideally MSS search rates would approach that achievable with the other principal EOD search sensor, side scan sonar. The likelihood of this degree of improvement in a MSS that utilizes a single total field magnetometer is nil. There are however, indications that a more advanced multiple sensor MSS utilizing spatial and temporal gradiometric processing would come close to matching the search rates of high quality side scan sonar systems. This long term objective is the focal point of the program subsequent to this quick look study.

The short term, or more accurately, immediate objective is to improve the current MSS as much as possible and at reasonable cost. This study, in part fulfills this objective. The degree of improvement, reasonably achievable, is defined in terms of impact upon search rates and timeliness of reduced and interpreted data. This brief study presents the study teams' conclusions concerning the current MSS configuration and two distinct recommendations. The first, presented in Section Five, covers quick equipment fixes and analysis procedures that will improve the accuracy of the anomaly charting process. These recommendations can all be implemented in the immediate future by EODTC personnel.

A second set of recommendations is presented in Section Six. These concern the automation of magnetometer signal processing and real-time charting of sensed anomalies. The

digital signal processing and charting system recommended could be implemented within 12 months and would provide a real-time output of accurately measured and charted magnetic anomalies. This system would provide the upper limit in search capability possible with a single magnetometer configuration.

CHAPTER 2

MSS CONFIGURATION, PROCEDURES AND STATUS

2.0 MSS Configuration, Procedures and Status

The MSS, in evolving from the hardware used at Suez, has inherited a few of the problems from the equipment that has been retained and a few from the modifications necessary for the single sensor configuration. There are also interactions between old and new components that frequently cause the loss of data during search operations. This section provides a concise description of the current system and its operational procedures as background against which the results of the "quick look" analyses and sea trials are discussed. There is also a fairly detailed discussion on the operational status of the system at the time it was used in the April sea trials.

2.1 System Configuration

The currently used system was briefly introduced in Section 1.2. There are only a few elements of the system that need to be discussed in greater detail as a background to the analyses, conclusions and recommendations of this "Quick Look" Study. There are the magnetometer signal processing, the process of determining sensor position and the problems in maintaining proper sensor orientation with respect to the earths ambient magnetic field.

2.1.1. Magnetometer Signal Processing

The processing of the LARMOR frequency output from the single cell VARIAN cesium sensor is the most critical circuitry in the system. The ultimate sensitivity and stability of the system is dependent upon the characteristics of the sensor, the signal processing equipment and the attitude stability of the cesium sensor as it is towed through the water. The following material is based upon the material

documented in the NCSL Report on the Suez equipment (Ref. 1). There are some interesting inconsistencies in this report which are noted.

The simplified block diagram of the magnetometer signal processing circuit is shown in Figure 2-1. The VARIAN Cesium sensor output is a low frequency RF signal that is proportional to the earths total magnetic field at the sensor site. This is a scalar measurement; a single sensor is incapable of measuring the vector components of the field. The ultimate sensitivity of the sensor exceeds the resolution of the remainder of the system. The sensor has a linear relationship between the Larmar frequency and the earths field. As the ambient field varies from 20 to 80 kilogamma, the larmor output will vary from 70 to 280 kHz. This corresponds to an approximate 3.5 Hz/gamma scale factor.

The FT-01 Frequency Translator is normally only utilized when a system is configured to utilize a reference cesium sensor (in the far field of the anomaly) and measure the difference (gradient) between the search and reference sensors. This is the configuration shown in Figure 2-1. This arrangement is rarely used in the EODTC system. It could be of value for zeroing the system or with an external magnetometer to null out large perturbations in the ambient field such as those caused by micropulsations.

The normal signal circuit for a single sensor system would have switch One in the "B" position where the reference frequency is provided by a stable RF Frequency Synthesizer. In this position, the FT-01 Frequency Translator is completely out of the system. In this configuration, the system is set-up prior to the start of the run by setting the frequency synthesizer at approximately 1 kHz above the Larmor frequency from the search sensor. The zero adjust on the MP-01 Magnetic Processor can then be set to the center of the linear dis-

Figure 2.1

Magnetometer signal processing path

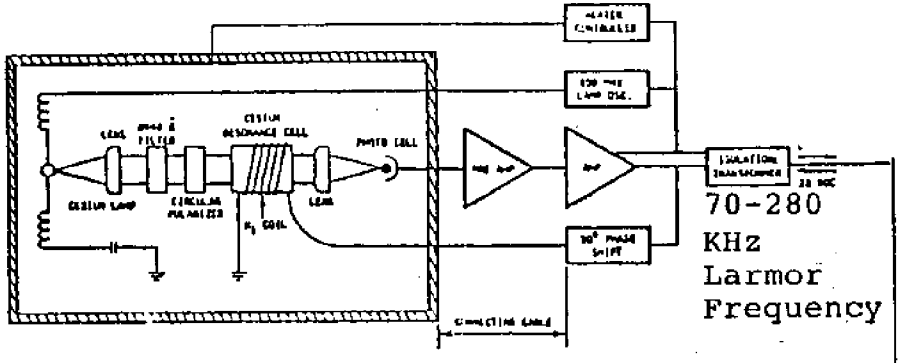

Single Cell Sensor

70-280 KHz Larmor Frequency

NCSL FT-01 Frequency Translator

A

B

Frequency Synthesizer (71-281 KHz)

Switch Two

Reference Frequency $f_R + f_L$

MFE-1600 Strip Chart Recorder

50 Gamma Dymanic range selected.

NCSL MP-01 Magnetic Processor

A

B

Switch One

Frequency Synthesizer (71-281 KHz)

Linear Frequency Discriminator
1800 Hz Dynamic Range
0.1 Hz Resolution 0.03Gamma
Output: LowPass filtered(0-1Hz)
: Zero offset and scale factor adjustable.

criminator range or to zero scale the pen on the recorder. The search would be run with the frequency synthesizer fixed unless area gradient or diurnal changes in the ambient field necessitates adjustments to bring the recorder back on scale. This arrangement will work quite well as long as the output of the frequency synthesizer is stable and free of spurious signals. If there are spurious signals or noise in the output of the frequency synthesizer, these may result in unwanted cross-modulation products in the mixer in the MP-01 with resultant non-linearities in the discriminator output.

This can be minimized by inputing RF reference signal into the Frequency Translator in place of the reference sensor Larmor signal. It would be set up as before except that the frequency synthesizer would be set to the same frequency as the Larmor signal from the search sensor. The FT-01 unit would generate the difference frequency internally and the phase lock loop (PLL) would effectively reject any spurious signals.

There are some interesting aspects to this signal processing scheme that could cause operational problems and hence require some explanation. The first concerns the stability of the processors when the Larmor signal is lost. This is a frequent problem that should be well understood. The Varian cesium magnetometer must be aligned in a fairly precise attitude with respect to the earth's ambient field. The alignment used in the EODTC system is shown in Figure 2-2. The primary axis of the sensor is vertical in the tow body and the active zone (shaded angle) covers from about 15^{o} above the horizontal plane to about 15^{o} from the vertical. The optimum earth's field angle is about 45^{o} off the sensor axis. The inclination of the earth's ambient field at the test site is a nominal 67 degrees, also shown in Figure 2-2. This is less than 10 degrees form the polar dead zone centered on the principle axis of the sensor. Any significant tilting of the

Figure 2.2

Active Zone of Varian 49-544 Magnetometer

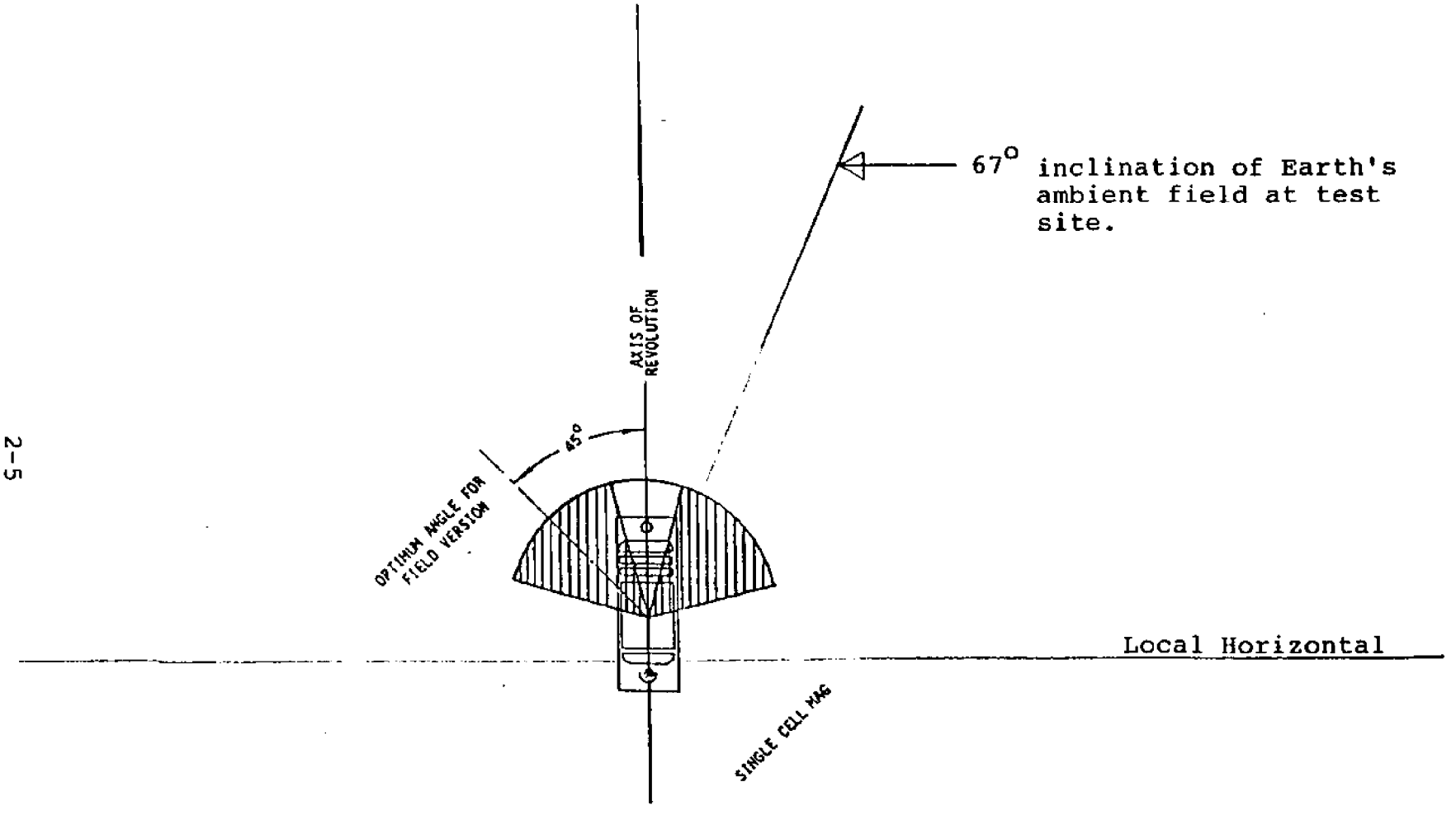

sensor from the local vertical would result in a rapid fall-off in Larmor signal amplitude and eventual loss of signal. In fact, Larmor signal amplitude should be well down (from peak at 45° field inclination) even when the sensor is vertical. It should be remembered that the sensor active zone is a conical section of revolution. The geometry is therefore independent of tow body heading. N-S, S-N, E-W and W-E courses would all see the same geometric relationship. The problems of maintaining proper sensor orientation with respect to the earths field will be further discussed in Section 2.1.3.

Temporary loss of signal from the magnetometer is not a serious problem as long as it does not persist for more than a small fraction of the time. It persistently occurred during the April trials. Possible causes for this will be discussed in the discussion on tow body configuration. When the sensor returns to the desired orientation the Larmor signal should return and the Magnetic Processor will again function normally. There is one potential problem in the system that could occur when a reference sensor is being used to derive the reference frequency input to the search sensors' Magnetic Processor. If the Larmor frequency into the Frequency Translator is temporarily lost, the Phase Lock Loop (PLL) will lose lock and the voltage controlled oscillator will cycle between its lower limit and a frequency that corresponds to the highest Larmor frequency to be found on earth. When the input Larmor signal is restored, the PLL can lock on a frequency exactly one kHz below instead of above the Larmor. this will fully satisfy the PLL circuit but will produce a reference frequency offset from that on which the Magnetic Processor has been set. Since the gain and zero offset controls on the MP-01 output have been set for a 50 gamma full scale input to the recorder, this may shift the output off scale at the recorder. This problem will not occur if the lower frequency limit on the VCO sweep is set at or near the

expected Larmor frequency. It cannot occur if a RF Synthesizer is providing the reference signal, either directly to the Magnetic Processor or through the Frequency Translator.

The concept utilized by NCSL in the development of the MP-01 and FT-01 was and remains one of the most effective means of precisely measuring the output of the Cesium sensor. It is far more precise than could be implemented by direct frequency counting. It also provides essentially an instantaneous measurement which is not possible in a counter. Between the need for a counter interval and the + one count error problem, the counter approach lacks the precision of the MP-01 by at least an order of magnetitude. The NCSL Magnetometer Processor would be retained in any computer based processing scheme proposed herein. The Frequency Translator is necessary whenever a reference magnetometer (either fixed or towed) is incorporated into the system. These potential improvements will be introduced in Section 3 and described in Section 4 of this report.

2.1.2. Determination of Sensor Position

One of the more significant difficulties in obtaining an accurate fix on the position of a sensed anomaly is determining the location of the sensor relative to the precision radio positioning system on the tow vessel. The technique used during the April sea trials was ad hoc since the slant range measurement system was not functioning. It is reasonably accurate in shallow waters where the cable scope is relatively short. This technique is described in Section 2.3.

Even when slant range is measured, the problem of determining sensor position can be quite complex if there are strong cross-currents or if the water is deep requiring a long scope in the tow cable. The techniques for determining sensor position relative to the vessel can be quite complex, po-

tentially requiring instrumentation more sophisticated than simple slant range and depth measurements. The mechanics of this problem and some calculation routines to determine sensor location are covered in Chapter 4. The impact of these errors surface as problems in locating and measuring the magnetic moment of an anomaly and in assuring that there are no holidays in the search pattern. The single magnetometer system is particularly difficult to utilize successfully when positional errors are in the order of the spacing between adjacent tracks.

2.1.3. Sensor Orientation

The orientation of the Cesium magnetometer with respect to the earths ambient field is one of the most serious problems in the system. The discussion in Section 2.1.1 indicates the scant margin for mis-alignment in the current configuration. The April tests, in which almost half the tracks resulted in no data is a severe example of the problem. The suspicion is that the sensor tow body has dynamic trim problems and that it is actually flying at a significant (5-10^{o} or more) pitch angle. This would move the earth's field angle closer to the optimum (45^{o}) angle on the south to north heading. On the reverse course, the pitch angle would result in the polar dead zone and hence loss of signal. The margin of correct alignment is narrow when the sensor is fixed in the tow body for all possible tow headings. Varian, in their literature suggests double cell sensors, which would not help the situation. They alternately picture the use of six cells to provide essentially full spherical coverage. This is an expensive over-kill. There are other more reasonable alternates.

Before these are discussed, it is useful to examine the problems in using the current configuration when the search pattern is other than generally N-S. As the extreme on E-W

set of tracks will result in proper sensor alignment being dependent upon the roll stability of the "torpedo" shaped tow body. Unless unusual steps are taken to achieve reasonable roll stability, the system will become extremely sensitive to cross currents and course changes of the tow vessel. The roll stability problem exists at all headings but is far less severe for N-S course bearings.

2.2 Current Data Acquisition and Analysis Procedures

Search patterns are typically conducted in a north -south pattern. The track separation is usually at 10 meters. The trail distance of the sensor is estimated by making several passes (at least 2) in a north to south and south to north direction over a known target. This value of trail distance is used in all subsequent position calculations.

As the search is conducted data was collected and recorded in the format shown in Table 2-1.

Table 2-1

Data Collected During Search Operations

Source	Signal Name	Type of Record	Recording Medium
Magnetometer	Gamma	analog	Strip chart
Altitude sonar	Altitude	analog	Strip chart
Pressure guage	Depth	analog	Strip chart
Radio navigation system	x y	output from HP 9825 computer	Paper printout and terminal

The post data reduction consists of marking the steep positive to negative slope equivalent to half the maximum gamma peak recorded. This mark (hit) is then allocated an XY position from between three event marks (Figure 2-3). The fraction at which point the event took place, plus the first and third XY position are punched into the HP 9825. Using the trail information, the HP 9825 prints out a calculated XY position of the hit (Table 2-2). Using still another program, the HP 9825 plots the positions of the hits on a plotter for a visual presentation (See Figure 2-4). Ideally, with this information, it would appear possible to plot positions and gamma strengths and get some idea of where the target is located as is shown in Figure 2-5. In reality though, the picture normally looks like Figure 2-6. As you can see, the hits are scattered in the x axis, rather than being aligned as in Figure 2-5. Such a hit pattern is probably due to inaccuracy of magnetometer position estimates.

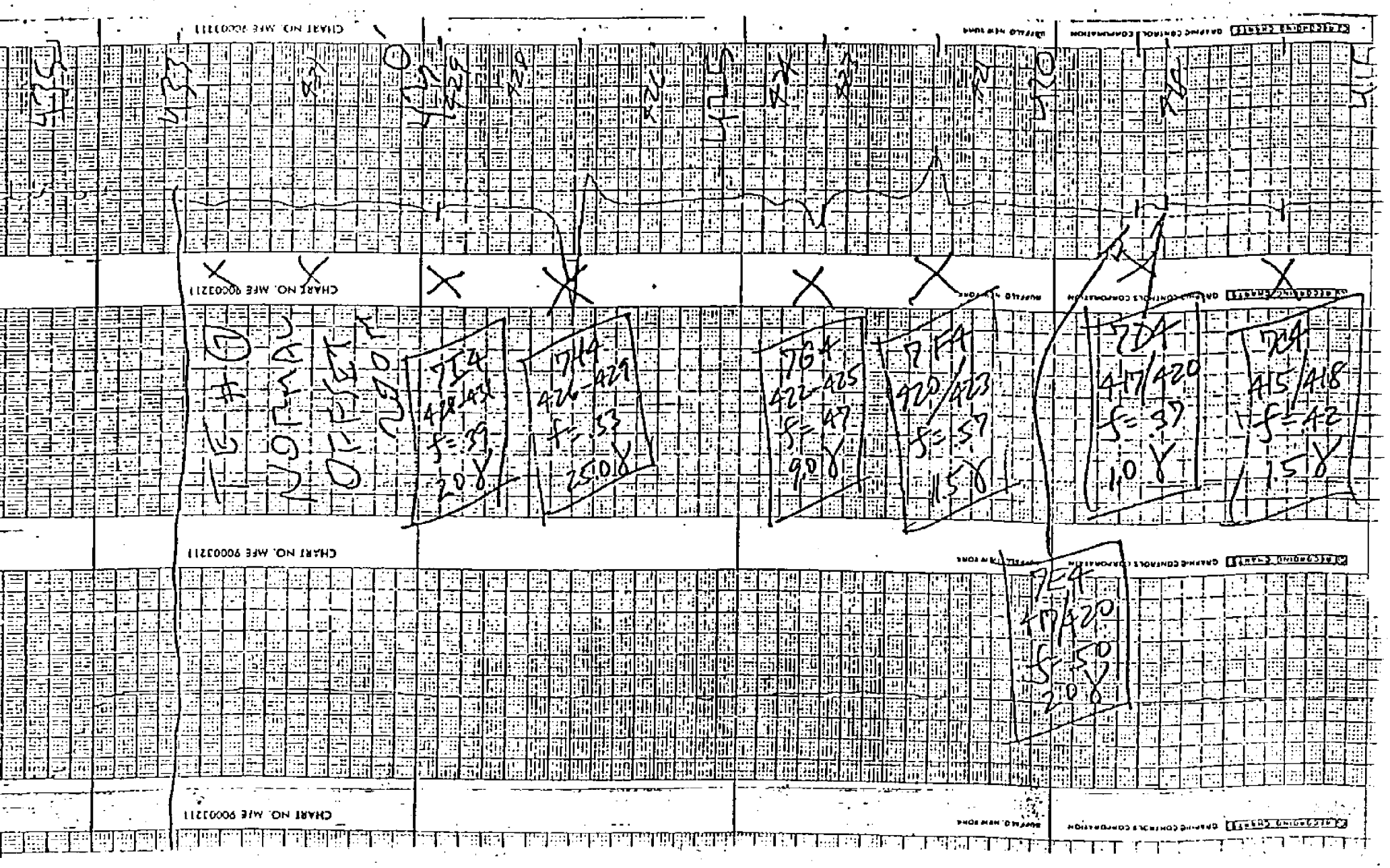

Figure 2-3 Analysis of Recorded Gamma Data

Table 2-2

START FILE 1

MAG/CDDTEST 11/83

NAME	FRAC	TRAIL	AMP	X1	Y1	X2	Y2	X	Y
1A4	0.36	81.335	4	1384	1015	1518	1014	1350.905	1014.5
1B4	0.36	81.335	4	1560	1013	1689	1015	1525.105	1014.0
2A4	0.52	81.335	2	2297	1023	2180	1026	2317.495	1024.5
2B4	0.70	81.335	2	2064	1026	1945	1022	2062.035	1024.0
2C4	0.71	81.335	6	1869	1025	1756	1024	1870.105	1024.5
2D4	0.43	81.335	2	1565	1026	1451	1026	1597.315	1026.0
2E4	0.58	81.335	4	1490	1026	1372	1024	1502.895	1025.0
2F4	0.51	81.335	4	1296	1023	1176	1025	1316.135	1024.0
2G4	0.53	81.335	3	1176	1025	1062	1025	1196.915	1025.0
2H4	0.50	81.335	4	943	1024	825	1023	965.335	1023.5
2I4	0.47	81.335	3	865	1023	745	1022	889.935	1022.5
3A4	0.22	81.335	2	1395	1038	1522	1036	1341.605	1037.0
3B4	0.32	81.335	2	1436	1035	1566	1034	1396.265	1034.5
3C4	0.32	81.335	1	1608	1037	1726	1035	1564.425	1036.0
3D4	0.49	81.335	7	1920	1032	2037	1037	1895.995	1034.5
3E4	0.44	81.335	10	2116	1031	2231	1033	2085.265	1032.0
3F4	0.29	81.335	2	2387	1030	2505	1034	2339.885	1032.0
4A4	0.48	81.335	0	2039	1048	1919	1048	2062.735	1048.0
4B4	0.34	81.335	7	1919	1048	1796	1044	1958.515	1046.0
4C4	0.36	81.335	26	1879	1046	1756	1040	1916.055	1043.0
4D4	0.62	81.335	1	1598	1038	1476	1046	1603.695	1042.0
4E4	0.31	81.335	1	1515	1046	1397	1046	1559.755	1046.0
4F4	0.18	81.335	1	1476	1046	1357	1040	1535.915	1043.0
4G4	0.42	81.335	1	1476	1046	1357	1040	1507.355	1043.0
4H4	0.17	81.335	1	1397	1046	1277	1040	1457.935	1043.0
4I4	0.20	81.335	1	1319	1037	1197	1046	1375.935	1041.5
6D4	0.42	81.335	3	1600	1058	1483	1058	1632.195	1058.0
4K4	0.44	81.335	1	1157	1046	1035	1041	1184.655	1043.5
6F4	0.42	81.335	26	1257	1068	1145	1068	1291.295	1068.0
5A4	0.36	81.335	3	1218	1055	1341	1053	1180.945	1054.0
5B4	0.27	81.335	4	1506	1055	1630	1057	1458.145	1056.0
5C4	0.51	81.335	23	1954	1054	2078	1057	1935.905	1055.5
5D4	0.37	81.335	28	2037	1055	2158	1057	2000.435	1056.0
5E4	0.40	81.335	3	2519	1056	2635	1052	2484.065	1054.0
6A4	0.61	81.335	3	2313	1066	2200	1067	2325.405	1066.5
6B4	0.33	81.335	1	2163	1064	2048	1066	2206.385	1065.0
6C4	0.67	81.335	47	1973	1064	1860	1060	1978.625	1062.0
6E4	0.44	81.335	4	1405	1068	1292	1069	1436.615	1068.5
7A4	0.39	81.335	19	1350	1072	1468	1071	1314.685	1071.5
7B4	0.21	81.335	17	1709	1075	1831	1075	1653.285	1075.0
7C4	0.42	81.335	2	1950	1077	2067	1076	1917.805	1076.5
7D4	0.37	81.335	1	2028	1076	2145	1074	1989.955	1075.0
7E4	0.50	81.335	2	2028	1076	2145	1074	2005.165	1075.0
7F4	0.57	81.335	12	2145	1074	2263	1080	2130.925	1077.0
7G4	0.47	81.335	9	2223	1080	2345	1076	2199.005	1078.0
7H4	0.33	81.335	25	2386	1076	2505	1076	2343.935	1076.0
7I4	0.39	81.335	2	2464	1075	2584	1073	2429.465	1074.0
8A4	0.27	81.335	3	1314	1083	1430	1087	1263.985	1085.0
8B4	0.39	81.335	3	1352	1082	1467	1081	1315.515	1081.5
8C4	0.26	81.335	2	1389	1086	1504	1081	1337.565	1083.5
8D4	0.30	81.335	3	1701	1081	1822	1087	1655.965	1084.0
8E4	0.54	81.335	17	2144	1088	2258	1082	2124.225	1085.0
8F4	0.31	81.335	22	2218	1085	2339	1086	2174.175	1085.5
8G4	0.47	81.335	4	2376	1089	2493	1087	2349.655	1088.0
8H4	0.23	81.335	1	2493	1087	2605	1082	2437.425	1084.5
9A4	0.32	81.335	20	1218	1100	1319	1097	1168.985	1098.5
9B4	0.61	81.335	4	1934	1098	2044	1096	1916.750	1097.0

Table 2-2 (continued)

9E4	0.39	81.335	6	2185	1092	2294	1097	2146.175	1094.5
9H4	0.50	81.335	6	2525	1097	2645	1099	2503.665	1098.0
$$$	0.39	81.335	4	2444	1104	2342	1106	2485.555	1105.0
$$$	0.38	81.335	3	2374	1110	2272	1100	2416.575	1105.0
$$	0.37	81.335	2	2234	1094	2123	1101	2274.265	1097.5
$$$	0.60	81.335	1	2234	1094	2123	1101	2248.735	1097.5

LOWEST X = 890

LOWEST Y = 1014

HIGHEST X = 2504

HIGHEST Y = 1105

END OF FILE 1

START FILE 3

MAG/CDD TEST 11/83 CONT

NAME	FRAC	TRAIL	AMP	X1	Y1	X2	Y2	X	Y
4M4	0.52	81.335	35	2510	1040	2396	1045	2450.720	1042.5
4J4	0.30	81.335	2	1277	1040	1157	1046	1322.335	1043.0
4L4	0.29	81.335	2	1035	1041	909	1045	1079.795	1043.0
9F4	0.49	81.335	5	2222	1097	2332	1097	2194.565	1097.0
9G4	0.28	81.335	2	2489	1100	2606	1100	2440.425	1100.0
$$$	0.41	81.335	4	2244	1100	2111	1100	2270.805	1100.0
$$$	0.47	81.335	4	2111	1101	1980	1101	2130.765	1101.0
$$	0.70	81.335	8	2111	1101	1980	1101	2100.635	1101.0
$$$	0.40	81.335	3	1748	1098	1614	1098	1775.735	1098.0
$$$	0.69	81.335	8	1748	1098	1614	1098	1736.875	1098.0
$$$	0.51	81.335	9	1284	1091	1146	1091	1294.955	1091.0
$$$	0.89	81.335	2	1284	1091	1146	1091	1242.515	1091.0
$$$	0.22	81.335	4	1096	1104	962	1104	1147.855	1104.0
$$$	0.70	81.335	21	1096	1104	962	1104	1083.535	1104.0

LOWEST X = 1080

LOWEST Y = 1043

HIGHEST X = 2451

HIGHEST Y = 1104

END OF FILE 3

Figure 2-4

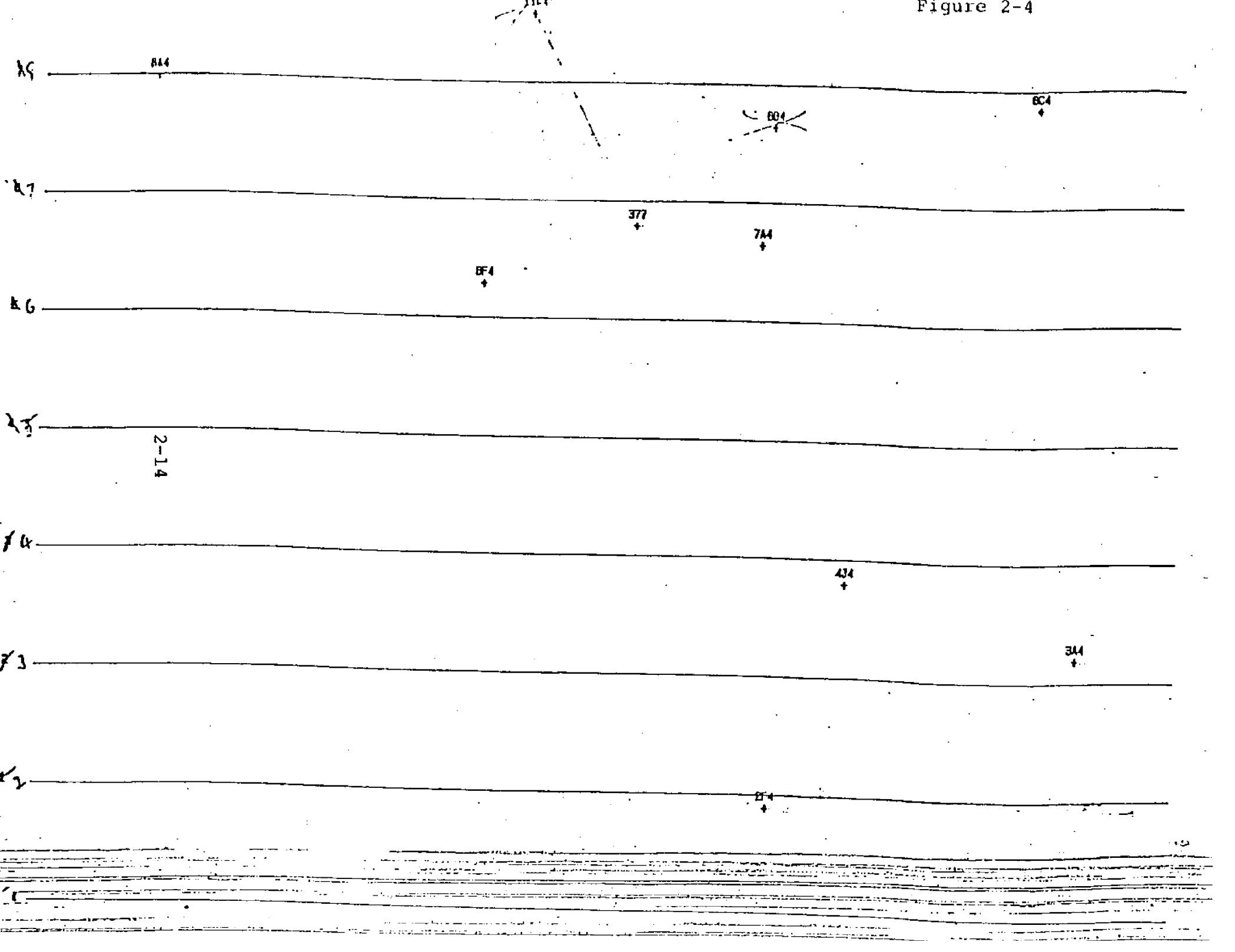

Figure 2-5

Gamma Readings Plotted in Theory

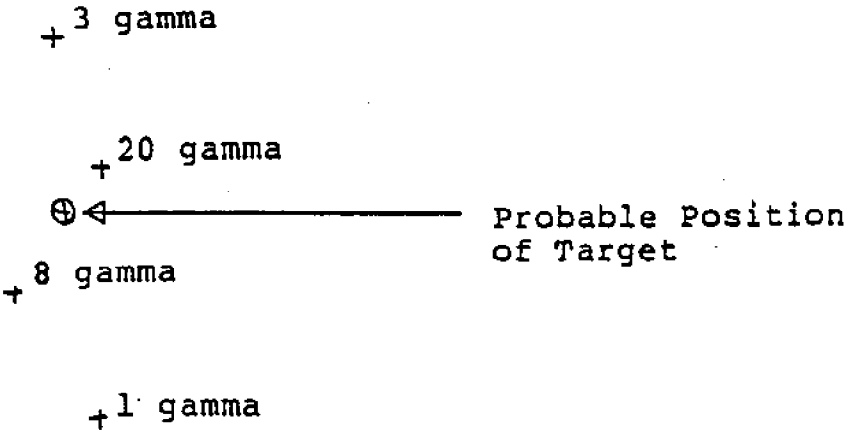

Figure 2-6

Gamma Readings Plotted in Actuality

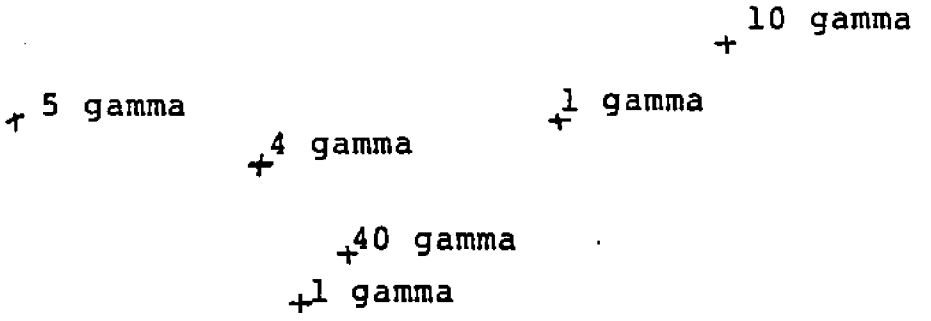

Possible reasons for the difference between actual and theoretical readings are the peturbations between the true and actual positions of the sensor in relationship to the tow vessels position and its height above sea bed, and inaccurate estimation of trail distance.

2.3 Current MSS Status

The analysis of data from the April trials and recommendations for improvements to the system must take into account the condition of the equipment, its operational use and the results that it currently is able to attain. This section is detailed and as factual as possible. It does provide some insight into basic design, maintenance and operational problems that are real and persistent. The discussion is generally terse.

2.3.1 Equipment Status

2.3.1.1 CDD Vehicle

(a) #2 CDD Partially Operational

(i) Operating with an externally mounted modified Mesotech 807 altimeter (Frequency 225KHz)

(ii) Operating without slant range (slant range vehicle electronic circuit card corroded)

(iii) Operating with a wing prone to flooding

(iv) Operating with a possible signal cross talk between data channels

(v) Operating without cable scope to depth parameters

(b) #1 CDD Status Not Operational

(i) Used as spare parts

(ii) Previous flight qualities good

2.3.1.2 CDD Control Box

#1 CDD Control Box Operational

(i) Operating without a back-up control box

(ii) Operating with an altimeter set point control that is in error from the actual control point by a factor of five .

(iii) Operating with uncertain calibration of the loop gain control.

(iv) Operating without a warning lamp to indicate "reset/normal mode" from "fast mode"

2.3.1.3 Magnetometer Sensors

#2 Magnetometer sensor: operational
#1 Magnetometer sensor: non-operational

(i) Operating with a possible signal cross talk problem

(ii) Operating without known tuning for the reference signal from the synthesizer

(iii) Operating with the through water orientation of the sensor unknown and probably at a pitch angle relative to the horizontal

(iv) Operating without the ability to fine adjust the sensor orientation within the sensor housing

2.3.1.4 Cubic Autotape

Operating with two areas of radio interference within the trial area.

2.3.1.5 HP Desk Top Computer 9825

Operating without a de-bugged CDD boat program. The depth and slant range data cannot be used for calculations of tow body position.

2.3.1.6 NAVSCHOLEOD Search Vessel

The recent trials indicated that the search vessel employed was ideal for the task. It was stable, with adequate covered and open work space. Another point in its favor was the addition of a competent crew who could relieve the R&D group of the added responsibility and concern of running the vessel.

It was noted that accurate revolutions to speed had not been calibrated.

2.3.2 Search Operations

2.3.2.1 CDD Operational Status

Although the CDD was fitted with an external altimeter it did not appear to degrade its excellent flying capabilities. It gave good and rapid response to climb and dive commands. During the 18 April trial it flew between 2 and 4 feet below

the set point altitude for the majority of the mission with occasional excursions to 6 feet below set point. However, periods of instability were experienced and are outlined:

(a) Porpoising. Occasionally the CDD would pass into an oscillating phase which would make it climb and dive in increments of approximately 5 to 12 feet. If the CDD is receiving the correct set point then the major cause may be the stress experienced in recovering from a turn and most frequently occurs in water depths under 60 feet (Figure 2-7). Boat speed changes of 0.4 knots were experienced during the porpoising motion.

(b) Deep Water. Another occasion when the CDD became unstable was in water depths over 80 feet (Figure 2-8). It can be seen from the photo-stat of the strip chart that the CDD is being tugged through the water erratically (arrows indicate) apparently in an attempt to get deeper but having insufficient scope to attain depth. Proof that the CDD is no longer working efficiently can be derived from the significant increase in drag shown by the extra strain slowing the search vessel from 5.5 kts at 65 ft to 5.4 kts at 73 ft to 5.3 kts at 81 ft and to 5.2 kts at 88 ft when the CDD is attempting to maintain an altitude of about 15 to 20 feet. When the CDD was in constant water depths of 80 feet it could achieve stability and fly level at approximately 15 to 20 feet altitude with only a loss of 0.1 knot. The importance of correctly monitoring the CDD is emphasized in Figure 2-9 which shows the area of incomplete search due to CDD instability. Approximately 47% of the data was unreliable. It is

Figure 2-7

Distortion Due To Sensor Porpoising

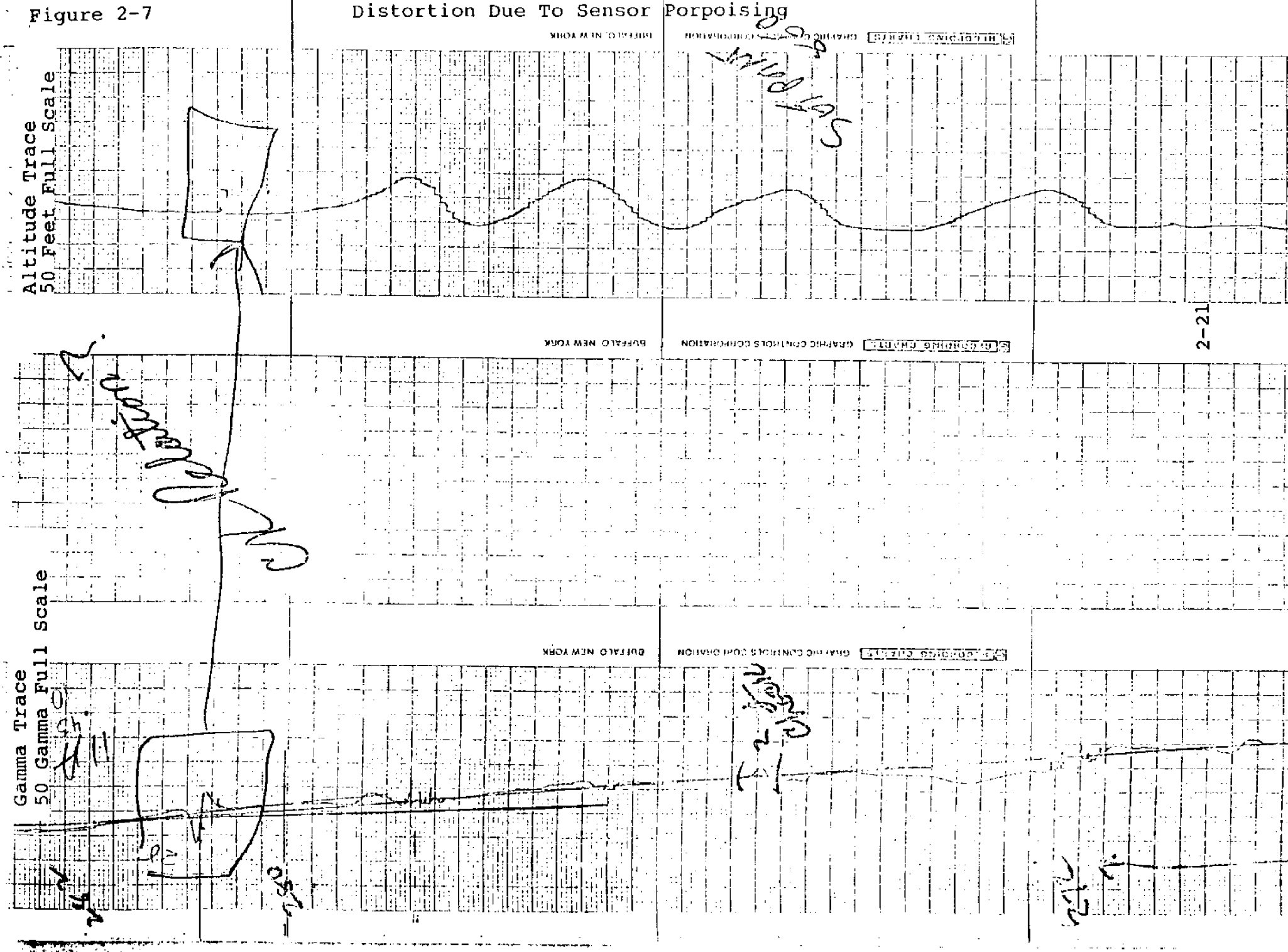

Figure 2-8

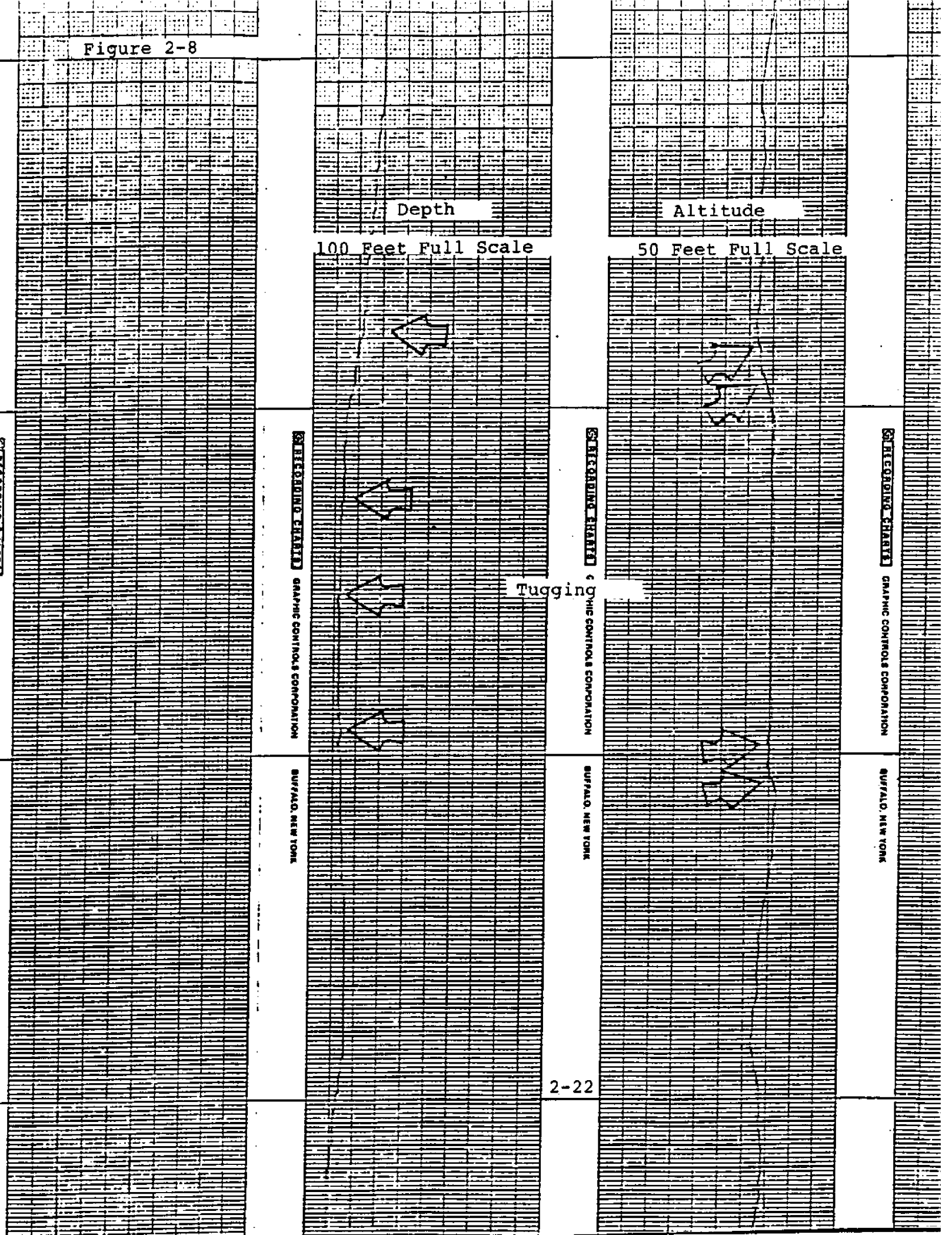
Depth
100 Feet Full Scale
Altitude
50 Feet Full Scale
RECORDING CHARTS
GRAPHIC CONTROLS CORPORATION
BUFFALO, NEW YORK
Tugging

Figure 2-9

Area of Incomplete Search Due to CDD Behaviour 12 Apr 84

Lines Indicate Areas of CDD Instability

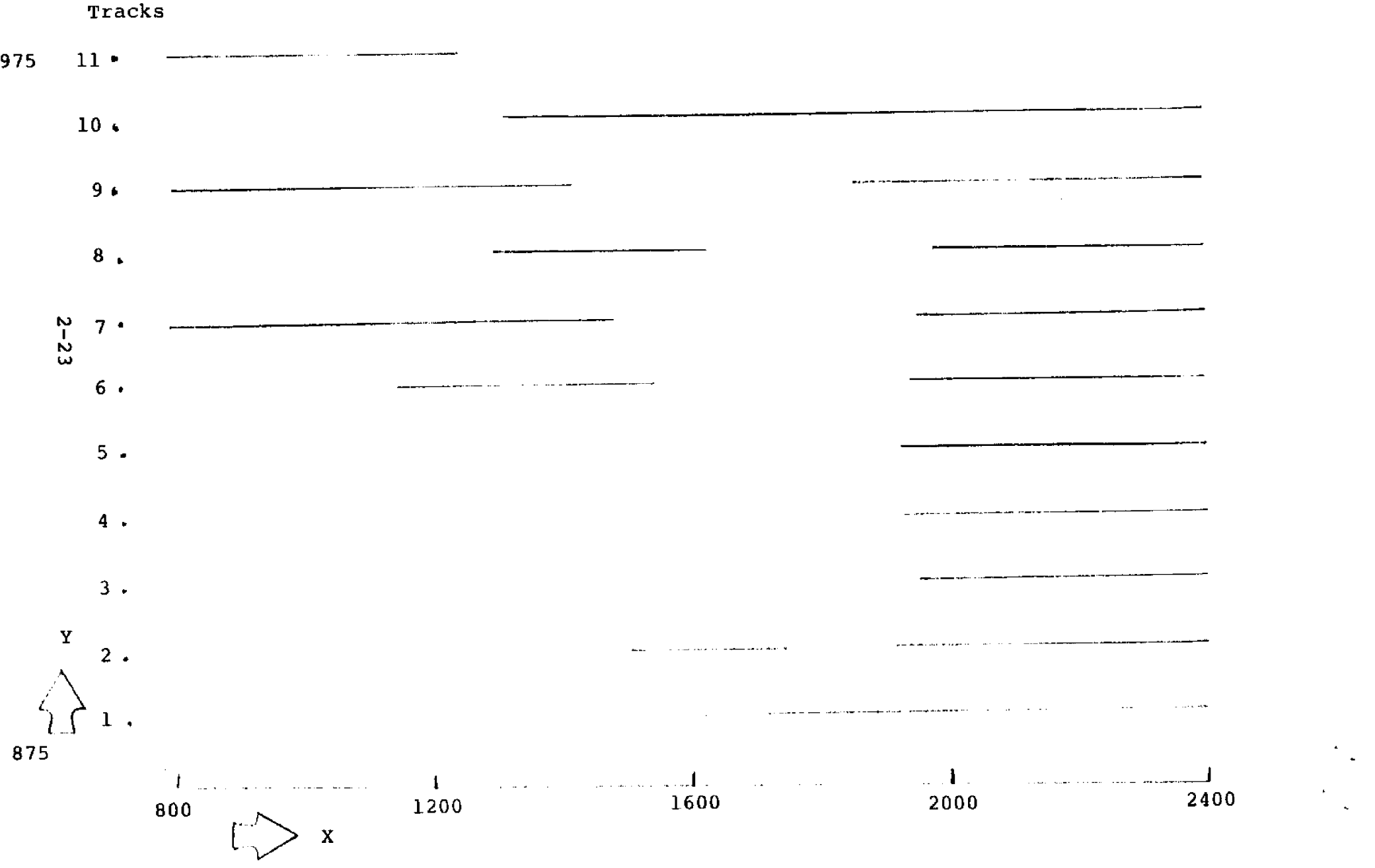

appreciated that scope/depth tables have not yet been compiled, therefore, a guide for future trials is submitted in Chapter 5 of this report.

2.3.2.2 Magnetometer Sensor Operation Status

The magnetometer data appears to be degraded on the following occasions:

(a) When the gradient slope runs the gamma signal to either side of the strip chart

(b) When the sensor exceeds 25 feet altitude

(c) When the sensor approaches or drops below 10 feet altitude

(d) When the sensor porpoises through changes of 10 feet or more in altitude

(e) When crosstalk is experienced

(f) When in the vicinity of gross magnetic targets

(g) When the sensor approaches the limits of the polar dead zone

The problem in (a) is self explanatory in that it results in the loss of peak analog signals that should normally indicate the maximum positive or negative gamma readings.

Exceeding 25 feet altitude (b) results in the loss of outer signal coverage for the target. (Chapter 3)

Study of the trial data has indicated that when the sensor approaches to within 10 feet or less altitude (c) background noise due to close proximity to the sea bed surface and small magnetic anomalies distorts the clean gradient. The resultant signals mask target anomalies.

Sensor porpoising in excess of six feet (d) distorts the gamma signal by changing the target anomalies expected signal strength thereby making judgement of a contact difficult to impossible (Figure 2-7).

There is still sufficient evidence to conclude that crosstalk (e) is emanating between the altimeter and the magnetometer signals (Figure 2-10).

Gross targets (f) such as the submarine not only distorts the gradient their sheer intensity masks out any lesser signals.

Table 2-3 tabulates the data loss due to erratic CDD behavior and the magnetic anomaly of the submarine. It also illustrates the average gamma gradient shift for the search area.

On 18 April 1984, #2 magnetometer lost lock on South to North headings (g). It was naturally assumed that the sensor had tilted into the polar dead zone. It was also assumed that water current speed or direction was to blame for this condition. A thorough study of the conditions on that day were compared to other trial days when the magnetometer did not lose lock. No excessive currents existed, in fact the current changed direction during 18 April trial with no appreciable change in magnetometer data (Table 2-4). Therefore, speed and direction of current were discounted as a cause. The next thought was perhaps the sensor head had moved inside the housing, knowing how tight a fit that is, this

Figure 2-10 Cross Talk Between Altimeter and Magnetometer

Table 2-3

Data Loss and Gradient 12 April 84

Track #	Track Duration Secs	Bad Data Secs	% Good Data Rate	Averaged Gradient + or - Gamma	Submarine Signature Effect (m)
1	540	460	15 %	+33n-s	350
2	700	320	55 %	-39s-n	734
3	620	240	62 %	+37n-s	720
4	680	300	56 %	-33s-n	660
5	600	200	66 %	+41n-s	600
6	700	260	63 %	-38s-n	630
7	560	380	33 %	+37n-s	670
8	750	260	66 %	-46s-4	670
9	NK	NK	NK	NK	NK
10	640	440	32 %	NK	NK
11	580	80	87 %	NA	300

Average gradient due to spatial effect = 38 gamma for 1600m

Average good data recording rate = 53%

Average signature influence from submarine to Y 945 = 630m

Table 2-4

Appendix 3

Track Information Record

Operator Tierney Richardson Program Cart # Boat Normal ~~Sonar~~ Mag #2 Single Sensor

Date 18 Apr 84 Data Set (Data Table) S Range S

Location Solomons Search Axis 030/210 Lane Spacing 10 meters

Sea State 2 Wind West 6kts Current South on Surface

Deck Trail 6.56m Towpoint Offset NIL

Mag #2 13.96m Trail (no Slant Rge) 114.5

Offset	Track #	Direction Nor	Direction Rev	Time In	Time Out	Avg ~~Scope~~ Speed	Result	Dif
1070	Trail Calc 1			1032	1036	5.2	Bad Y/on X/off all	
1070	" 2			1039	1044	6.17	Good Y/on X/on	.9
1070	" 3			1047	1052	5.16	Bad Y/off 4mE X/off all	
1070	" 4			1055	1059	6.19	Good Y/on X/on	1.0 .4
1020	" 5			1059	1103	5.7	Good Y/on X/off all	.6
1020	" 6			1108	1111	5.1	Bad Y/on X/off all	.5
1020	" 7			1119	1121	5.65	Good Y/off 3mW X/on	.4
1020	" 8			1126	1128	5.17	Bad Y/on X/off all	
Course	Test #9			1130	1138	--	000 Bad 060 P.Good 050 Good 340 Good	
900	10			1152	1200	4.82	Good Y/on X/on	
970	11			1237	1247	--	No Data	
970	12			1250	1309	5.27	Good Y/on X/off/1004.1587	.5
980	13			1305	1313	5.8	Bad & Trying Y/on X/off Tide Change	
990	14			1317	1330	4.92	Good & Y/on X/on	.2
1000	15			1336	1342	5.2	Trying to Good Yat1630 4m off NoX/1497/2500	
1010	16			1346	1357	4.87	Good Y/on X/on	.4
1020	17			1401	1413	5.29	Occasional Gliche Y/off 1300/2400 X/on	
1030	18			1415	1427	4.83	Good Y/off 1800/2400 X/on	.6
1040	19			1431	1441	5.42	Occasional Gliche 2160 Y/off 1400/1900 X/off 2514	
1050	20		2-28	1446	1457	4.9	Good Y/off 2000/2300 O/on	

argument was also discounted. Diurnal or Sunspot activity would effect the magnetometer equally, no matter in which direction it travels. Erratic movement by the CDD does adversely effect the magnetic signature response but does not effect it for prolonged periods. it would, therefore, appear that something else was different on that day. Admittedly, the UNH/SSC recording was being conducted that day, but like the Diurnal and Sunspot activity, that must also be discounted as North to South runs were unaffected. This leaves only one possible suspect area. The setting of the frequency on the NCSL Magnetic Processor and synthesizer that day were set to give positive polarity for the recording media. Normally the NCSL equipment should be adjusted to a count of 1000Hz above the Larmor frequency due to the ambient field.

The present method of judging the 1000 Hz setting is a rather hit and miss affair. Usually if a signal appears on the strip chart it is felt that, with minor adjustments, the instruments will perform. It is likely that this method of alignment of the instruments is unsatisfactory and results in a signal close to the edge of the MP-01's dynamic range. Exceeding the dynamic range will cause output fold-over to occur, resulting in the signal observed on South/North headings as the sensor becomes increasingly sensitive to its orientation.

2.3.2.3 Reference Sensor

Trials were not conducted using a reference mag sensor, therefore, it is not known at this time whether this addition to the system would be of specific value.

2.3.2.4 Trial Area

The trial area used for the test is suitable but is far from ideal. Prior to the target field first being laid, it would have been preferable to map the natural magnetic anomalies that already exist there. This was not possible as the CDD and a method of accurate sensor location did not exist at the time the targets were laid. Therefore, magnetic anomalies that are not due to a target's influence will continue to either mask or confuse the overall picture when data analysis is undertaken (in many ways this improves the situation by making it more realistic). Targets have been located and identified as accurately as possible but this task requires continual updating if accurate data analysis is to be achieved.

2.3.2.5 Speed and Maneuvering

(a) The calculated average speed over the ground for the 18 April trial was from 4.8 to 6.2 kts (it will be noticed form para 2.3.2.1 that the CDD exerts considerable drag on the towing vessel reducing its speed for short periods by as much as 0.5 kts at maximum wing depression).

(b) The search vessels speed was controlled by remaining at constant shaft RPM regardless of the direction of travel. If current velocity is present, constant RPM will produce strip chart records of uneven length thereby making visual track to track data comparison difficult.

(c) At the end of track, Williamson turns were executed at set RPM with the CDD in the dived state. The CDD was set at 20 feet altitude controlled by the altimeter.

(d) The average distance from track start to the vessel being on course with the CDD at the correct altitude was between 200 and 400 meters. At the deep south end late recovery was due to the CDD not attaining depth before reaching track start. At the shallow North end late recovery was due on three occasions to the CDD descending to the sea bed or approaching to within 2 to 7 feet altitude (Figure 2-11).

(e) CDD oscillations appeared to be cured by temporarily increasing the set point by 20 feet altitude.

(f) Most CDD and magnetometer recoveries were conducted with the search vessel at dead stop. Fouling of the screws occurred on two occasions.

2.3.2.6 Navigation and Tracking

(a) The search courses actually steered continue only to be as accurate as the skill of the helmsman. This factor makes the task of predicting search coverage achieved difficult. Study of the data in Table 2-5 highlight the problem of the approach to track start. It took an average of 154 meters into the track to approach to within 2 meters of the intended track. Possible reasons for this error are:

(i) Incorrect turning procedure
(ii) Influence of the dived CDD
(iii) Insufficient turning space (Shallow water)
(iv) Control of helmsman by the operators

Figure 2-11

CDD Behavior during turn at end of track #9

Gamma Trace
50 Gamma Full Scale

Altitude Trace
50 Feet Full Scale

Table 2-5

Navigation Error 12 April 84 Trial

Track #	Track Direction	Distance To 2m of Track	% of Track	Error Over 2m of Track	% of Track	Possible NAV Inter-ference Error	% of Track
1	NOR	428	24 %	525	29 %	100	4 %
2	REV	30	2 %	155	9 %		
3	NOR	320	18 %	520	29 %		
4	REV	0	0	290	16 %		
5	NOR	225	12 %	630	34 %	170	7 %
6	REV	0	0	530	29 %	100	4 %
7	NOR	200	11 %	630	35 %		
8	REV	70	4 %	158	9 %		
9	NOR	230	13 %	800	44 %	170	7 %
10	REV	40	2 %	310	17 %	40	2 %
11	NOR	815	45 %	160s	89 %	560	22 %

A. Average distance to on track within 2m = 214m
B. Average percentage off track in excess of 2m due to helmsman error 31%
C. Average percentage off track in excess of 2m due to Nav interference 8%
D. (A) without track II 154m
E. (B) without track II 25%
F. (C) without track II 5%

(v) Helmsman inefficiency

It can be seen that recovery to track distance was greater at the shallow Northern end of the track.

It can also be judged that although Table 2-5 and the jagged ships track trace in Figure 2-12 highlight the areas where the Navigation equipment appears to be giving bad data, the problem is very small (5%) when compared to other tracking errors.

2.3.2.7 Scope and Trail

(a) The following method of trail calculation was recommended by SSC staff as an interim in the absence of slant range information. It was used in the April trial with reasonable success:

(i) Target. The target can be a placed magnetic dipole (dummy mine) or an anomaly that gives an approximate equivalent dipole reading. It is convenient if the exact XY coordinates are known but it is not essential.

(ii) Method. Run past the dipole North to South with the HP 9825 printing a position every two seconds, with a corresponding event mark on the strip chart recorder. On completion of the run, the anomaly on the strip chart should be studied and a position line should be drawn on the positive to negative slope on the Northern side to coincide with the 1/2 value gamma, i.e., the gradient line is first projected through the anomaly and the peak gamma reading is taken; say 10 gamma. A line is then drawn at 5 gamma through the positive to negative slope

Figure 2-12 Navigation Interference

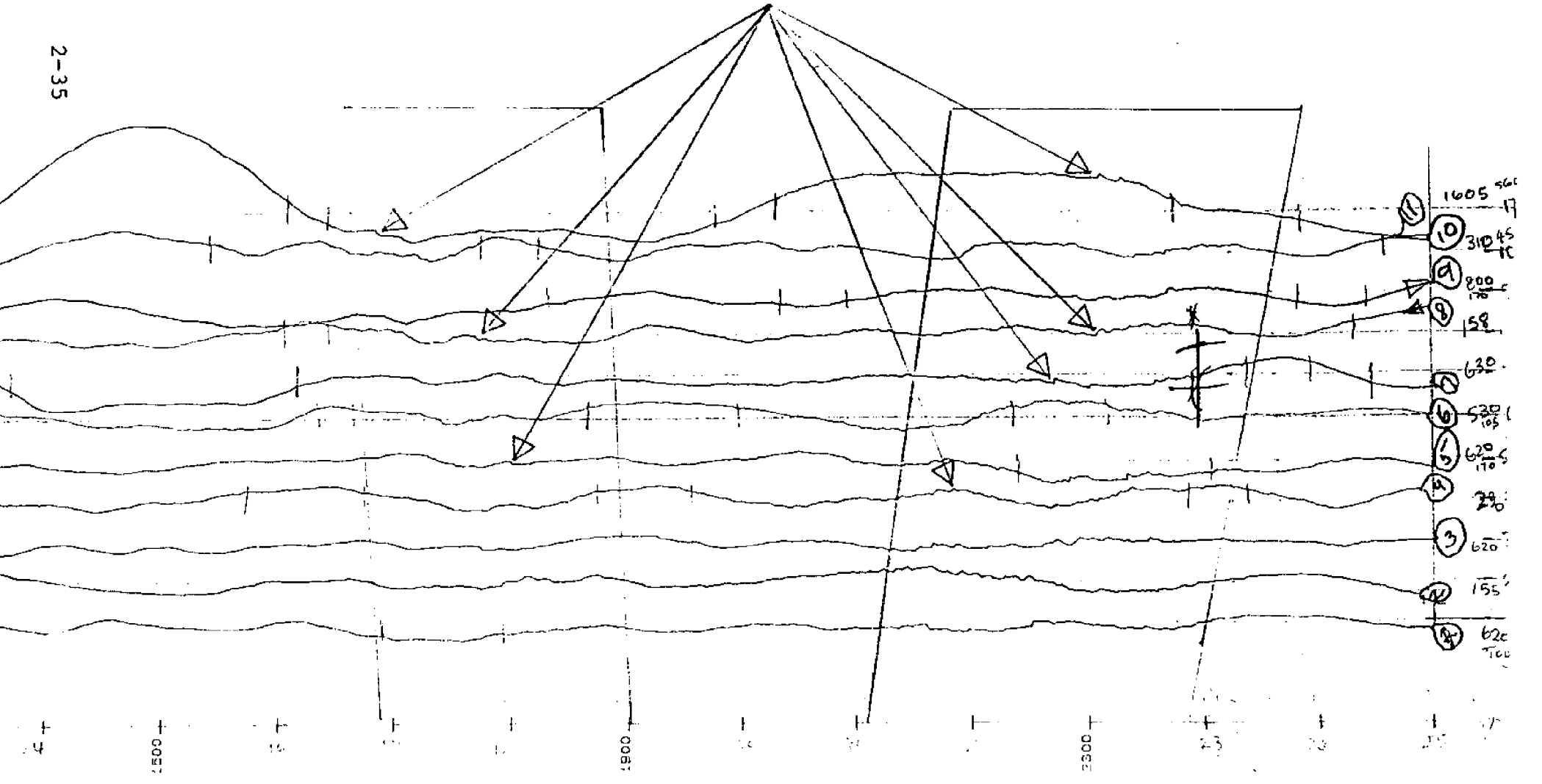

to indicate the position. This position is noted by interpolating between the two second event marks. The whole process is repeated on a South to North run. The initial track X position is then subtracted from the reverse track X position. The resultant is divided by two for the trail distance. This process should be checked again with two more runs (Figure 2-13).

(b) The boat tow configuration for the April trials is depicted in Figure 2.14. It can be seen that if the deck trail of 10m (A), the cable scope of 91.44m (B) and the magnetometer trail of 13.96 m (C) are added together, the resultant length is equal to 115.4 meters. As the calculated trail was 114.5 meters a loss of only 0.9 meter for the catenary was recorded, therefore, it must be assumed that a mistake occurred somewhere either during the measurement of the cable or the estimation of the trail. Trail estimation by contact comparison of the 12 April data is 111m which approximates the calculated trail as the search was being conducted in deeper water. However as the difference is small it will be assumed that slightly more than 300 feet of cable was paid out and that the estimation of 114.5m was slightly high.

2.3.3 Data Reduction

2.3.3.1 Time

Although a time consuming and boring task, the accurate data reduction performed by the NAVEODTECHCEN staff has greatly aided the UNH/SSC staff to complete this report. The method of data reduction was covered in Section 2.2. so will not be repeated in this section. Based on the time taken to

Figure 2-13

TRAIL CALCULATION

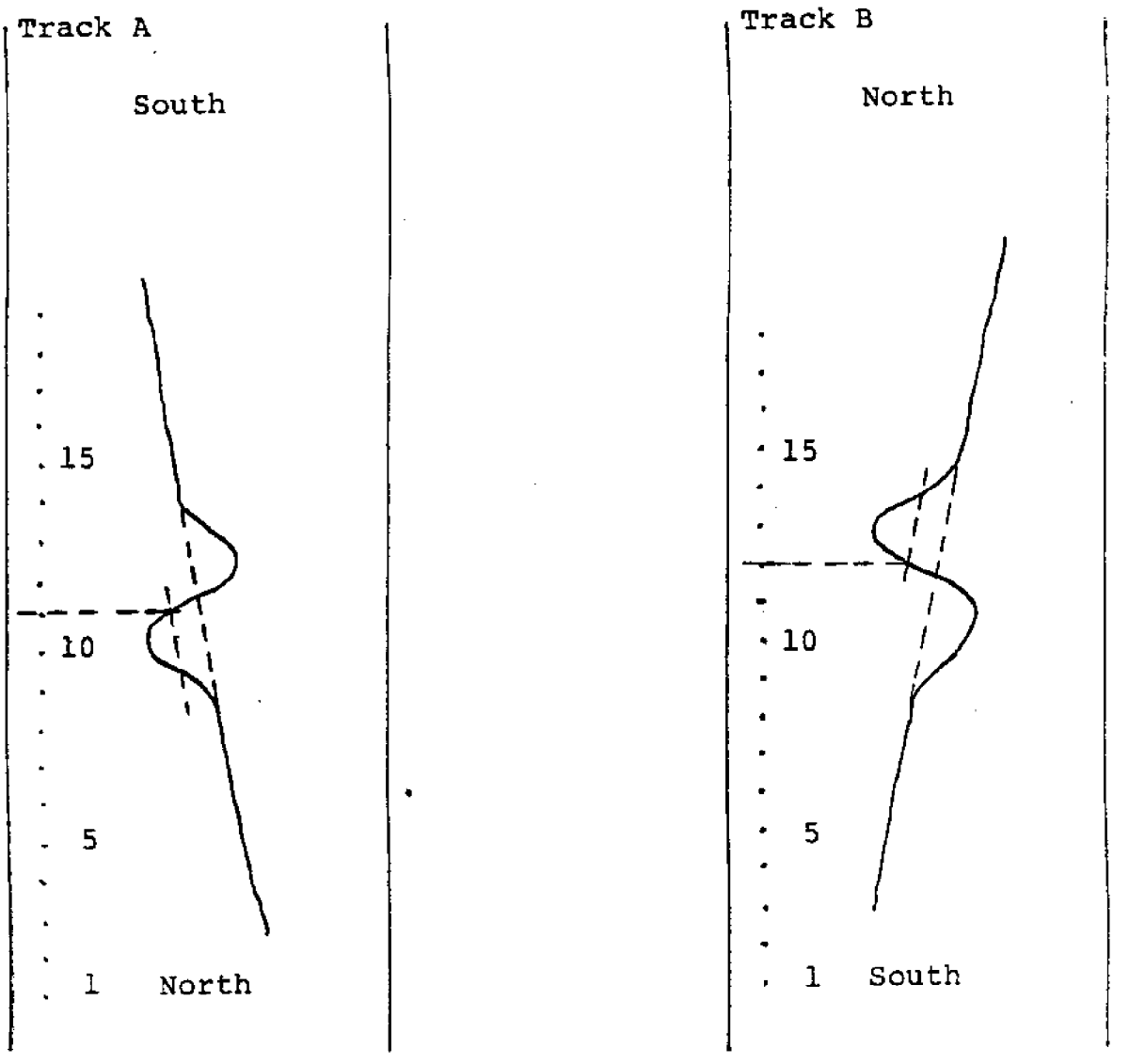

Track A event mark 11 corresponds to x = 1373

Track B event mark 12 corresponds to x = 1233

Difference = 140

Trail = $\frac{140}{2}$ = 70 meters

Figure 2-14

Tow Configuration

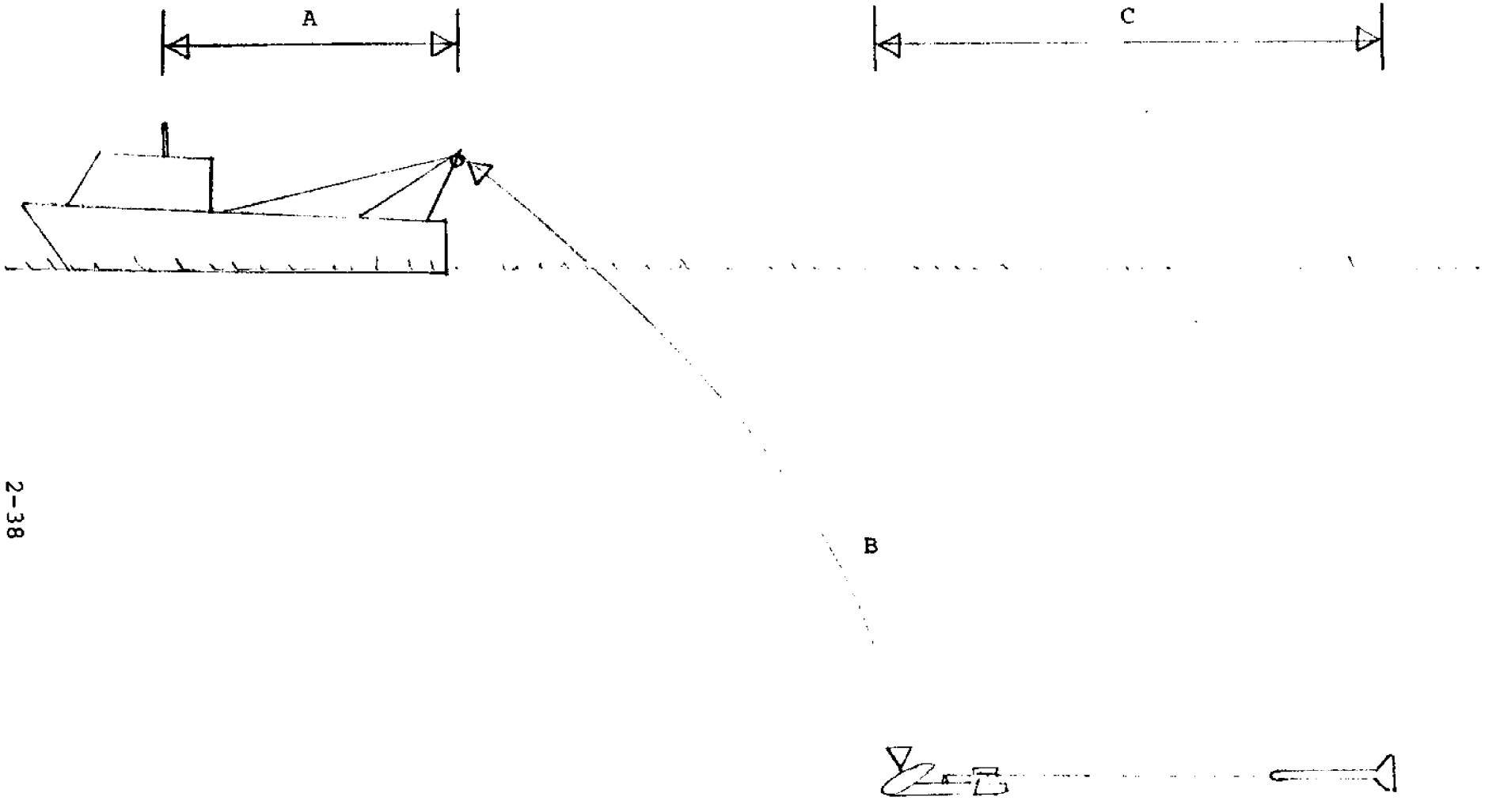

reduce the data for the 12 April trial it is estimated that it would take about 600 man hours to reduce the data from the search of a one kilometer square area. However, improvements to the plotting procedures, greater operator familiarity and cleaner magnetic sea beds should greatly reduce the data reduction time.

Using data extrapolated from Tables 2-6 and 2-7 the following conclusions are reached for a search conducted within the trial area.

2.3.3.2 Average Target

An average target magnetic anomaly will be represented by +9.3 gamma south followed immediately the a -1.2 gamma to the North. The average distance between start of anomaly and finish of anomaly will be 42 meters.

2.3.3.3 Detection

The average target will be detected by a sensor at an average altitude of 19.4 (6 meters) feet if the sensor approaches to within Y coordinate distance of 5.7 meters.

2.3.3.4 Probability

Assuming that the magnetometer can produce good data for 53% of the search it will have a probability of detection of 70% if the search vessel remains within 2 meters of track for 75% of the search.

2.3.3.5 Area

The sensor will detect approximately one magnetic anomaly every 19 seconds in a 1 sq km area containing 765 magnetic anomaly responses.

Table 2-6

Mag Trial 12 April 84 Target Hits

Course Dir^{n}	Target # Hit #	Positive Gamma Orientation	Negative Gamma	Target Length(m) +0 to -0	Altitude Ft (m)	Proximity to Target X	Y
NOR	31 1A	6.0	--	23	19 (5.79)	+12	-26 *
REV	31 2C	8.0s	1.0n	37	19 (5.79)	+29	- 5 *
NOR	31 3B	7.5s	0.5n	40	20 (6.09)	+38	- 9 *
REV	33 4F	3.5n	1.5s	40	20 (6.09)	- 6	- 9
REV	32 4E	8.5s	1.0n	39	20 (6.09)	- 5	- 9
REV	30 4D	14.5s	2.0n	39	20 (6.09)	- 5	- 1
NOR	30 5C	1.5n	1.5s	40	20 (6.09)	-21	+ 8
NOR	32 5B	6.0s	1.5n	35	18 (5.49)	+ 3	- 5
REV	29 6E	1.5s	1.0n	42	22 (6.7)	- 4	- 7
REV	28 8C	20mid	1.5s 1.0n	53	15 (4.57)	- 7	- 2
NOR	28 9D	4.0s	1.0n	43	19 (5.79)	0	+ 3
NOR	27 11B	20s	1.0n	55	20 (6.09)	+ 1	-12
NOR	26 11C	20mid	0.5s 1.0n	60	20 (6.09)	+ 2	- 1

* Target Position Suspect

Average Target Length 42m
Average Altitude 19.38ft
Average X range (not *) 4.9m
Average Y range (not *) 5.7m

Average Positive Gamma 9.3 south
Average Negative Gamma 1.2 north

Table 2-7

Target Analysis 12 April 84 Trial

Track #	Track Direction	# of Anomalies under 3 gamma	# of Anomalies 3 gamma and over	Possible Di-pole Targets 3 gamma and over	Possible Di-pole Targets under 3 gamma	TECHCEN gamma Contacts Marked	Likely gamma Anomalies Missed	Actual Targets On Track	TECHCEN # of Hits
1	NOR	27	3	NIL	2	5	1	NIL	NIL
2	REV	13	7	NIL	NIL	3	NIL	1	1
3	NOR	15	5	4	4	4	NIL	2	1
4	REV	4	7	6	NIL	6	NIL	4	3
5	NOR	6	6	3	6	7	2	3	2
6	REV	6	5	NIL	7	7	1	1	1
7	NOR	8	7	3	2	3	NIL	2	NIL
8	REV	10	3	2	3	5	NIL	2	1
9	NOR	NK	NK	NK	NK	8	NK	2	1
10	REV	10	2	1	1	2	NIL	2	1
11	NOR	3	6	4	3	7	NIL	3	3
TOTALS:		102	51	23	28	57	4/2.6%	20	14/70%

NK= Not Known

2.3.3.6 Density

Assuming a density of 40 mine-like targets per sq km approximately 24% of the anomalies identified as mine-like targets were actual mines.

NOTE 1: It should be appreciated that the above information is based on the work of the operator who reduced the 12 April trials. Identification of target gamma anomalies is subjective and entirely dependent upon the skill, experience and patience of the analyzer.

NOTE 2: This data is valid only for the area in which the test took place. Further trials using alternative areas are required so that the Probability of Detection can be further evaluated for differing conditions.

CHAPTER 3

MAGNETIC SIGNATURE STUDY

3.0 Analyses and Interpretation

The primary purpose of this quick look study has been to evaluate how the MSS System could be improved in the near future. The study teams background knowledge of the system supported the need for a short set of sea trials of the system to evaluate current operational problems. This sea trial, accomplished in April 1984, also tested an interface between the magnetic processor analog output and a microcomputer controlled data acquisition system. This was the first step toward the development of a real-time system to analyze and interpret magnetic search data. Section 3.1 briefly describes this ad hoc instrumentation set-up and the problems that occurred during the sea trials. The lessons learned during the trials would be incorporated into the configuration recommended in Chapter 6 as part of an improvement program.

Computer analysis of magnetic search data is most efficient when the expected characteristics of magnetic anomalies can be modeled in mathematical terms. The computer can then compare sensed data to these models and compute the best fit for magnetic moment and position (location) of the sensed anomaly.

Section 3.2 derives a mathematical model of the anomaly contours for a dipole configuration typical of mine like objects. This model and associated data analysis algorithms are then tested using data acquired during sea trials in November 1983 (good data) and April 1984 (poorer data). This simple test shows that the computer analysis of magnetic anomaly data is feasible and as accurate as any other means. With automated acquisition of data and direct computer entry, real time analysis is both feasible and achievable at reasonable cost.

The April sea trials encountered many equipment and operational problems that reduced the effectiveness of search operations regardless of the techniques used to analyze the data. Chapter 5 discusses a series of recommendations aimed at making the current system function to the limits of its configuration. The chapter also provides some operational guidance of use in setting up and controlling routine survey operations.

Chapter 4 addresses the problem of determining sensor position relative to the radio positioning system on the tow platform. This is one of the more persistent problems in MSS search operations and unless adequately resolved can become a disabling factor when attempting to interpret search data. A guide to reducing these errors is also included in this Chapter.

3.1 Magnetometer Data Acquisition Test Description

On April 17 and 18 a field test was conducted at the EOD test site to acquire magnetometer data pertaining to specific targets. The objective of the project was to interface digital data collection equipment to the existing system and record search data on a digital cassette deck.

Since several instruments were being tied together a master or controlling device was required to integrate the system. This task was performed by a Motorola 68000 based microcomputer which buffered data between instruments and formatted records for output. A block diagram of the data collection system is shown in Figure 3-1. The microcomputer also accepted rough sensor position data from the HP 9825 computer. The HP computer calculates the XY position within the test area from ranges supplied by the Cubic navigation

Figure 3-1

Block diagram of data collection system

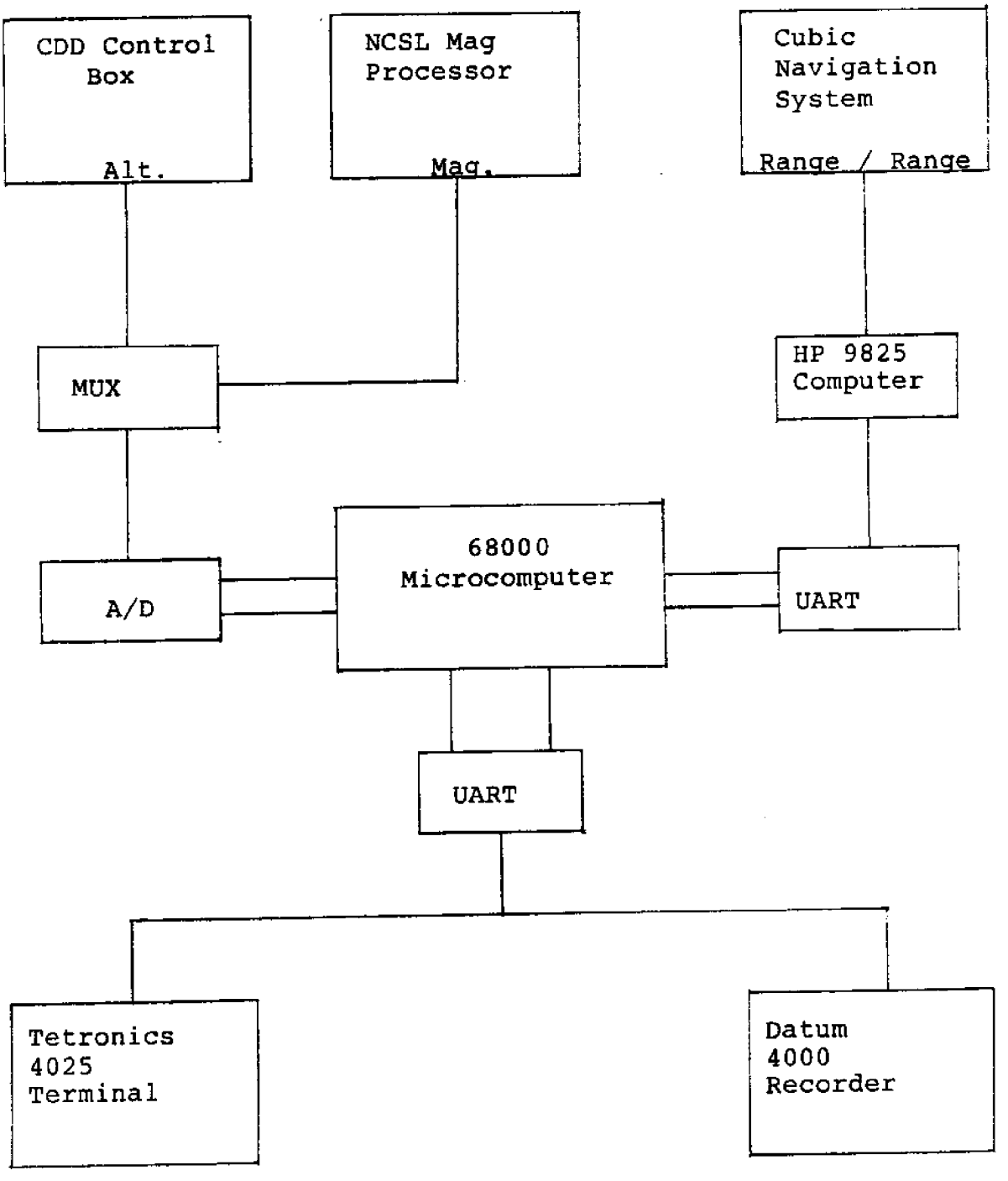

systems. The transfer from the HP computer to the 68000 was via a 1200 baud RS-232 serial link. The position update rate was about once per second.

The remaining data used in the test was available in analog form. For this reason, the 68000 microcomputer was equipped with a 6 channel analog multiplexer and a 12 bit analog to digital converter. Analog outputs from the CDD control unit and the Magnetic Processor were digitized and assembled with the position data to form a record. Within a record the magnetometer channel was sampled twice while the altimeter was sampled once. The format for a typical record is shown below.

The record begins with a Z identifier followed by the sensor x position in meters; next, a Y marks the y position in meters. The M identifier is followed by the digitized magnetometer reading in hexadecimal units while the A preceeds the digitized altimeter reading. In each record there are two magnetometer samples. Prior to the test, calibration was done on the A/D system with the following results:

magnetometer	1 gamma = 14.05
altimeter	1 foot = 81.14

After each record was assembled in the microcomputer it was output to a Tektronix 4025 terminal and a Datum Model 4000 digital cassette recorder.

There were some modifications which had to be made to the existing magnetometer equipment in order to be compatible with the microcomputer which operated from a +5 volt and ground power supply. The magnetometer output of the Magnetic Processor is typically an analog voltage of -10 to +10 volt output, although this decreased the resolution for the strip chart it still provided a useable system.

3.1.1 Problems

There were some problems evident in the testing that should be mentioned. The slant range measurement equipment was not functioning on the CDD, therefore the trail distance could not accurately be known. Also the magnetometer acted very erratically when towed on the northbound tracks.

A problem with the analog digitizing system was present in the form of substantial noise on the signal. For a constant DC input, the output varied over 4 bits. This corresponds to an error of + or -5% full scale or 50 gamma.

3.1.2 Retrieving Data from Tape

As part of the equipment setup procedure approximately 4 minutes of sample data was recorded on tape and replayed to verify the integrity of the recorded data. Upon completion of this process it was concluded that it was indeed possible to record digital data and retrieve it successfully. Upon determining this, the team proceeded to the test site and began data collection; the entire data collection process lasted 5-6 hours.

Once back at MSEL the process of transferring the data from cassette tape to floppy began. Early indications showed that the data transfer from cassette to terminal were not reliable. A complete playback of the data on Tape A showed that only about 5% of the records were uncorrupted. The actual content typically showed 10-20 good records followed by up to 30 seconds of completely corrupted characters. The playback of Tape B (only 5 minutes data) had a much higher success rate. Almost all the records were extracted correctly from this tape. The only difference between the two tapes is

the drive on which each was produced: Tape A on Drive A and Tape B. All connections were identical since the digital recorder automatically switched drives.

All data that was recoverable was placed on floppy disks for further processing. Only the data from tape B contained any significant information.

3.1.3. Conclusion

In summary there are several points which one can draw from the test results. At first it was proposed to record data on the 2 drive cassette recorder and transport the single drive unit to UNH for data reduction. Experience has shown that mixing data tapes and recorders is very risky at best. Also, the use of mechanically driven devices in a hostile operating environment is not completely reliable. Another setback suffered in the data acquisition was the incomplete or incorrect specification of the signal characteristics. An example of this is evidenced by the magnetometer signal which has a -10 to +10 volt range.

This test, however, did prove that it is possible to electronically digitize and record data for this system. The magnetometer channel should be sampled 2 to 4 times per second in order to achieve the resolution required for typical signal speeds.

It is not necessary to store all magnetometer information. The background and unimportant data could be filtered out.

3.2 Development of Magnetic Anomaly Analysis Procedures

A description of the system and its operation was presented earlier in sections 1 and 2. In order to assess and improve the current system, it is important to understand the nature of a magnetic anomaly pattern, the magnetometer output format, and how these two correlate.

A Cesium Vapor magnetometer measures the total magnetic field intensity. This is a scalar quantity. The output signal is a frequency (LARMOR) which is proportional to the total field intensity. The undisturbed magnetic field of the earth is on the order of 50,000 gammas and the disturbances which is being measured is typically 3 to 4 orders of magnitude smaller. It therefore can be shown that the total signal being measured is very nearly in the direction of the undisturbed Earth's magnetic field. This is a valid assumption except in the very near field of large objects. The magnetometer output therefore measures the field essentially parallel to the Earth's magnetic field at that location. In conjunction with this statement, the analyses must then correlate the Earth's field direction at the particular location where measurements are made.

3.2.1 Theoretical Anomaly Signature Derivation

Assuming that the object to be detected and located appears as a dipole, it is useful to derive a simplified model of its effect on the ambient magnetic field. The objective is to arrive at a 3 dimensional representation of the signal which the magnetometer detects.

Once this is done and if the model is somewhat representative of the object type to be detected, the analyst can deduce optimum search track width, search direction and search

altitude above the object based on the minimum gamma signal deemed reliable in the search environment and the range of magnetic moments of the objects. it may also be possible to derive an algorithm based on the signature which could be implemented in a computer to locate the target and indicate its probable magnetic moment.

3.2.1.1 Dipole Signature/Interpretation

A dipole has a field with magnitude and direction given by radial and tangential components T_r and T_θ. These can be expressed (See Figure 3-1A) by:

$$T_r = \frac{2M\cos\theta}{r^3} \qquad \text{(Eq. 3.1)}$$

$$T_\theta = \frac{-M\sin\theta}{r^3} \qquad \text{(Eq. 3.2)}$$

where M is the magnetic moment of the object, and T is the amplitude of the anomaly. If the dipole is induced by a vertical magnetic field the total field measured by a magnetometer would be:

$$T_z = T_r \cos\theta + T_\theta \sin\theta \qquad \text{(Eq. 3.3)}$$

Combining the above equations yields:

$$T_z = \frac{M}{r^3} (3\cos\theta - 1) \qquad \text{(Eq. 3.4)}$$

$$\theta = \arcsin \frac{x}{(x^2 + z^2)\,1/2} = \arctan \frac{x}{z}$$

Since the magnetometer effectively measures the field in the direction of the Earth's magnetic field, introduction of the angle of inclination (B) enables the computation of the component along the Earth's magnetic field. If the geometry is analyzed, it follows that the filed components of T_r and T_o along the Earth's field lines are given by:

$$T_m = T_r \cos(\theta - 90^o + B) + T_\theta \sin(\theta - 90^o + B) \qquad \text{(Eq. 3.5)}$$

FIGURE 3-1A

Field Geometry.

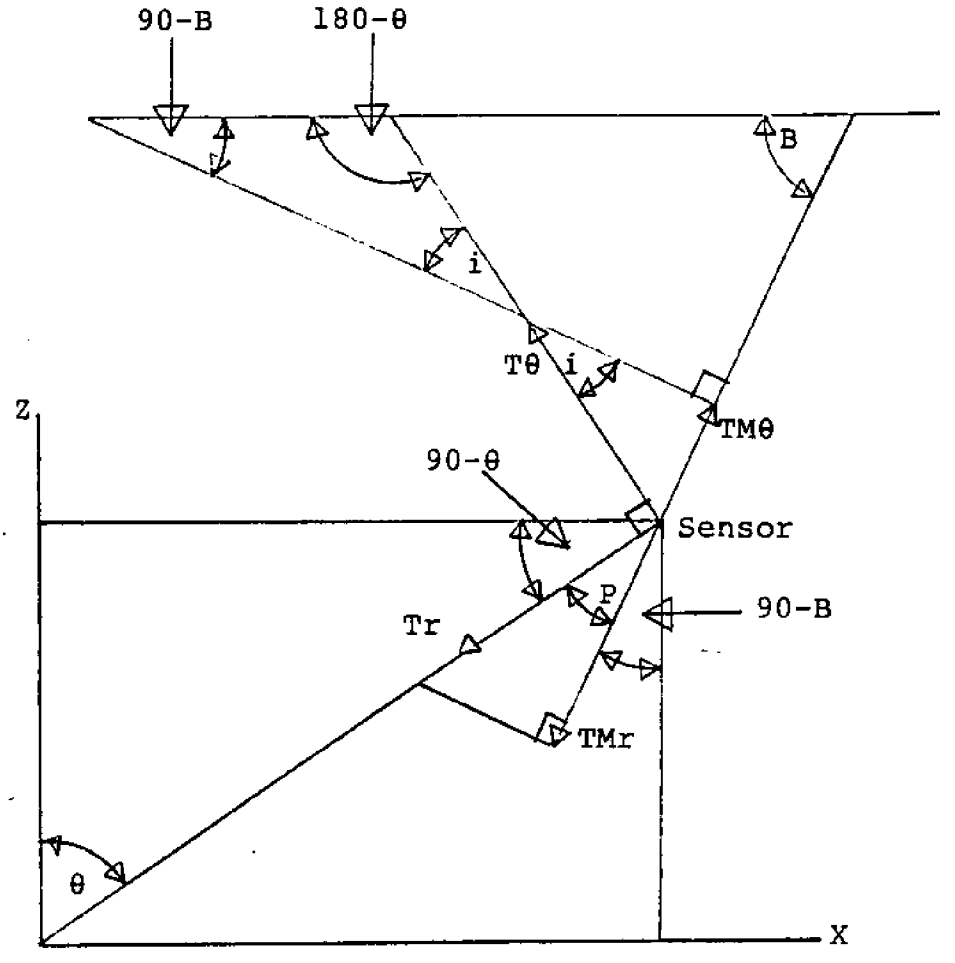

$$i+90^{\circ}-B+180-\theta=180^{\circ}$$

$$i=\theta-90^{\circ}+B$$

$$TM\theta = T\theta \sin(\theta-90^{\circ}+B)$$

$$P+90^{\circ}-\theta+90^{\circ}-B=90^{\circ}$$

$$P=\theta-90^{\circ}+B$$

$$TMr=Tr \cos(\theta-90^{\circ}+B)$$

where B is the angle of inclination of the Earth's magnetic field. Substituting Equations 3.1 and 3.2 into this equation yields:

$$Tm = \frac{M}{r^3} \quad 2\cos\theta\cos(\theta - 90^o + B) - \sin\theta\sin(\theta - 90^o + B)$$

assume for near vertical fields that $\theta = \theta - 90^o + B$, then the result becomes:

$$T_m = \frac{M}{r^3} (3 \cos^2 [\theta - 90^o + B] - 1) \qquad \text{(Eq. 3.6)}$$

where: M = Magnetic moment of dipole

$$r = [x^2 + y^2 + z^2]^{1/2}$$

$$\theta = \arcsin \frac{x}{[x^2 - z^2]^{1/2}} = \arctan \frac{x}{z}$$

A 3 dimensional plot of the signal amplitude (T) in the xy plane at a given depth z would look like Figure 3-2. The values chosen for this plot are $B = 68^o$, $M = 50 \times 10^3$ (cgs), x = 10 feet above the dipole. In order to understand the variation of the signal strength as the sensor altitude above the dipole is varied, T (in gammas) is plotted along the x axis (y = 0) for various altitudes (z) in Figure 3-3 and 3-4 which reveal several important facts as listed below:

1. Peak signal strength (gamma level) decreases with altitude (z).

2. The peak occurs south of the x = 0 location (approximately x = 0.3z).

3. For this angle of inclination, a negative peak occurs just north of the axis crossing.

4. The negative peak is much smaller than the positive peak

Figure 3.2

3D Plot of Eqation 4-6

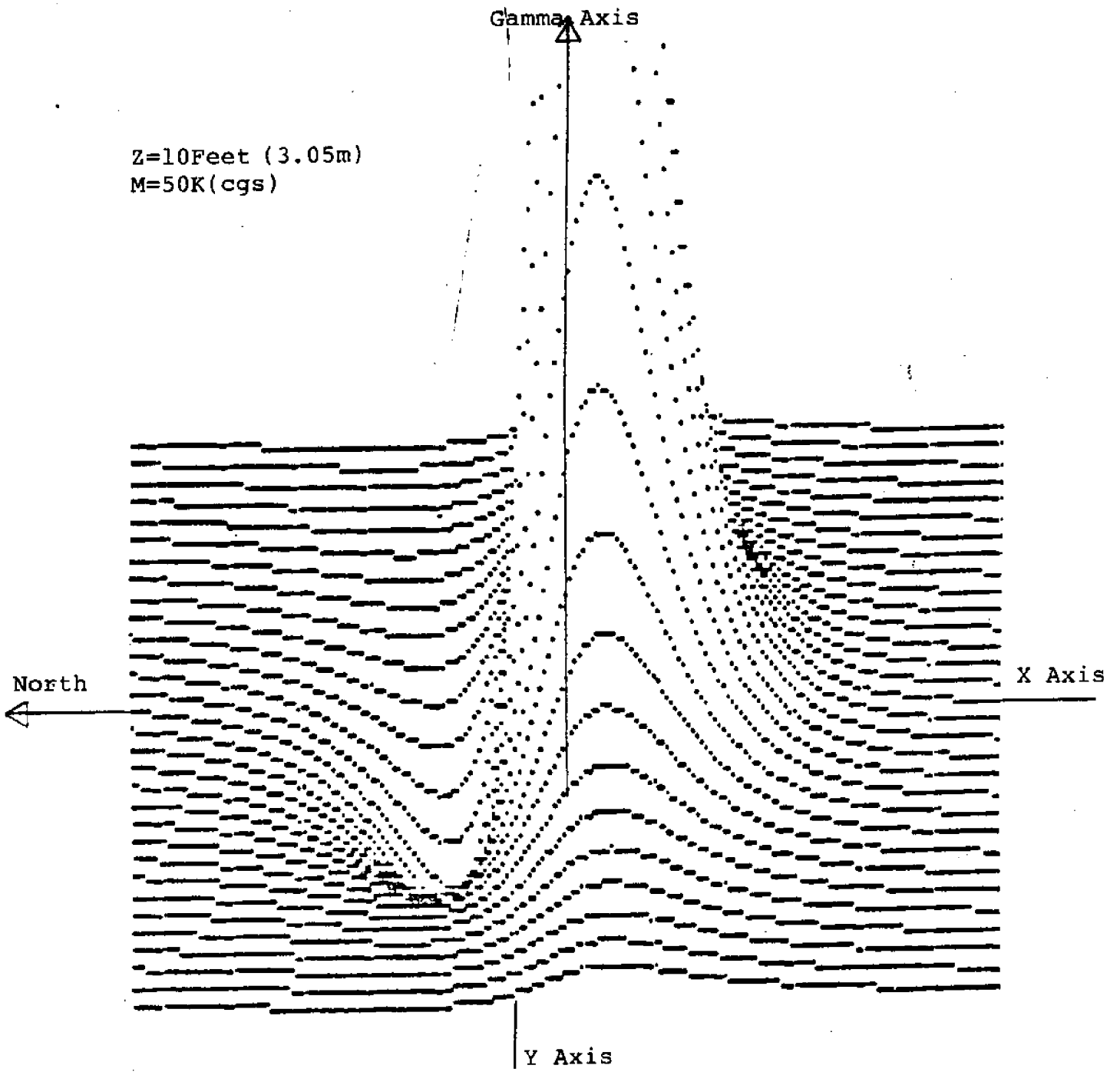

Figure 3.3

Dipole Signature on X Axis.

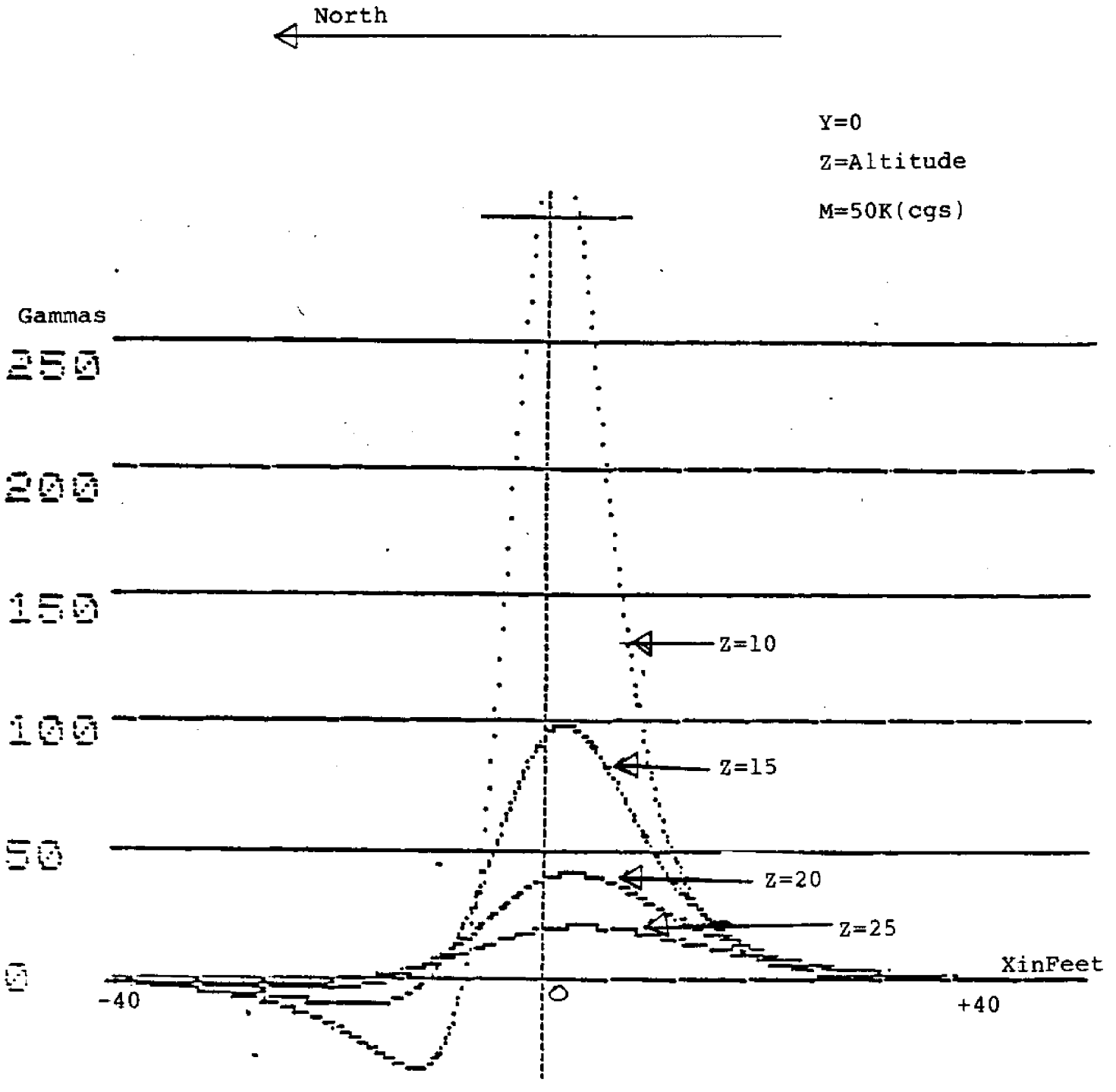

Figure 3.4

Expanded scale of Figure 3.3

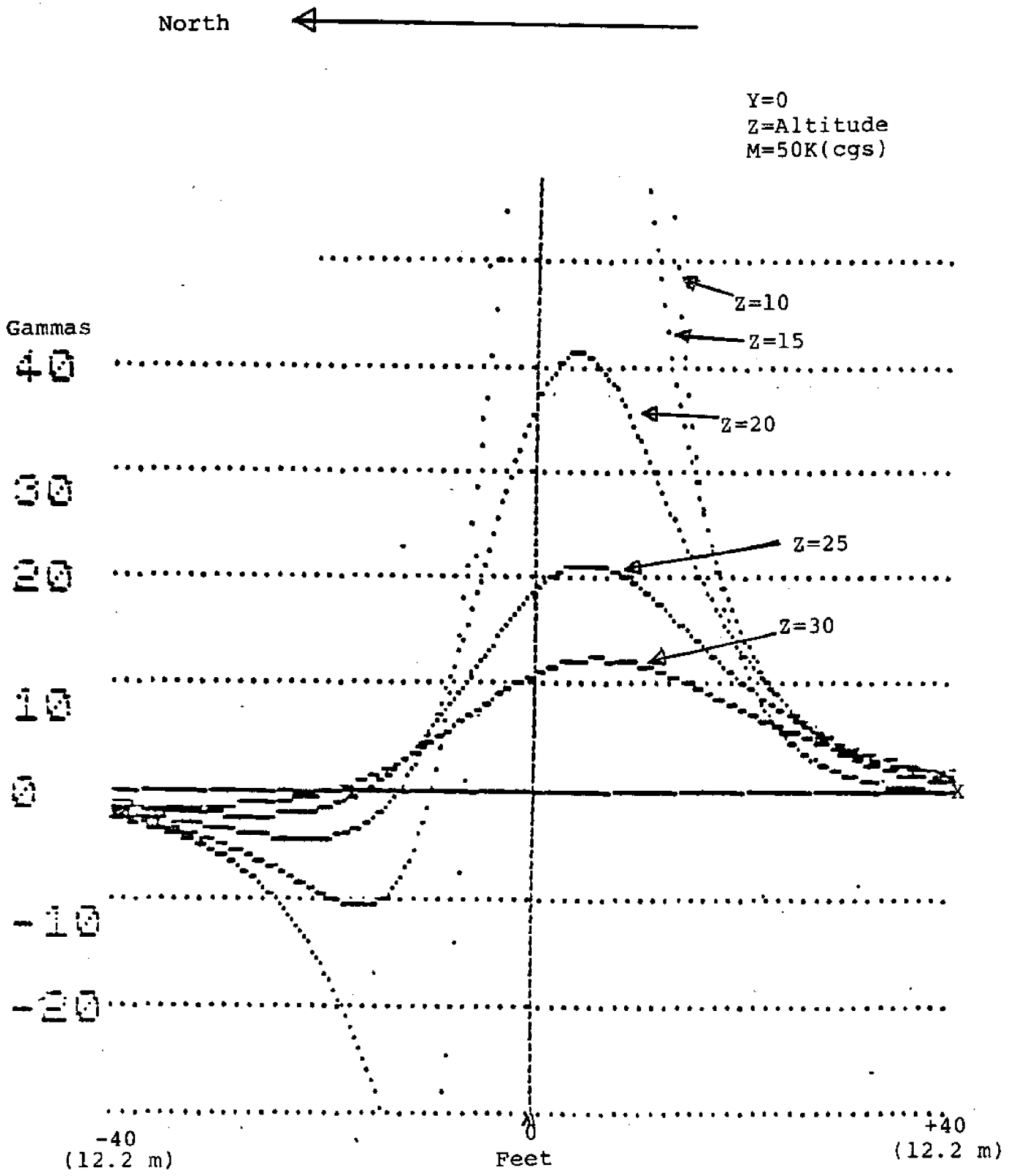

5. As the sensor moves out on the +x axis, the signal takes off from the axis earlier at higher altitudes. This implies an increasing footprint width in the north-south axis with increasing altitude.

Figure 3-5 is a plot along the y axis (x = 0) of the same conditions as above. It is symmetrical in the +y axis. Also notice that the footprint in this axis (E-W) decreases with increasing altitude.

These plots are for an angle of inclination of B = 68°. As B gets larger, the profile on the x axis shows less of a negative excursion and finally at B = 90°, the profile would be symmetrical with no negative excursions. The next phase of this project will include extending this work in Signature/-Anomaly Analysis to include angles of inclination that will encompass using the system anywhere in the world.

3.2.2 Constant Intensity Plots/Interpretation

In order to determine the optimum depth at which to search for magnetic anomalies, as well as the search path to take, lines of constant field intensity have been plotted at several altitudes. These are displayed in Figures 3-6 through 3-11. These plots are also for a dipole of magnetic movement M = 50 k (cgs). It is a simple matter, however, to scale the constant gamma lines for other values M. For example, if a plot was desired for a dipole having a magnetic moment M = 70 k, simply multiply each gamma value on the plot by 1.4 (i.e., 70/50). Inspection of these plots confirms the fact that the footprint decreases in the E-W (y-axis) direction with increasing altitude. It also shown that the footprint in the N-S (x axis increases as altitude is increased initially, but then begins to decrease with higher sensor altitudes.

Figure 3.5

Dipole signature on Y Axis

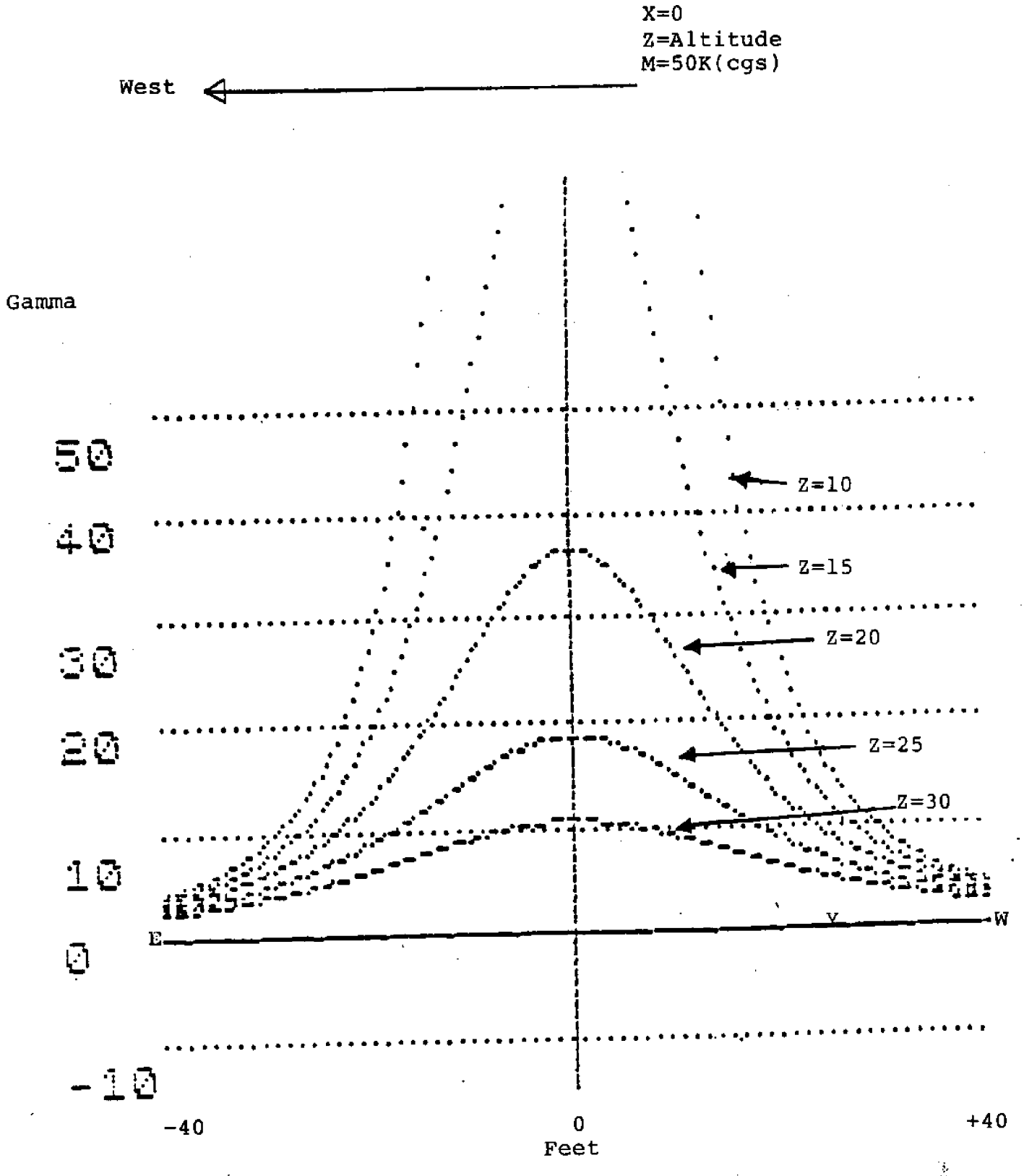

Figure 3.6

Constant intensity plot Z=10 feet

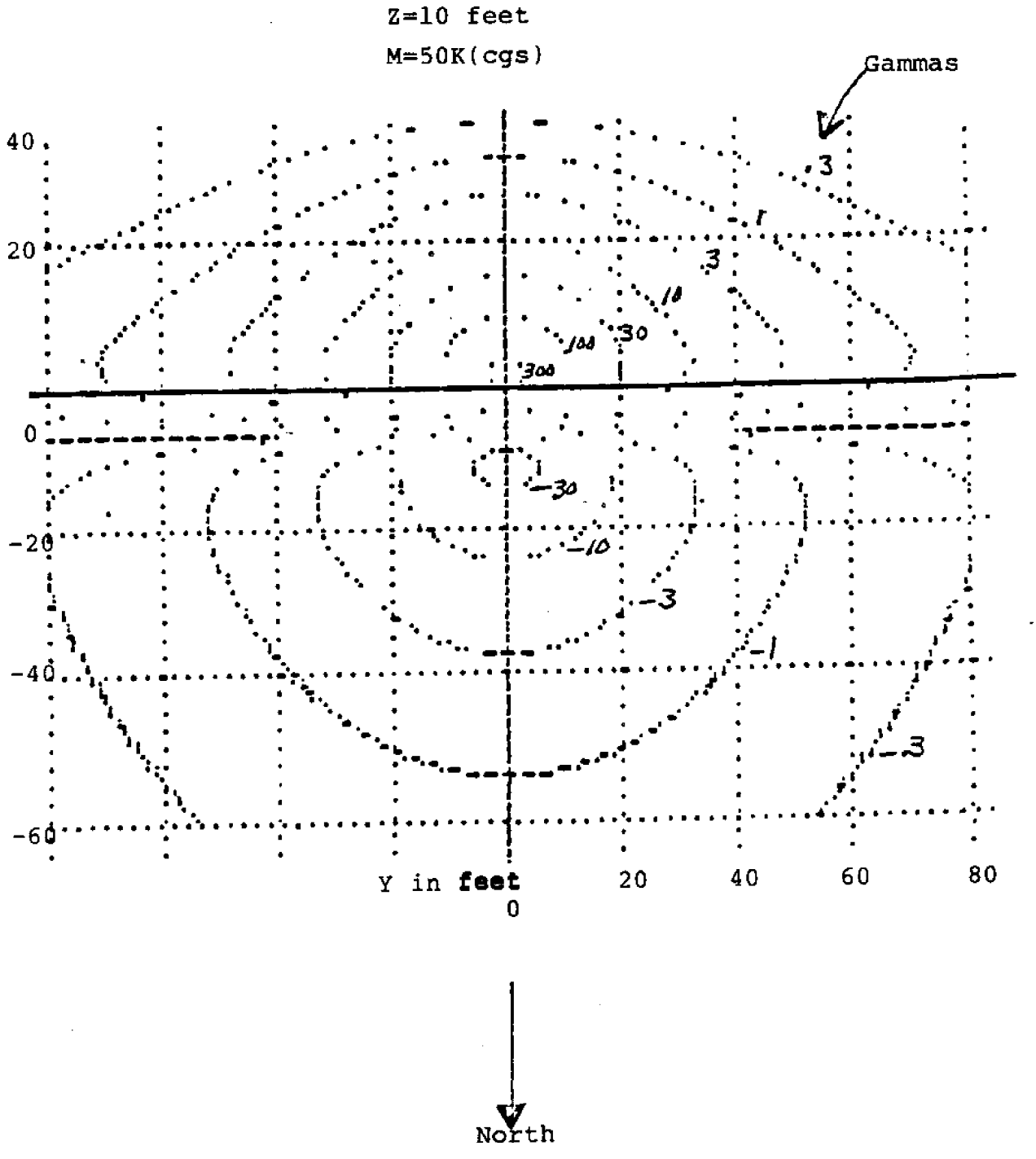

Figure 3.7

Constant intensity plot Z=15 feet

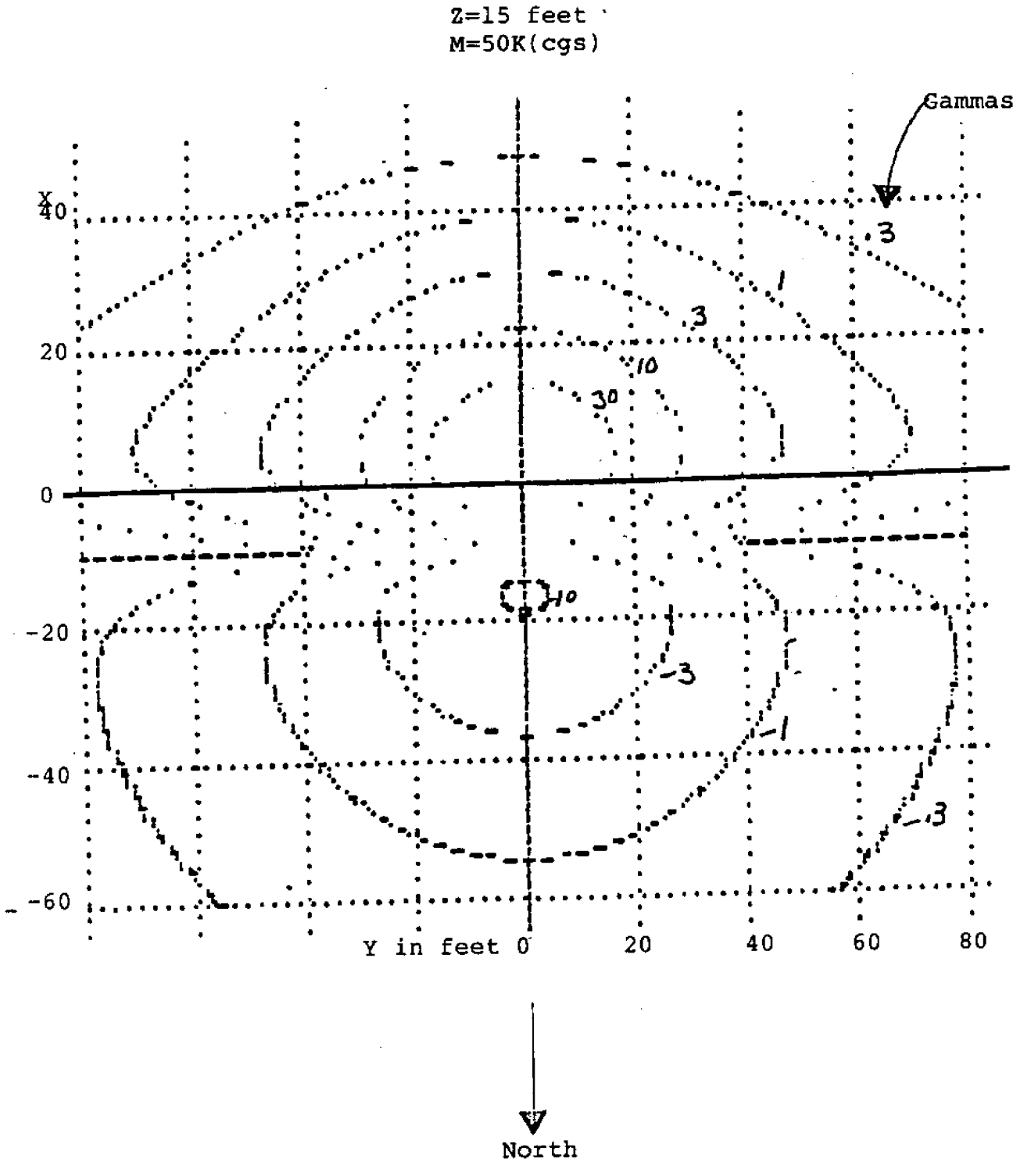

Figure 3.8

Constant intensity plot Z=20 feet

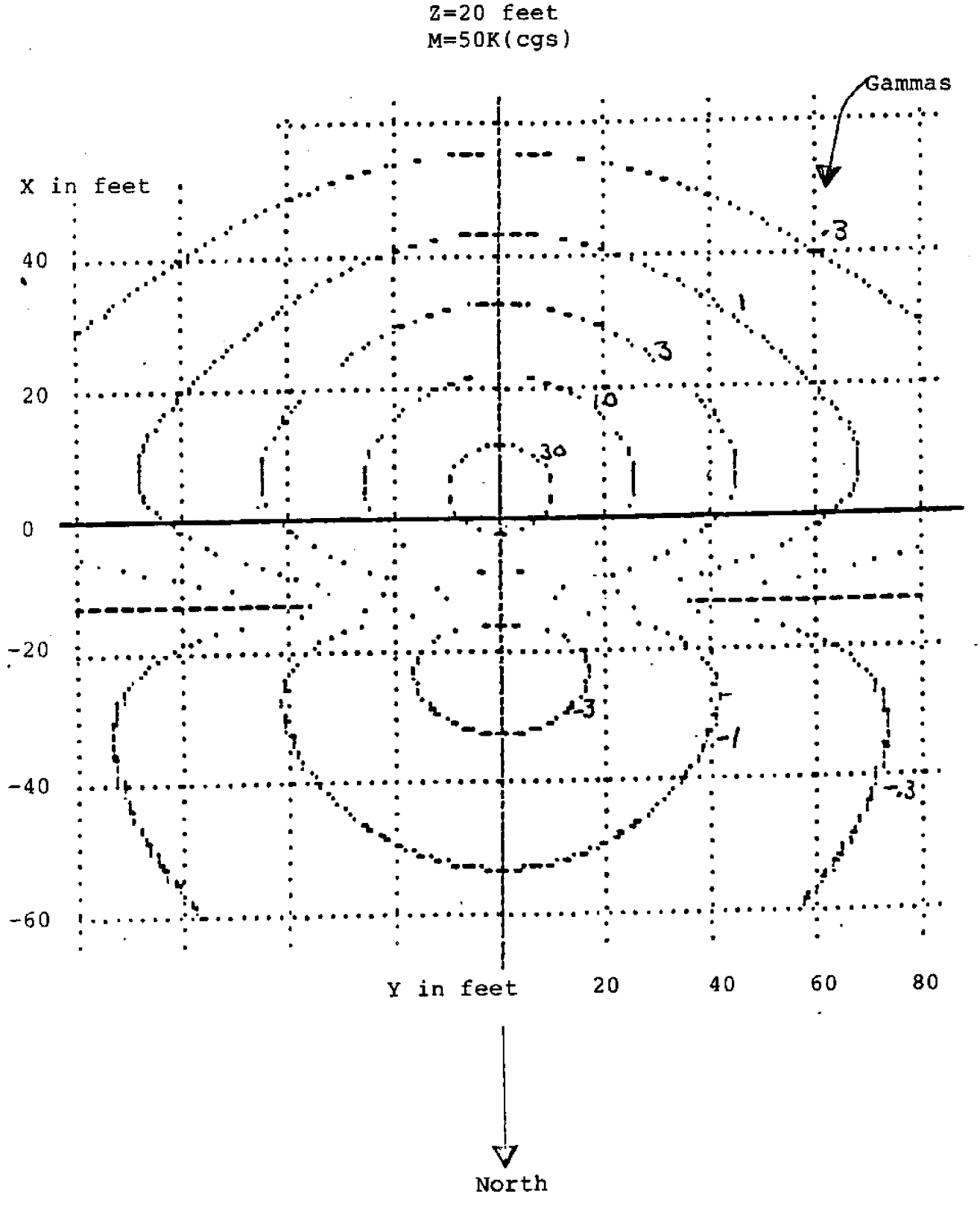

Figure 3.9

Constant intesity plot Z=25 feet

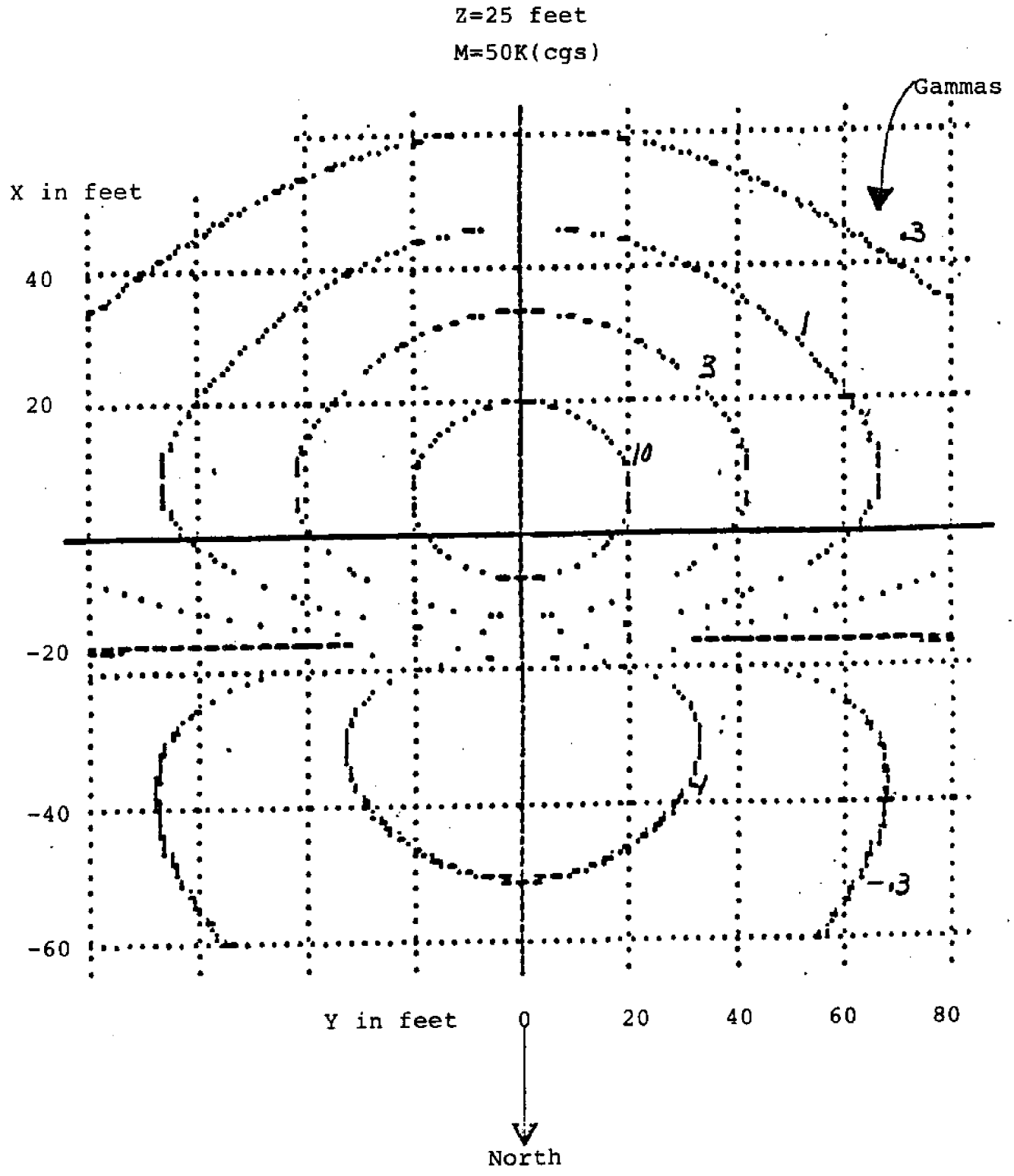

Figure 3.10

Constant intensity plot Z=30 feet

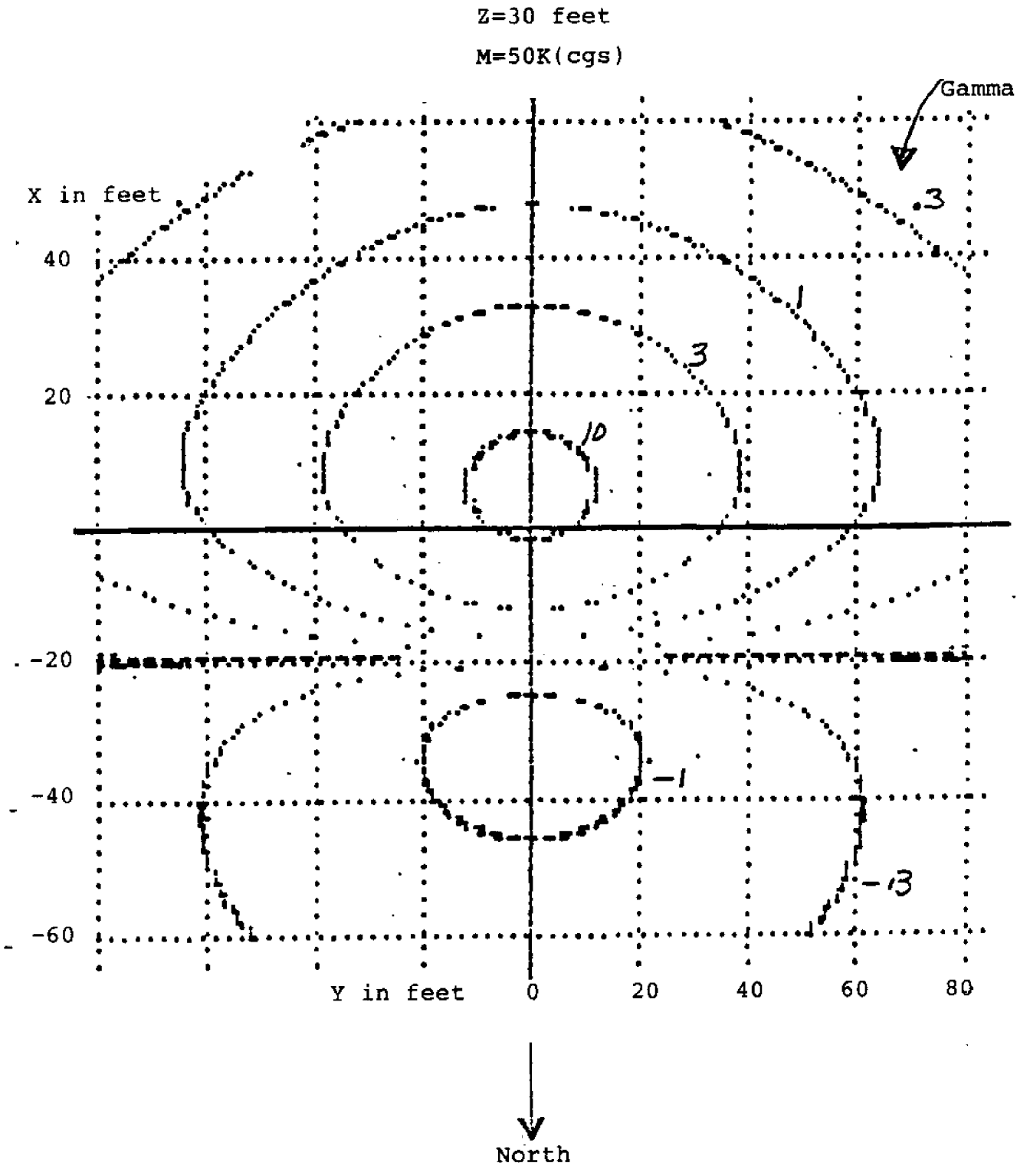

Figure 3.11

Constant intensity plot Z=40 feet

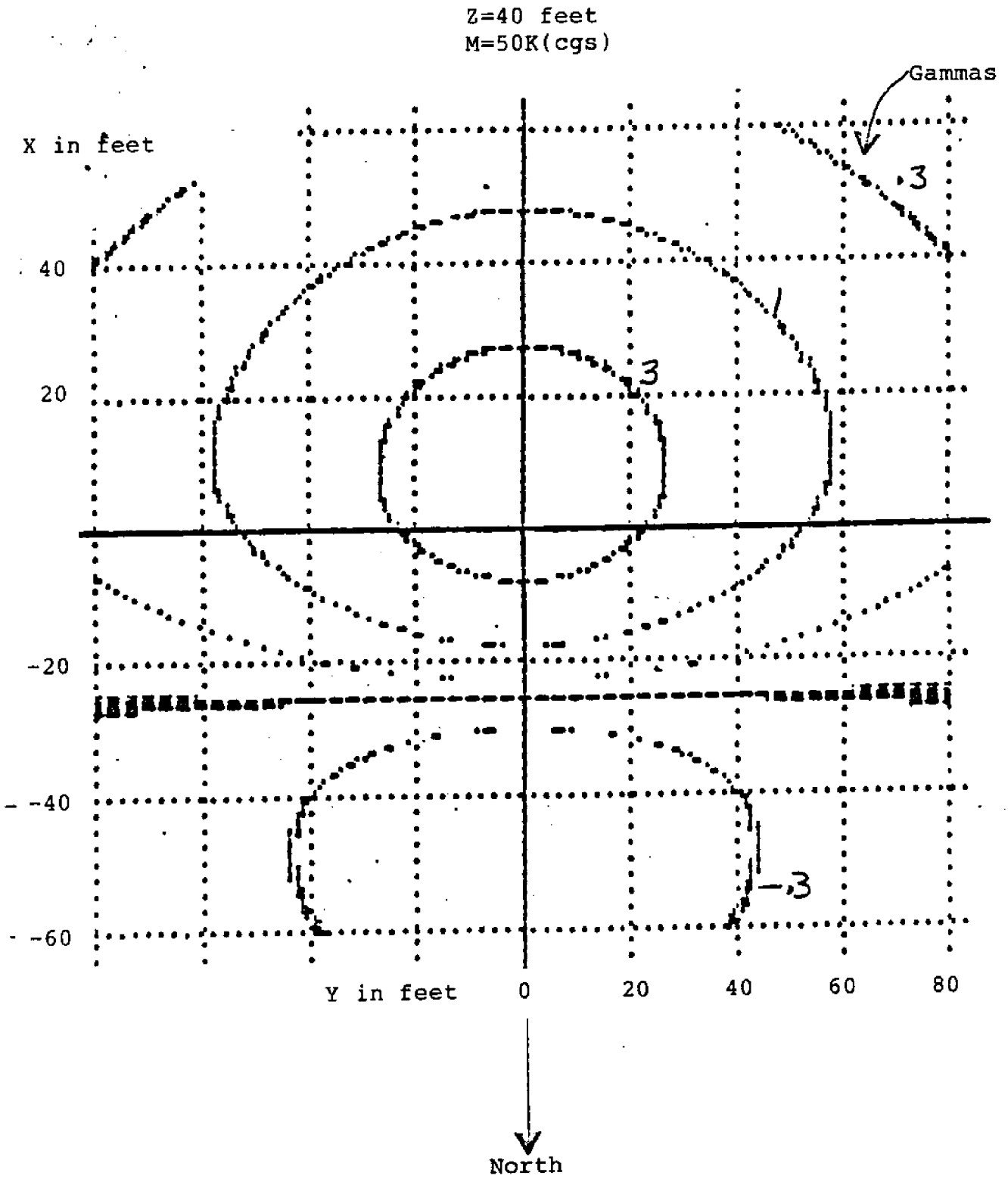

Perhaps a better way to show this is to superimpose constant gamma lines at various altitudes on the same plot. This was done and a sample plot is shown in Figure 3-12 for a 3 gamma signal. This type of representation is very useful in determining both optimum depth and track width or search pattern. This information when combined with system noise and sensor positioning errors provides an excellent tool for search path planning.

3.2.3 Locating the Dipole

There are various well known methods suggested in the literature (References 2,3,4) in regard to locating a target. They all have one thing in common. They are time consuming, manpower intensive and tedious, however, if looking for a few targets and time is not a factor, they can be used successfully.

Since the objective is to locate potentially large numbers of signatures, analyze them and locate their position in a reasonable period of time it is necessary to devise a method of target location which can be implemented in a small computer.

3.2.3.1 A Computer Algorithm to Locate the Dipole

Analyzing the signatures and footprints of a dipole and assuming a N-S search pattern, it becomes obvious that the peak positive gamma reading will occur at a point south of the x axis which is predictable. (See Figure 3-13.) Obviously if the track is not exactly N-S, or the signature is skewed to one side or the other, this will introduce some error, however, the errors should not be very large by comparison with currently used methods. For example if the track was west of North by 20^{o}, the position error in y would be on the

Figure 3.12

Constant intensity plot (3 gamma)

X in feet

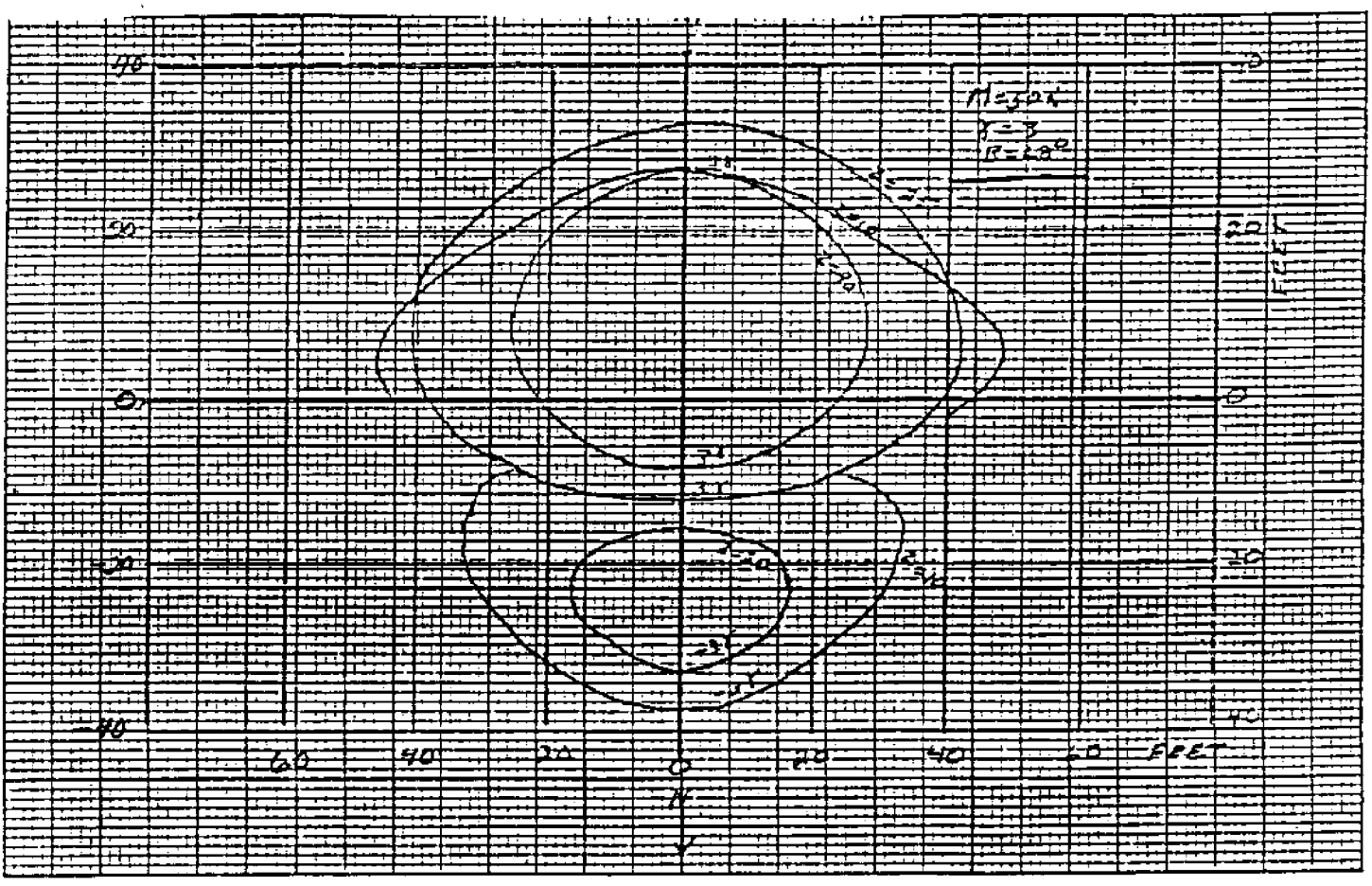

Y in feet

Figure 3.13

20° Offtrack effect on Y value

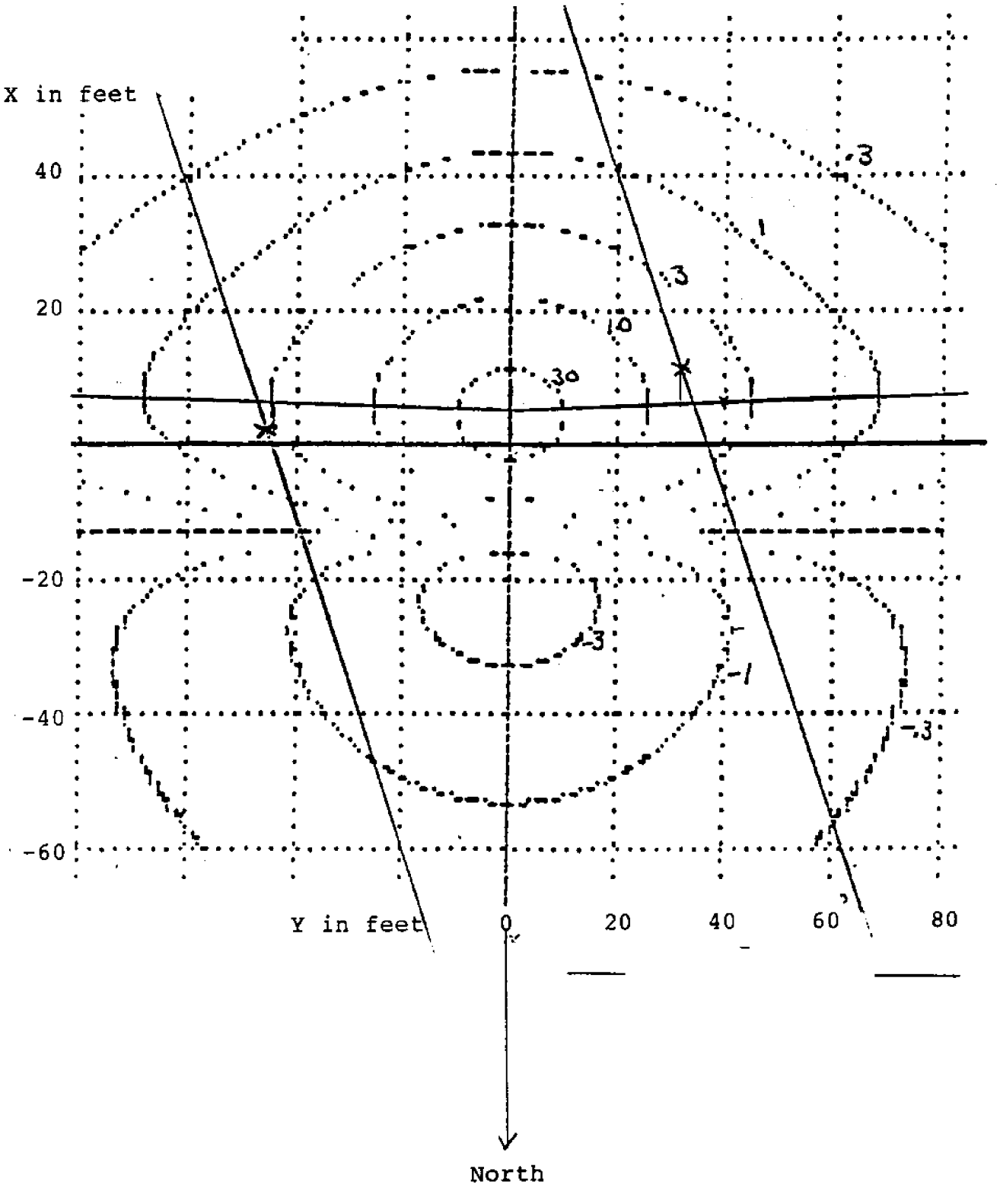

order of a few feet at most. The error discussion is left for now, it will be re-examined when the results of locating targets utilyzing the method have been developed.

Remember that the equation which is used to plot the preceeding signatures and footprints is:

$$T = \frac{M}{r^3} \left(3 \cos^2 (\theta - 90^\circ + B) - 1\right) \qquad \text{(Eq. 3.7)}$$

where $\theta = \arctan \frac{x}{z}$ and $r = (x^2 + y^2 + z^2)^{1/2}$

The peak value of gamma will occur when the angle:

$$\theta - 90^\circ + B = 0$$

Substitution yields:

$$\arctan \frac{x}{z} = 90^\circ - B$$

for our example, $B = 68^\circ$, hence:

$$\arctan \frac{x}{z} = -22^\circ$$

and $x = 0.41\ z$ (Eq. 3.9)

Substituting this value of x into equation 3.7 and solving for y yields:

$$y = +(K - 1.17z^2)^{1/2} \qquad \text{(Eq. 3.10)}$$

where $K = \left(\frac{2M}{T}\right)^{2/3}$

This equation indicates how far the sensor was from the x axis when the peak occurred. Obviously if there is only one detection, the equation yields two possible solutions. If there are at least 2 detections (hits) however, it is relatively easy discriminate against the erroneous solution.

One way to implement this idea when searching for a range of different size (M value) targets is described in the following example.

Assume the search is for dipoles in the range of 25 k to 50 k (M in cgs). The detections in the example occurred as shown in Figure 3-14. First calculate a value of y for hit 1 for M = 25 and M = 50 k and do the same for hit 2. Incidentally, the value of z for the sensor is known within a reasonable error. With this information solve for the intersection in y of the two solutions to determine distance to the dipole's x axis. Once the y value is known, the x values for hit 1 and hit 2 are averaged in the event the track was not exactly N-S or that the actual dipole footprint is skewed. This x value is then translated to the south by the amount 0.41z.

This algorithm works even if both hits are detected to one side of the target. This was proved through inputting of data from the November tests.

As a correllary to the above, it can be seen that having solved for the target location, the algorithm can go back to equation 3.10 and calculate the value of M for the target which yielded the solution, hence there is an indication of target size as well.

Algorithm for Locating a Target

Read input xhit, yhit, z, T T is target strength

$$K_L = \left(\frac{2M_L}{T}\right)^{2/3}$$

M_L is the smallest expected mass

Figure 3.14

Target loction example

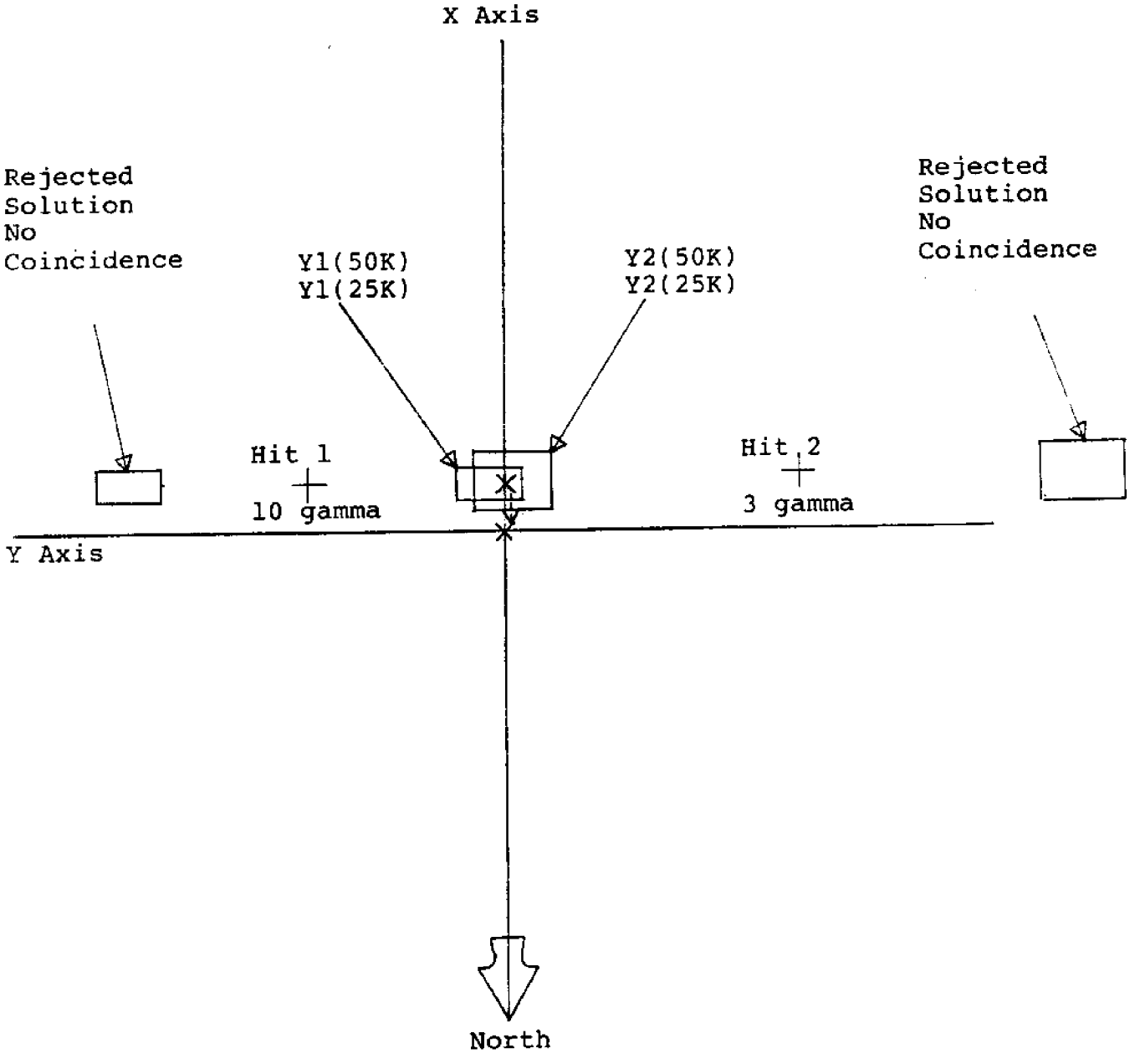

$$K_H = \left(\frac{2M_H}{T}\right)^{2/3}$$

M_H is the largest expected mass

$$yplus1 = yhit + \sqrt{K_L - 1.168z^2}$$

$$yplus2 = y\ hit + \sqrt{K_H - 1.168z^2}$$

$$yminus1 = yhit - \sqrt{K_L - 1.168z^2}$$

$$yminus2 = yhit - \sqrt{K_H - 1.168z^2}$$

yplus = (yplus1 + yplus2)/2

yminus = (yminus1 + yminus2)/2

ytar = (xhit - 0.412)

Do above for 2 "hits"

find minimum difference between 2 sets of

yplus (1)	yminus (1)
yplus (2)	yminus (2)

to find target location

ytar = (y1 + y2)/2

where y1 and y2 are closest

the size is determined after the position is fixed at xtar, ytar, z

$$\text{Size} = \left(\frac{t}{2} \left[(\text{ytar} - \text{hit})^2 + 1.168z^2 \right] \right)^{3/2}$$

NOTE: This algorithm was written for an angle of inclination of 68°, however it will apply within + 10° of B = 68°. The next phase of this project will extend the analysis and algorithm development to a global system.

3.2.3.2 Implementation and Testing of the Algorithm

The above algorithm was implemented with the added feature that if there was no intersection of the solutions (which implies either a value of target magnetic moment outside the range initially selected the value of altitude (z) is in error) the algorithm could increment z downward until it achieved a solution.

Data from a November 1983 search was provided for analysis. The program is given a value of peak gamma and the hit location in x, y, and z for at least 2 hits. The program outputs the target location in x, y coordinates as well as the size of the target which yielded the solution. The value of M in this printout Table 3-2 is the average of both solutions.

The above data results were correlated with the position of known target locations. A tabulation of the known target locations computed by this algorithm is shown in Table 3.3.

Several factors regarding the data used in Table 3.3 are of significance:

1. There is no figure available regarding the accuracy of the actual position of the known targets, therefore it will be difficult to assess the absolute

Table 3.1

Sample printout for Target Location Algorithm

November Data

(More details on this algorithm and its code in 'C' language is presented Appendix A)

```
Wed May 09 11:11:24 1984  targ5  Page 1
```

						Target Name
Data for Target # 101						
xhit = 2077.0	yhit = 1048.0	zhit =	40.0	t =	2.5	
error flag: new z =	38.9					22
xhit = 2077.0	yhit = 1032.0	zhit =	40.0	t =	10.0	
error flag: new z =	24.5					
xtar=2073.1	ytar=1038.8	msize=	52			
Data for Target # 102						
xhit = 2077.0	yhit = 1048.0	zhit =	40.0	t =	2.5	
error flag: new z =	38.9					22
xhit = 2083.0	yhit = 1024.0	zhit =	40.0	t =	2.0	
xtar=2075.2	ytar=1037.4	msize=	60			
Data for Target # 103						
xhit = 2336.0	yhit = 1024.0	zhit =	50.0	t =	2.0	
error flag: new z =	41.9					19
xhit = 2331.0	yhit = 1032.0	zhit =	50.0	t =	2.0	
error flag: new z =	41.9					
xtar=2328.4	ytar=1028.0	msize=	28			
Data for Target # 104						
xhit = 1644.0	yhit = 1058.0	zhit =	20.0	t =	3.0	36
xhit = 1641.0	yhit = 1075.0	zhit =	20.0	t =	17.0	
xtar=1640.0	ytar=1070.8	msize=	42			
Data for Target # 105						
xhit = 1307.0	yhit = 1068.0	zhit =	20.0	t =	26.0	
error flag: new z =	17.8					37
xhit = 1308.0	yhit = 1072.0	zhit =	20.0	t =	19.0	
error flag: new z =	19.8					
xtar=1305.2	ytar=1069.8	msize=	29			

Table 3.2

Estimate of errors

	Target name	Actual Location (meters)		Calculated Location (meters)		Error (meters)		Average Target Strength	Calculated Estimate of Strength	Target Orientation (degrees)
		x	y	x	y	x	y			
November	19	2325	1023	2328	1028	+3	+5	50	28	270 - 90
	21	2173	1087	2181	1087	+8	0	35	76	no info.
	22	2078	1036	2075 2079	1037 1039	-3 +1	+1 +3	70	52 60	vertical
	24	1880	1020	1879	1029	-1	+9	unknown	37	250 - 70
	36	1640	1073	1640	1070	0	-3	70	42	180 - 0
	37	1304	1073	1305	1069	+1	-4	unknown	29	340 - 160
April	28	1528	946	1522	938	-6	-8	70	43	170 - 350
	30	1350	905	1334	900	-16	-5	50	41	45 - 225
	32	1109	915	1105	900	-4	-15	50	45	350 - 170

differences between the position locations and the calculated values of Magnetic Moment. It was estimated that the actual locations are 'probably' within +15 meters.

2. The altitude sonar and the ranging sonar were not operating during the November trials. The depth (z) input to the algorithm is therefore an estimate. The trail calculated for this test was a fixed value estimated by the operators because the sonar ranging systems was inoperable.

3. The sonar ranging system was also not operating for the April trials, hence, once again the trail is a fixed estimate based on tracking over a known target in 2 directions (N-S) (S-N). During the April trials, the magnetometer readings were very erratic, as was the CDD depth control.

3.2.3.3 Analysis and Conclusions Derived from the Algorithm Generated Data

The calculated target locations for the November data correlates very well with the actual locations. The errors in x average less than 3 meters and the error average in y is less than 4 meters.

Targets can be located even if both hits are to one side of the target. The average error for the April trials are typically 9 meters in x and 9 meters in y. Based largely on the November data (since the April data is suspect) it is obvious that the target location algorithm can indeed by used to locate targets electronically.

Incidentally, the targets used in these tests varied in orientation over the entire 360° spectrum which would indicate that the footprints of the real target must have the general orientation and shape of the model footprint. Because the model assumes a very small or near point source, however, it is expected that the field of the real targets is somewhat distorted relative to the model since it is utilizing measurements taken within 5 or 10 lengths of its dimensions. This does not, however, seem to invalidate the algorithm's ability to locate the target.

In analyzing the algorithm's ability to approximate the target strength, the estimate appears to be low with the exception of one particular type of target (the 35K target). The fact that the estimate is on average about 30% lower than the actual value indicates that the width of the model's footprint (E-W) is probably larger than the footprint of a real target. It should be possible by conducting more tests to acquire sufficient data which could be used to modify the algorithm in such a way that its estimate of size of target would be much closer to the real value.

The procedures and results of this set of analyses were reviewed in comparison to the detailed magnetic signature measurements made by the Naval Coastal Systems laboratory (NCSL) (Reference 1) over twenty years ago. The nature of the algorithm developed herein appears to be fully capable of localizing and measuring the magnetic moment of any of the potential targets of interest. It should be noted that search patterns in the E-W direction versus the N-S produce significantly different sensed data. However, algorithms can be developed that are a function of search track orientation.

It should be noted that the NCSL concludes that the measurement of the vertical gradient of the anomaly provides the best data on magnetic moment of the object regardless of object orientation or search track angle. This vector component also works for monopoles as well as dipoles.

It should also be noted that implementation of this algorithm requires that two hits be made on the object. Without at least two, the solution becomes both ambiguous and much looser in measuring magnetic moment. The two hit criteria sets the allowable track separation quite close and limits area search rates.

A single hit system utilizing multiple axis gradiometers is the subject of the next phase of this program.

3.2.3.4 A Computer Algorithm To Correlate A List of Hits Into Groups

The current method of correlating hits to specific targets is described in Section 2.2 Essentially, the data is plotted on an x, y plotter and the analyst has to attempt to group the hits visually. This is very time consuming and prone to error.

Having described the iso-intensity footprints in some detail, a logical step was to determine whether the parameters of these plots could be used to mathematically sort and group the large number of hits which are typically seen during a search.

A list of hits from the November trial is shown in Table 3-4 below. If we check the minimum signal amplitude detected during this trial namely 1 gamma, and inspect our iso-intensity plots, we can arrive at a y axis footprint for 1 gamma of approximately 41 meters for sensor altitude of 25 feet and

Table 3.3

NOVEMBER 1983
TRIAL DATA

Name	Frac	Trail	Y	X_1	Y_1	X_2	Y_2
1A4	0.36	81.3	4	1884	1015	1518	1014
1B4	0.36	81.3	4	1560	1013	1689	1015
2A4	0.52	81.3	2	2297	1023	2180	1026
2B4	0.70	81.3	7	2064	1026	1945	1022
2C4	0.71	81.3	6	1869	1025	1756	1024
2D4	0.48	81.3	2	1565	1026	1451	1026
2E4	0.58	81.3	4	1490	1026	1372	1024
2F4	0.51	81.3	4	1296	1023	1176	1025
2G4	0.53	81.3	3	1175	1025	1067	1025
2H4	0.50	81.3	4	943	1024	825	1023
2I4	0.47	81.3	3	865	1023	745	1022
3A4	0.33	81.3	7	1995	1038	1532	1036
3B4	0.32	81.3	2	1486	1035	1566	1034
3C4	0.32	81.3	1	1608	1037	1726	1035
3D4	0.49	81.3	7	1929	1032	2087	1037
3E4	0.44	81.3	10	2116	1031	2231	1033
3F4	0.29	81.3	2	2887	1030	2505	1034
4B4	0.34	81.3	7	1519	1048	1796	1044
4C4	0.36	81.3	25	1879	1046	1756	1040
4D4	0.62	81.3	1	1598	1038	1476	1046
4E4	0.31	81.3	1	1515	1046	1397	1046
4F4	0.18	81.3	1	1476	1046	1357	1040
4G4	0.42	81.3	1	1476	1046	1357	1040
4H4	0.17	81.3	1	1397	1046	1277	1040
4I4	0.20	81.3	1	1318	1037	1197	1046
6D4	0.42	81.3	5	1600	1058	1483	1058
4K4	0.44	81.3	1	1157	1046	1035	1041
6F4	0.42	81.3	36	1257	1068	1145	1068
5A4	0.36	81.3	3	1218	1055	1341	1053
5B4	0.27	81.3	4	1506	1053	1630	1057
5C4	0.51	81.3	23	1954	1054	2078	1057
5D4	0.37	81.3	78	2037	1055	2158	1057
5E4	0.40	81.3	3	2513	1056	2635	1052
6A4	0.61	81.3	5	2313	1066	2200	1067
6B4	0.33	81.3	1	2163	1064	2048	1066
6C4	0.67	81.3	47	1978	1064	1860	1060
6E4	0.44	81.3	4	1403	1068	1292	1069
7A4	0.39	81.3	19	1350	1072	1488	1071
7B4	0.21	81.3	17	1709	1075	1831	1075
7C4	0.42	81.3	3	1950	1077	2067	1076
7D4	0.37	81.3	1	2028	1076	2145	1074
7E4	0.50	81.3	2	2028	1076	2145	1074
7F4	0.57	81.3	12	2145	1074	2263	1080
7G4	0.47	81.3	9	2223	1080	2345	1076
7H4	0.33	81.3	23	2286	1076	2505	1073
7I4	0.39	81.3	3	2464	1075	2584	1073
8A4	0.27	81.3	3	1814	1083	1430	1087
8B4	0.39	81.3	5	1952	1082	1467	1081
8C4	0.26	81.3	2	1883	1086	1504	1081
8D4	0.30	81.3	5	1701	1081	1822	1087
8E4	0.54	81.3	17	2144	1088	2258	1082
8F4	0.31	81.3	92	2218	1085	2339	1086
8G4	0.47	81.3	4	2375	1089	2493	1087
8H4	0.33	81.3	1	2493	1087	2605	1082
6A4	0.32	81.3	20	1218	1100	1319	1097
9E4	0.39	81.3	6	2185	1092	2294	1097
9H4	0.50	81.3	6	2523	1097	2645	1099
4M4	0.52	81.3	65	2510	1040	2395	1045
4J4	0.30	81.3	2	1277	1040	1157	1046
4L4	0.29	81.3	7	1085	1041	909	1045
9F4	0.49	81.3	5	2223	1097	2332	1097
9G4	0.28	81.3	2	2423	1100	2606	1100

END

above as it was in the November trial. If we look at the x axis variation where the peak gamma occurs, we find that this value occurs within 1 or 2 meters even for boat tracks off N-S line by 20 degrees. Because we suspect errors in trail calculation as well as other sources of position error we chose a correlation value along the x axis of 7 meters.

The procedures for sorting hits is quite straightforward.

First the hits are placed in descending order of x position.

Next a comparison of the x position is made on each entry using the value of 7 meters to establish correlation with a group.

All the hits are grouped according to x location and the values which do not correlate are discarded.

Within each group the sorting proceeds to determine which y values fall within the 41 meter range.

Once all the data is sorted, the algorithm outputs a table (see Table 3-5) in which hits are grouped to a target. The algorithm also outputs the values of x, y location and peak gamma for each hit.

The output in Table 3-5 is the actual output from an algorithm implemented in 'C' language and the input was the data from the November trials.

Analysis of the groupings revealed that the algorithm grouped the data perfectly. The only errors which occurred were due to errors in manually inputting the table to the computer.

Table 3.3

Name	X_{LDC}	Y_{LDC}	y'	
9C4	2428.5	1100.0	2.0	Group 1
8H4	2425.5	1084.5	1.0	
8C4	2387.7	1086.0	4.0	
6A4	2387.4	1066.5	3.0	Group 2
7H4	2382.0	1076.0	25.0	
2A4	2329.5	1024.5	2.0	Group 3
3F4	2327.9	1032.0	2.0	
7C4	2187.0	1078.0	9.0	Group 4
9F4	2182.6	1087.0	5.0	
7F4	2119.0	1077.0	13.0	Group 5
8E4	2112.3	1085.0	17.0	
2B4	2074.0	1024.0	3.0	Group 6
3E4	2073.3	1032.0	10.0	
7E4	1993.3	1075.0	2.0	
6C4	1990.6	1052.0	47.0	Group 7
5D4	1988.5	1056.0	28.0	
4C4	1928.0	1048.0	26.0	Group 8
5C4	1923.9	1055.5	23.0	
3D4	1884.0	1034.5	7.0	Group 9
2C4	1882.1	1024.5	6.0	
6D4	1644.2	1058.0	3.0	
8D4	1644.0	1084.0	3.0	Group 10
7E4	1641.3	1075.0	17.0	
4D4	1615.7	1042.0	1.0	Group 11
2D4	1609.3	1026.0	2.0	
3C4	1552.5	1036.0	1.0	Group 12
4F4	1547.9	1043.0	1.0	
4C4	1519.5	1048.0	1.0	
2E4	1514.9	1025.0	4.0	Group 13
1B4	1513.1	1014.0	4.0	
6E4	1448.6	1058.5	4.0	Group 14
5B4	1446.3	1056.0	4.0	
4I4	1387.9	1041.5	1.0	Group 15
3B4	1384.4	1004.5	2.0	
1A4	1338.9	1014.5	4.0	Group 16
4J4	1334.3	1048.0	2.0	
3A4	1329.6	1037.0	2.0	Group 17
2F4	1328.1	1024.0	4.0	
8E4	1303.5	1081.5	3.0	Group 18
6F4	1303.3	1068.0	26.0	
7A4	1302.7	1071.5	19.0	

OUTPUT OF CORRELATION ALGORITHM

More details on this algorithm and its code in 'C' language is presented Appendix B.

Note: The values of x and y listed in Table 3-4 were found to be incorrect due to an error in the trail estimate from the November test. A correction for this erroneous trail estimate by 12 meters was included in the beginning of our sorting algorithm.

As a final note, it is obvious that the output of this algorithm can be input into the algorithm to locate targets described earlier. This combination would provide a means of sorting hits, grouping hits and finally providing locations of targets for each group of hits. This would provide for great savings in time of data analysis and is as accurate as the best of operators.

3.2.4 Time Variations in the Earth's Magnetic Field

In addition to the spatial variations of the Earth's magnetic field there are also time variations. They are due to the effects of the solar wind and are divided into three types: daily (diurnal) variations, micropulsations, and magnetic storms.

Diurnal variations are seen largely during daylight hours and can vary by as much as 100 gammas over a period of a few hours.

Micropulsations are much shorter period variations and are quite random. They can range from 0.01 seconds up to several tens of minutes in length, and can have gamma amplitudes from several tens of gammas to thousands.

Magnetic storms can occur several times per month, have periods of one to several days, and can have gamma variation s of several hundred.

These variations are superimposed upon, and distort the Earth's magnetic field. They are mentioned here simply to indicate that any magnetometer system will have to discriminate against them in order to successfully detect target anomalies. Time correlated reference magnetometers and or various techniques of data processing can be used for this purpose.

The typical total anomaly signature at speeds of 5 knots would occur in a time period of 1 to 3 seconds with the fastest portion of the signature (fastest slope) occurring in approximately 0.2 to 0.6 seconds depending on the track over the target.

CHAPTER 4

SENSOR POSITION MEASUREMENT

4.0 Introduction

One of the most critical aspects of detecting anomalies is knowing the exact location of the sensor at all times during a survey. The error in position of the sensor obviously causes a corresponding error in determining the target location. There are several sources of this sensor position error. They will be discussed here with the objective of providing a tabulation of errors due to these sources.

Chapter 5 will present suggested methods to reduce or eliminate these errors.

4.1 Sources of Error - Magnetometer Location

The following sources of error are present in the current magnetometer system and are analyzed to determine their magnitude and effects on the system.

1. Crab Error - Wind and Sea Effects on Boat Angle:
   In order for the boat to maintain a straight course in a cross wind and or cross current, the boat must take a heading that is not aligned with the desired track. The crab angle results in the magnetometer being off track compared to its calculated position.

2. Cross Current Effects on Cable and Instruments:
   Cross currents cause an error displacement of the magnetometer in the y direction (assuming a course in the x direction).

3. Error Due to Trail Calculation:
   When the slant range measurement system is non-operational, a horizontal trail calculation is experimentally determined and assumed constant over

the entire search area. Since the CDD is tracking a fixed altitude above the ocean floor the horizontal trail does vary as water depth changes. This causes an error in the along track (x axis) location of the magnetometer.

4. Slant Range Sonar Beam Angle:
When the sonar system is working, it has a 15° conical beam. This beam angle is fixed but the CDD is moving vertically and can also be offset in the horizontal plane by a significant amount. An analytical correlation between cable scope, sonar aiming angle and desired sensor depth can be used to keep the CDD within the beam (Table 5-4).

5. Piloting Error:
This is due to inability to maintain the desired boat track. Trial data is investigated to determine the size of this error.

6. Navigation Error:
This is the result of accuracy limits of the land based radio navigation system used to determine boat position.

4.1.1 Crab Error - Wind and Current Effects on Boat/Magnetometer

In order to stay on a straight course while in a wind or current the boat may need to crab. Consider the boat crabbing at an angle θ to the desired track (See Figure 4-1).

The error in the x and y direction, Ex and Ey, will depend on the distance between the navigation antenna and the tow point lb and the crabbing angle θ. This error is calculated as follows:

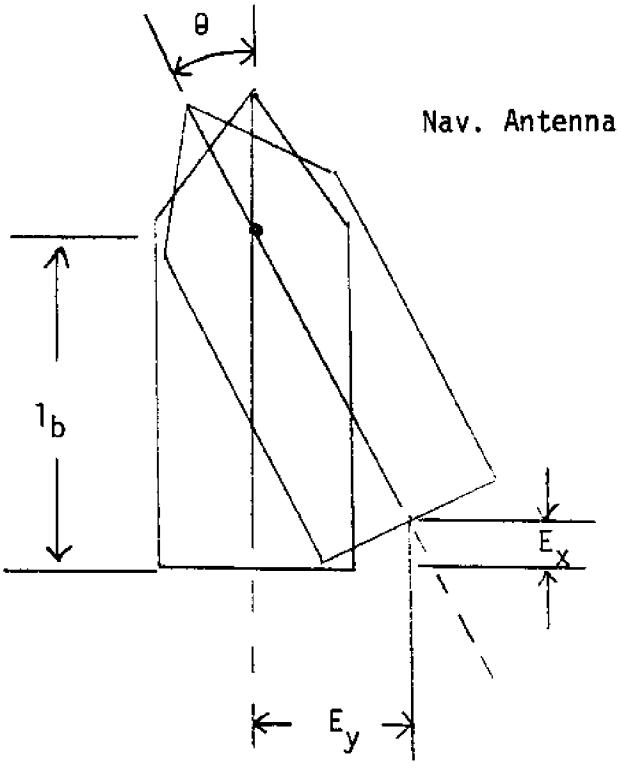

FIGURE 4-1 Boat Crab Error Geometry

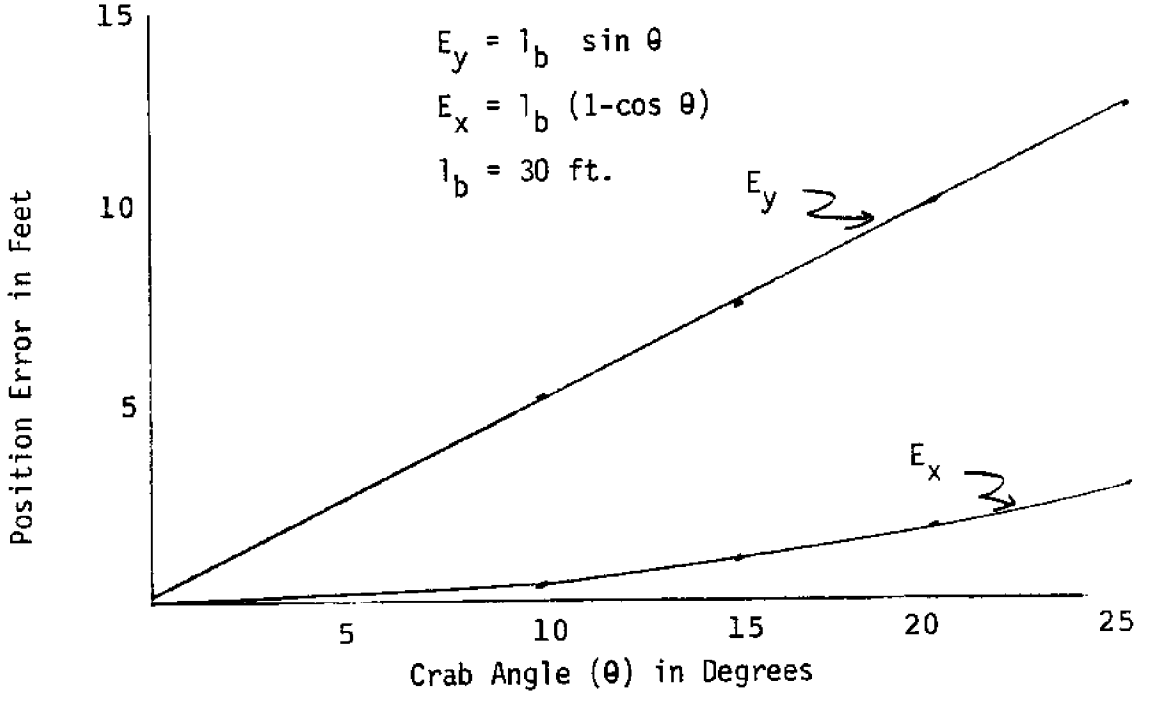

$$E_y = l_b \sin\theta \qquad \text{(Eq. 4.1)}$$

$$E_x = l_b \ (1 - \cos\theta) \qquad \text{(Eq. 4.2)}$$

if we assume an antenna to tow point separation of 30 feet and a crabbing angle of 15°, the resulting errors are:

E_y = 7.77 ft. (off track error)

E_x = 1.02 ft. (on track error)

The relationship between crab angle and the resulting error is shown in the graph in Figure 4-1. The numbers correspond to a 30 foot separation distance. For a larger boat the errors would be greater.

4.1.2 Cross Current Effects on Cable and Instruments

A cross current will result in a y displacement of the tow cables and instruments. The drag force on a 300 foot cable contributes the better part of the total displacement. Any drag force is given by the equation:

$$F_D = 1/2 \ C_D \ pAV^2 \qquad \text{(Eq. 4.3)}$$

Let R_y and R_x be the drag force per unit length of the cable when the cable is normal to the stream. For example: a 1/2 inch cable with a normal stream velocity of 4.5k will produce a drag force of:

$$F_D = 1/2 \ C_D pAV^2 = 1/2(1.2)(1.9885) \ \frac{(1/2 \text{ in})(12\text{in})}{144 \text{ in}^2/\text{ft}^2} \ [(4.5\text{k})(1.68\text{ft/s/k})]^2$$

F_D = 2.84 lb

The total y displacement can be obtained using the equilibrium equation summation of $F_y = 0$. The lateral force, (the drag force on the total length of the cables in the water) is countered by the drag force on the amount of cable protruding normal to the stream (See Figure 4-2).

so: $(Ry)Lc = (Rx)y$ where Lc is the cable length:

$$u = \frac{Ry}{Rx} Lc = \frac{1/2\ C_D PAVc^2}{1/2\ C_D PAV_B^2} Lc$$

This yields: $$Y = \left(\frac{Vc}{VB}\right)^2 Lc$$ Error due to cable (Eq. 4.4)

To find the displacement due to the CDD and the tow fish, we again use the equilibrium equation summation $F_y = 0$: (See Figure 4-2).

$$F_{Dx} = R_x y \qquad \text{(Eq. 4.5)}$$

$$\text{or} \quad y = \frac{F_{Dx}}{Rx}$$

where F_{dx} is the drag force on the instrument due to the cross current. This is of course dependent on the cross current velocity. Thus, the total y displacement due to a cross current is given by:

$$y = \left(\frac{V_C}{V_B}\right)^2 (L_{C1} + L_{C2}) + \frac{(F_{Dx})_{CDD} + (F_{Dx})\ \text{Tow Fish}}{Rx} \qquad \text{(Eq. 4.6)}$$

Substituting Eq. 4.3 into Eq. 4.6 yields the following:

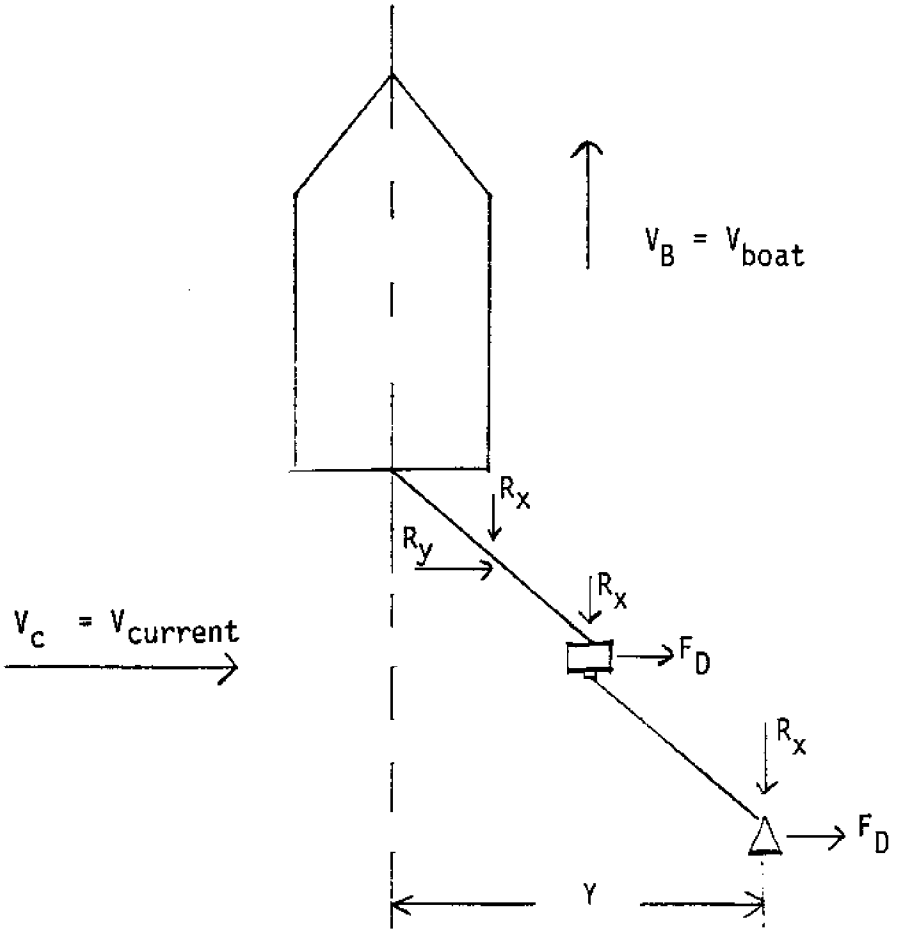

FIGURE 4-2 Cross Current Error Geometry (y)

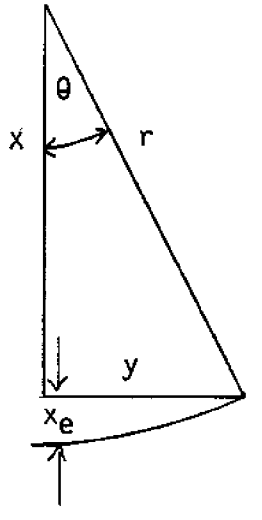

FIGURE 4-3 More Geometry (x) Error

$$\left\{ \frac{(F_{Dx})\ \text{CDD} + (F_{Dx})\ \text{Tow Fish}}{1/2 C_D\ PA_T\ V_B^2} = \frac{1/2\ PC_D\ A_{CDD}\ V_c^2 + 1/2 PC_D A_{TF}}{1/2 C_D\ PA\perp\ V_B^2} \right\}^V$$

$$\frac{(F_{DX})\text{CDD} + (F_{DX})\ \text{Tow Fish}}{Rx} = \frac{V_C^2\ (A_{CDD} + A_{TF})}{A\perp\ V_B^2}$$

since all the coefficients of drag and densities are equal. The off axis (y) error due to cross current effects on the CDD and the tow fish are shown in Eq. 4.7 where the y displacement error becomes:

$$y = \left(\frac{V_C}{V_B}\right)^2 (L_{C1} + L_{C2}) V_C + \frac{(A_{CDD} + A_{\text{Tow Fish}})}{V_B^2 A\perp} \quad \text{(Eq. 4.7)}$$

Total error due to cable, CDD and towfish

where V_C = velocity of cross current

V_B = velocity of boat

L_{C1} = length of cable connecting CDD to boat

L_{C2} = length of cable connecting towfish to CDD

(F_{Dx})CDD or towfish = instrument's drag force due to cross current AT cross current's normal velocity

Rx = drag force per unit length of the cable when the cable is normal to the stream. Stream velocity is boat speed

$A\perp$ = area per unit length of cable perpendicular to flow

NOTE: The total area of the instruments normal to a cross current stream is:

A_x CDD = 4.282 ft^2

A_x towfish = 3.25 ft^2

If the cross current creates a y displacement, a displacement in the x direction will also result. Note the triangle in Figure 4-3. Using x_e to represent the error in the x direction, the on axis (x) error due to cross current is given by:

$$x_e = r - (r^2 - y^2)^{1/2} \qquad \text{(Eq. 4.8)}$$

where $r = L_{C1} + L_{C2}$

EXAMPLE CALCULATION

In order to understand the magnitude of these errors we offer the following example. The assumptions made are as follows:

$V_B = 4.5k$
$V_C = 0.6k$
$L_{C1} = 300$ ft.
$L_{C2} = 300$ ft.
1/2" cable

Therefore:

$$y = \left(\frac{V_C}{V_B}\right)^2 (L_{C1} + L_{C2}) = \frac{V_C^2 (A_{CDD} + A_{TF})}{V_B^2 A_1}$$

$$y = \left(\frac{0.6K}{4.5K}\right)^2 (330 \text{ ft.}) + \frac{(0.6K)^2 (4.3 \text{ ft}^2 + 3.25 \text{ ft}^2)}{(4.5K)^2 \dfrac{(1/2 \text{ in})(12 \text{ in})}{\dfrac{144 \text{ in}^2}{\text{ft}^2}}}$$

$y = 9.2$ ft. Error in y axis under sample conditions

$$xe = r - \sqrt{r^2 - y^2} \quad \text{where } 4 = 330 \text{ ft.}$$
$$xe = 330 - \sqrt{(330)^2 - (9.1)^2}$$

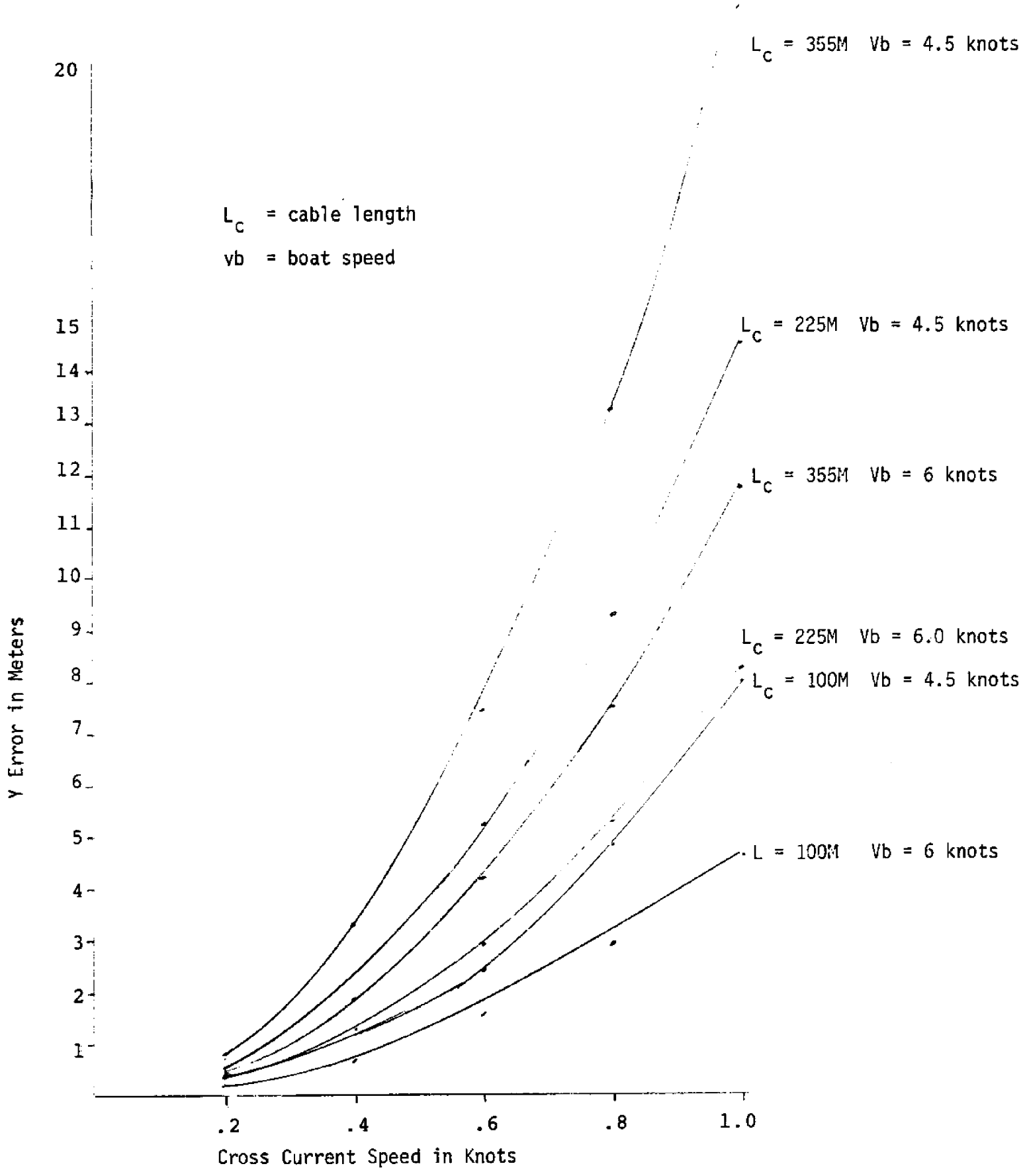

FIGURE 4-4 Sensor Error in y Axis Versus Cross Current

xe = 0.125 ft. = 1.5 in. (negligible) error in x axis under sample conditions. In the graph in Figure 4-4 for various cross currents and boat speeds, the results of the Y displacement are summarized.

4.1.3 Error Due to Absence of Slant Range Sonar System

When the slant range sonar is inoperable a trial run is made over a known target to estimate a total trail (distance from antenna to sensor). This trail is assumed constant when the slant range is not working. Because the horizontal (x) distance between the boat and CDD is a function of the angle θ hence depth of CDD (See Figure 4-5) an error is created by the assumption of a constant trail.

The following calculations are made to estimate the potential size of errors which accure due to the current method of assuming a constant trail at varying CDD depths.

A basic assumption made in the calculations is that the cable length is equal to the hypotenuse r_s. This is not precisely accurate, however, the magnitude of error calculations are representative.

For a trial run over a known target, r_s (slant range) can be determined by the relation (see Figure 4-6).

$rs = (d^2 + x^2)^{1/2}$: substituting X = T-X1-X2 yields

$$r_s = (d^2 + (T - x_1 - x_2)^2)^{1/2} \qquad \text{(Eq. 4.9)}$$

where d is the water depth to the CDD, x_1 is the distance from antenna to winch, x_2 is the distance from CDD to magnetometer and T is the trail that is calculated.

The trail can be approximated by the relation

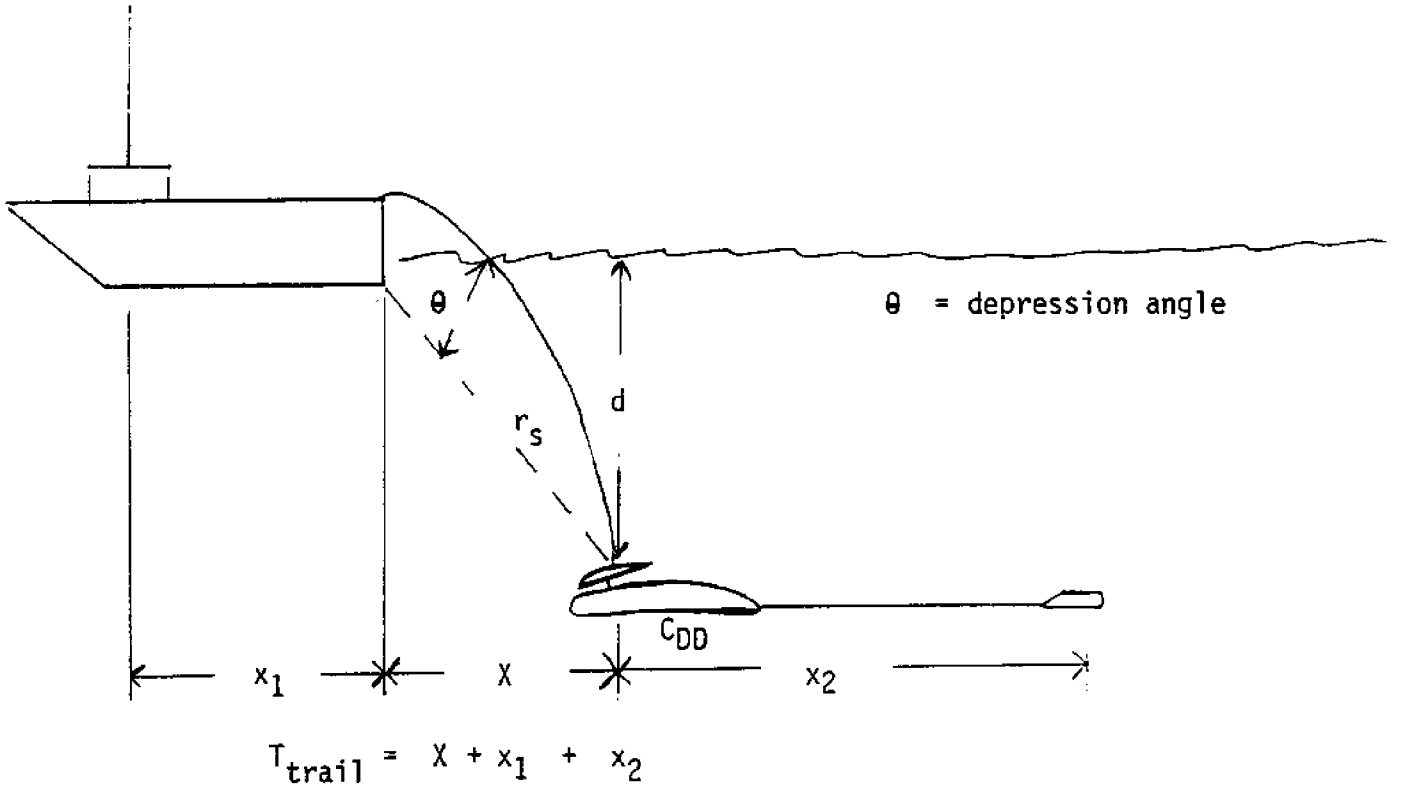

FIGURE 4-5 Trail Error Calculation Geometry

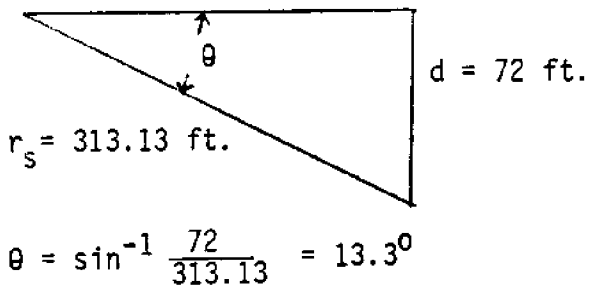

FIGURE 4-6 Geometry for Sample Calculation

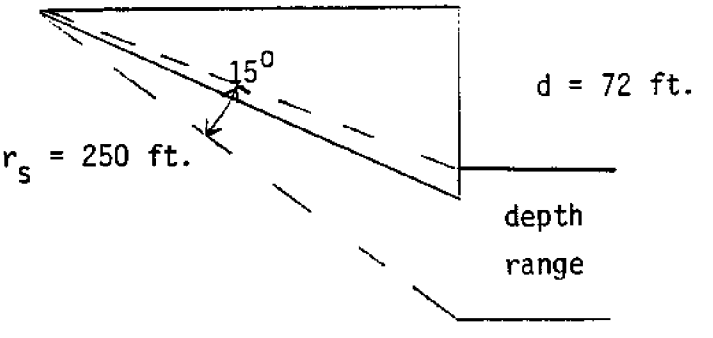

FIGURE 4-7 Geometry for Sample Calculation

$T = x_1 + x_2 + X$; substituting for X yields

$$T = x_1 + x_2 + r_s\cos\theta \qquad \text{(Eq. 4.10)}$$

where $\theta = \sin^{-1} d/r_s$

The error in trail would be the change in X as the CDD changed depth through an angle $d\theta$. To find the error E_1, we subtract the estimated distance X from the actual distance X as follows:

$$E = \left[(r_{so}\cos\theta)_{act}\right] - \left[(T_o - x_1 - x_2)_{est}\right]$$

where T_o is the initial trail calculation.

The trail error as a function of depth is:

$$E = (r_{so}\cos\left[\sin^{-1}d/r_{so}\right] - X_o) \qquad \text{(Eq. 4.11)}$$

EXAMPLE CALCULATION

For the trial runs of 16 April 1984 the trail was estimated as 375.65 ft. The distances were as follows:

$d_o = 60$ ft.
$x_1 = 30$ ft.
$x_2 = 30$ ft.

$$r_{so} = \left[(60)^2 + (375.65 - 30 - 30)^2\right]^{1/2}$$
$$= 321.3 \text{ ft.}$$

$$X_o = T - x_1 - x_2 = 375.65 - 30 - 30$$
$$= 315.65 \text{ ft.}$$

We now use these R_{so} and X_o values to find the error associated with a target at a different depth.

First take as a depth (d) the average depth in a sample target field. d = 72 ft., a 12 ft. difference from the test target depth. We now calculate the error due to this depth change:

$$E = (r_{dso}\cos\left[\sin^{-1}d/r_{so}\right] - X_o)$$

$$= (321.3)\ (\cos\left[\sin^{-1}72/321.3\right]\ ) - 315.65 \text{ ft.}$$

$$E_x = 2.52 \text{ ft.}$$

If we now consider the worst case of the deepest target located in this sample field, d = 120 ft., a 60 ft. difference from the test targets. The error in trail calculation becomes:

$$E = (321.3)(\cos\left[\sin^{-1}120/321.3\right]\ ) - 315.65 \text{ ft.}$$

E_x = 17.6 ft. This is a very significant error.

If we perform a similar calculation with a cable length of 1100 feet with the trail estimate made at the shallowest usable depth of 127 feet for that length of cable (See Table 5-4), we arrive at an estimated trail error of 63 feet when the CDD is operated at maximum depth of 390 feet.

It is clear then, that very significant errors in the x position of the sensor are built into the system as it is currently used. Methods of error correction are possible and are discussed in detail in Chapter 5, Section 3.9.

4.1.4 Slant Range Sonar Depression Angle

Presently the system includes a fixed sonar to determine the slant range to the CDD from the boat. This distance is needed to determine the horizontal distance in the x direction between the boat and CDD. Because the device is fixed at a certain angle on the bottom of the boat and has a limited field of vision, (i.e., A 15° cone) it is quite possible that the CDD could move outside it's field of vision (See Figure 4-7).

θ should be adjusted such that

$$\theta_A = \sin^{-1} (d/r_s)$$

where r_s is the slant range. The sonar will only be effective if θ is within $\pm 7.5^\circ$ of θ_A since the sonar forms a 15° conical field of view. to determine the likelihood of being outside of the beam, we look at a depression angle and calculate the range of depths this angle will satisfy. If this range is too narrow in relation to the usual range of depths encountered in a search area, then either the tactics of operation will have to take this into account, or alternative means of determining trail will have to be implemented.

EXAMPLE CALCULATION

Using the values of the trial runs of 16 April 1984 we will set the following as our slant range and depth:

$d = 72$ ft. (average target depth)

$r_s = (321.3 \text{ ft})(\cos[\sin^{-1} 72/321.3])$

$r_s = 313.13$ ft. (slant range)

The geometry is shown in Figure 4-6, and the depression angle is:

$\theta = \sin^{-1} 72/313.13 = 13^\circ$.

If we let θ range $\pm 7.5^\circ$ (from 5.8° to 20.8°) then:

$d_1 = r_s \sin\theta$

$= (313.13 \sin(5.8^{\circ})$

$d_1 = 31.66$ ft.

$d_2 = r_s \sin\theta$

$= (313.13 \sin(20.8^{\circ})$

$d_2 = 111.25$ ft.

So the range of operation for this configuration would have been for depths of 32 to 111 feet.

To calculate the corresponding ocean floor depth to be covered by these limits the CDD's altitude must be known, i.e., if the CDD flies 20 feet above the ocean floor and the cable is 200 feet long, the ocean depth for which the sonar will be effective is 67.03 ft. to 115.74 ft.

It is important to note, however, that this analysis assumes (1) that the sonar depression angle can be adjusted prior to a search and (2) that the boat is running smoothly across the water and not adding to the angle error.

Note also that if a displacement in the y direction forces the cable to exceed the angle of 7.5° from the x axis, then the CDD will again be "invisible" to the sonar.

With slant range of 300 feet, if a cross current forces the CDD to shift 39 feet, a condition of no working slant range will result. However, it does not appear that this is likely based on our calculations in Section 4.4.

A problem could result however, if the crabbing angle of the boat exceed 7.5° from the x axis. This is a more likely possibility and has to be considered. Table 5-4 shows transducer angle as a function of scope and operating depth.

4.1.5 Piloting Error

Due to wind, waves and other effects, pilots cannot maintain a straight course. When the boat is off course, the magnetometer is imparted with an off track error. Due to the tow cable length, the magnetometer will not take the exact course of the boat but will tend to "smooth" the piloting errors. Figure 4-8 depicts this effect. The solid line represents the path taken by the boat and the dashed line represents the trailing magnetometer's path. The magnetometer trails quite a distance (say 370 ft. for this example) behind the boat. At any time say t_1 point 1 can represent the locations of the boat and magnetometer. The assumption that the magnetometer follows directly behind the boat will produce the error y_e shown below. Examination of the courses taken in trials has shown that there is an average piloting error approximately equal to 2m = 6.56 ft. in the y direction (see Figure 4-9), while maximum pilot error from the charts inspected is on the order of 12 m or 39.36 ft. (Figure 4-10).

The interpolation method presently used to calculate the boat's position at the time of a target hit effectively acts as a position averaging mechanism. That is, at the time of a hit, the position recorded at some time past and the position of the boat at a position further down the course are effectively connected by a straight line. This approximation tends to diminish the piloting error. To demonstrate this with the most obvious case, note Figure 4-9. The pilot's true position is at Point 1. Points a and b are the positions used for interpolation; a straight line is drawn connecting them and the boat is assumed to lie on this line. Now note the

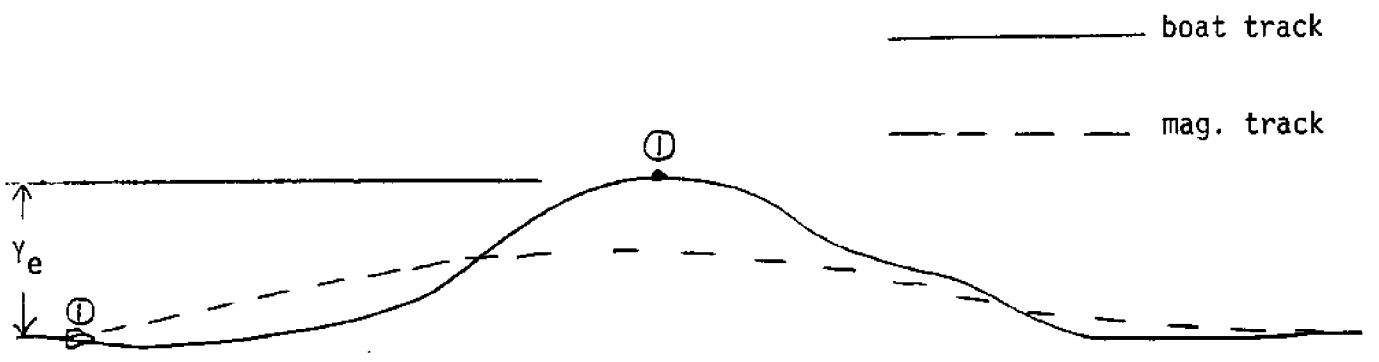

FIGURE 4-8 Typical Boat and Sensor Tracks

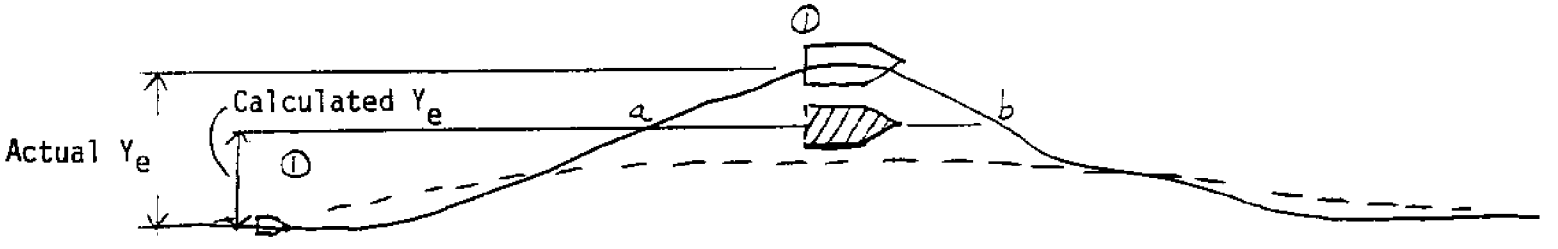

FIGURE 4-9 Piloting Error Calculation Sketch

Figure 4-10

Piloting errors
April trial

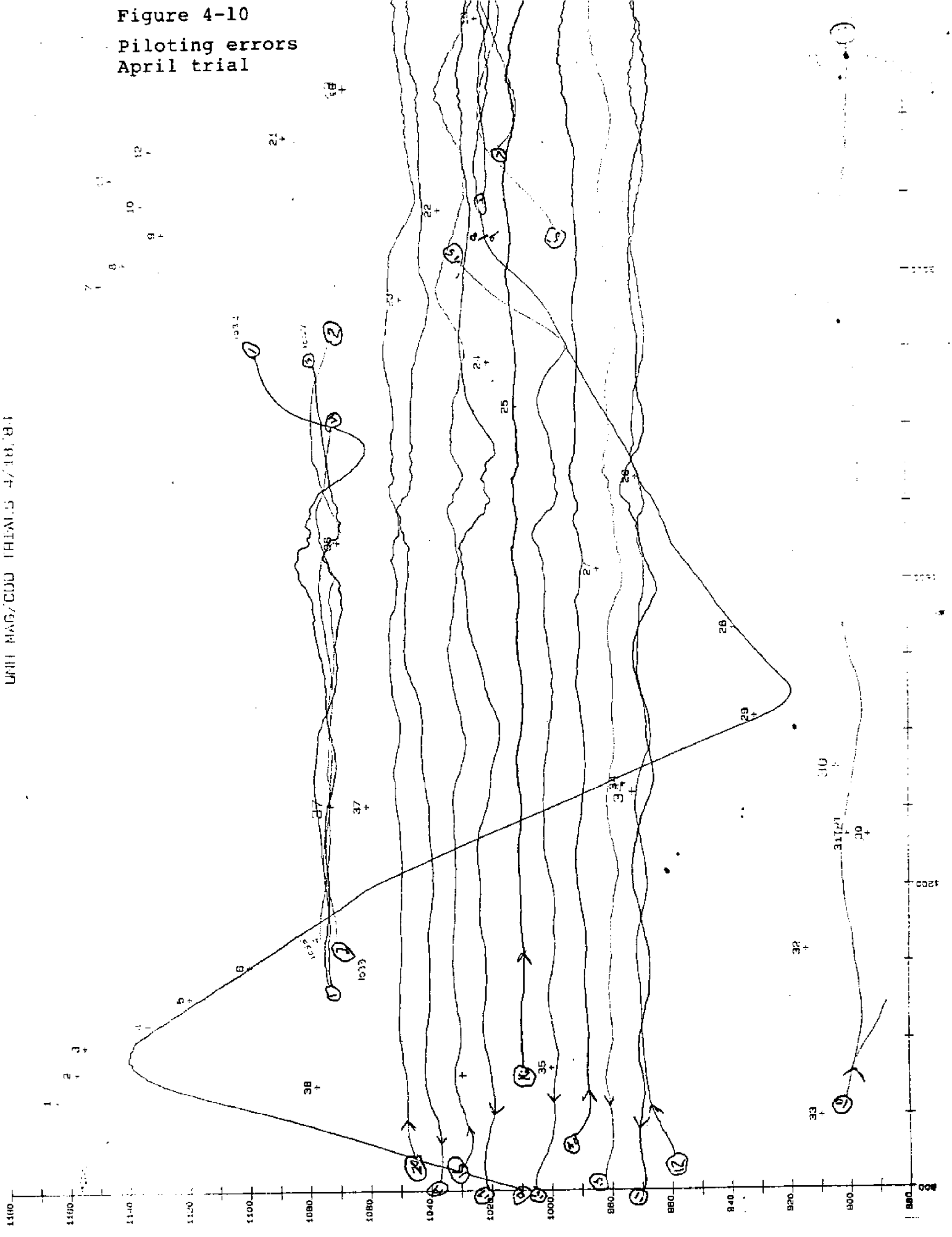

error due to the assumption that the magnetometer follows straight behind the boat. The piloting error has been reduced.

If we assume a velocity of 5 knots, a trail of 1200 meters, and position extrapolation as currently performed over 60 seconds, we find that the positions are extrapolated over approximately 170 meters in the on track (x) direction. For an average excursion of peak y_e = 2 meters, and delta x = 48 meters, we find that the error introduced in the y axis is negligible.

4.2 Summary and Conclusions of Magnetometer Position Errors

There are many variables to be considered in attempting to arrive at an error figure for the position calculation for the magnetometer. These are primarily due to the real ocean environment in which the tests are conducted, i.e., wind speed and direction, cross current speeds, trail estimates, etc. The following table attempts to show the range of errors which are achievable with the current system (See Table 4-1).

We can break down the errors into two groups, namely errors in x axis (along track) and y errors (90° to track).

The x axis errors are primarily due to two sources. Namely, the trail calculation with no slant range sonar and the land navigation system. Of the two, the trail calculation is the most significant and can be as much as 20 meters. In fact, the November 83 trial data was in error by 12 meters.

The y axis errors are attributable to two principle sources. namely, boat crab angle and cross-current effects. Both are largely dependent on sea conditions, and errors can be extremely large.

TABLE 4-1

Magnetometer Position Errors of Current System

ERROR TYPE	VARIABLE(s)	VARIABLE RANGE	RESULTANT ERRORS
Boat crab angle	Angle between track and boat	5^0 10^0 15^0 20^0	x meters: negligible, ", ", " y meters: .7, 1.4, 2.3, 3.0
Cross current effects See plots in Figure 4-4	Cross current speed V_C Cable length L_C Boat speed V_B V_B = 4.5 knots for this table.	V_C .2K .4K .6K .8K 1.0K	x meters: negligible, ", ", ", ", " y meters L_C=100M: .3, 1.0, 2.7, 5.0, 8.0 y meters L_C=225M: .6, 2.3, 5.2, 9.2, 14.5 y meters L_C=355M: .8, 3.3, 7.4, 13.2, 21.0
Trail Calculation No Slant Range Sonar	Depth of Magnetometer and Scope of Cable	Cable Length Ft. / Mag. Depth Range Ft.: 300 / 33-105 700 / 80-245 1100 / 127-390	X errors: 0-5.5M, 0-13M, 0-20M y meters: negligible, ", "
Trail Calculation With Slant Range Sonar			Negligible within accuracy of sonar
Depression Angle of Slant Range Sonar			See Table 5-4
Piloting Error			Negligible when extrapolating position over 60 seconds
Land Navigation System	2 Range Geometry (2M)	30^0-150^0 60^0-120^0 90^0	$\pm$ 7.7M $\pm$ 4.0M $\pm$ 2.8M

The effects of piloting error and depression angle are within reason if proper procedures are adhered to.

The cumulative effect of this multiplicity of errors is such that locating targets within a reasonable error (i.e. 5 - 10 meters) is often not possible.

We will present procedures, calculations and equipment recommendations to reduce these errors in Chapter 5.

In conclusion, the two most serious sources of error which prevent this system from having a 10 meter accuracy are (1) the trail calculation error when slant range is not working, and (2) the effects of cross currents on the sensor position.

Although it would make sense to eliminate all sources of error, eliminating these two would make the most dramatic improvement in system accuracy.

4.2.1 Recommendations for Eliminating Magnetometer Position Error

We will briefly describe a means of correcting each of the types of errors discussed in this Chapter. Some of the corrective measures overlap different categories.

Following these recommendations we will present a solution which would correct all of the error sources simultaneously.

4.2.2 Crab Angle Error Correction

The error due to boat angle can be accounted for or eliminated by the following method. This method requires that the boat be furnished with a compass which can be electroni-

cally interfaced to a computer. These are commercially available; many have digital outputs (10-100/second) and accuracies of +1°.

The first method utilized the computer to constantly (once per second) monitor the boat track (x,y position). This information is presently available in the HP 9825 computer. This track would be correlated with known positions of the navigation system to arrive at a magnetic track heading. The compass heading is compared to the track heading and the crab angle is determined. From this angle and the simple calculations presented in Section 4.1.1, a correction factor can be added to the magnetometer location (i.e., y axis correction).

4.2.3 Cross Current Error Correction

In order to correct for cross currents one must either be able to measure the currents or measure their effects on the sensor position in real time. Measuring the currents in real time is extremely difficult for this type of system, if not impossible. A more realistic mechanism would be to measure its effects on the sensor position.

This could be achieved using a short baseline acoustic navigation system, which could provide both range and bearing information from the CDD to the boat. Since the CDD depth is known, both the off track (y axis) and on track (x axis) errors can be calculated.

Because of the problems currently associated with a 15° conical beam system, it would be preferable to use a system with a wider beam angle.

4.2.4 Trail Error Correction (When Slant Range Sonar is Inoperable)

Since the trail error is due to assuming a constant estimate of trail over various depths of CDD a procedure can be used to account for the variation in trail with depth emperically.

A known target is placed at three depths: minimum, maximum, and mid-depth in the area to be searched. Using the proper cable length for this depth variation, a value of trail can be determined for each of the three depths. The computer can be programmed to extrapolate a value of trail thereafter for any depth in the test area. This method is discussed in more detail in 5.3.9 of this report.

4.2.5 Ranging Sonar Depression Angle Correction

If the existing sonar ranging system is used, it is a simple matter to establish the minimum and maximum depths over which the search is to take place. Once this is known, calculate the length of cable required to maintain the CDD within the 15° conical beam pattern (see Table 5-4). Note that if the boat has to maintain a crab angle greater than 7.5° to stay on track, that the CDD will be out of the beam cross section.

4.2.6 The Total Solution to Positioning Error

After considering all of the sources of error in this system, it becomes clear that most errors can be corrected.

A system which would not only correct for these errors, but would also be amenable to electronically automating the system at a later date would include a range/bearing acoustic sonar system and a solid state boat compass.

If this system was implemented with the addition of some computer algorithms to correct the data for position errors, the MSS would be capable of locating targets to within 5 to 10 meters. Most of this remaining error is due to the land navigation system.

The addition of this system would also save time in that trail data would be available in real time without having to make calibration passes over known targets.

This system would correct for boat crab angle, cross current effects. trail errors, and piloting errors. If the system had a beam larger than the 15° conical beam of the existing system, this would alleviate the problem of maintaining the CDD within that narrow angle.

Table 4-2 is an array to describe the major components required to correct specific errors.

TABLE 4-2

	Method of Correction		
Error Source	Equipment Needed	Procedure Needed	Computer Algorithm Needed
1. Boat crab angle	solid state compass	no	yes
2. Cross current effects	range/bearing sonar	no	yes
3. Trail calculation w/no slant range sonar	no	yes	yes
4. Trail calculation w/slant range sonar	no	no	yes
5. Depression angle of slant range sonar	no	yes	no, could add to make easier for operator
6. Piloting error	no	no	no
7. Land navigation system	other system	no	yes
8. All above except #7	solid state compass & range/bearing sonar	no	yes

CHAPTER 5

CONCLUSIONS AND RECOMMENDATIONS FOR IMMEDIATE SYSTEM IMPROVEMENT

5.0 Introduction

It is stressed that this Chapter's content is based on a limited data base. The improvements and equipment alterations are recommended with the possibility that further testing may indicate a need for additional changes. This section addresses improvements to the current MSS that are achievable without making major changes in its present configuration.

5.1 Conclusions

The primary conclusion is that the MSS is a reasonably well conceived and, considering the time frame and resources expended, well designed system. It has a series of operational problems that taken together hinder the efficient use of the system. Many of these are minor and concern discrete components that simply require repair or proper installation to fix. Others, such as the problem of maintaining an accurate sensor position are more serious, and may require the acquisition of the new equipment recommended in Chapter 6.

The most serious problem, inherent with the MSS's data handling configuration, is the amount of manpower and time it takes to reduce the data after the completion of the sensor runs. This is not serious during training or peace time search operations. It could be intolerable in a crisis. Within the context of the above comments, the specific conclusions are:

A. The single magnetometer search system is a viable approach to locating and measuring the approximate magnetic moment of buried or otherwise obscured ferrous objects.

B. The MSS system requires at least two transits through the anomaly pattern of an object (hits) in order to locate the object and approximate its size.

C. The majority of the operational problems with the MSS involve lost data and/or inaccurate positional information. These trace to a series of individual equipment and procedural problems that must be remedied even if no further technical improvements are made to the system.

D. With all of its limitations an upgraded MSS offers the best near-term system available. It may be the preferred system for small craft and shallow water search even when more advanced systems are available.

E. The MSS is and will remain the least costly means of detecting and localizing the buried mine for at least the next 5 to 7 years.

When the identified problem areas are fixed, the MSS will be capable of search rates that will be close to the intrinsic limitations of a single magnetometer system. The data reduction, analysis and interpretation process will still be post exercise and essentially manual.

5.2 Equipment Recommendations

5.2.1 CDD

(a) That #2 CDD should be made fully operational by:

(i) Requesting that Mesotech re-configure the 807 altimeter for internal mount within the CDD vehicle

(ii) Repairing the slant range vehicle electronic circuit card and sealing the housing to prevent further corrosion

(iii) Repairing the wing leak

(iv) Investigate and resolve the possible signal cross talk between Data Channels

(v) Initiating trials in water depths to 300 feet to determine proper cable scope for various depths (Covered in Section 5.3.15)

On completion of (i), (ii) and (iii) the CDD should be pressure tested to a depth of 450 feet to test for leaks.

On completion of (iv), the remainder of the system, i.e., the cable and the CDD control box should also be investigated for signal cross talk occurrences and remedied by filtering, shielding or establishment of a single point ground system for all signal circuits.

(b) That #1 CDD should be refurbished and that the modifications proven in trials to be successful on #2 CDD should be retrofitted to #1 CDD. On completion, trials should be conducted to assure its operational capability.

5.2.2 CDD Control Box

Consideration should be given to:

(a) Assembling a #2 "back-up" control box, or have duplicate spare boards made.

(b) Modifying the electronic circuit that controls the altimeter set point to give true reading altitude settings.

(c) Conducting a trial to ascertain the characterisics of the loop gain control. Tracks should be made over the same ground with different loop gain settings. On completion, an analysis should be made to ascertain the correct loop gain settings for various operational situations, e.g., in rough terrain where water depths vary in excess of 6 meters per 300 meters of track, the loop gain control should be set between 820 and 840. Over smooth level ground the loop gain should be set at 920 and not adjusted. When oscillations occur the loop gain should be reset to 850, etc.

(d) A warning lamp should be fitted to the front panel of the CDD control box to make operators aware of the operating mode. A warning legend should accompany it, informing the operators of the difference between "reset/normal mode" and "fast mode".

5.2.3 Magnetometer Sensors and Housing

Consideration should be given to making #1 magnetometer sensor operational.

(a) Resolution of the signal cross talk problem outlined in 2.3.2.2.

(b) Tests should be frequently under taken at the NAVEODTECHCEN to ascertain the true extent of the magnetometer sensor active and dead zones (both

polar and equatorial). This information will insure that the sensor is working correctly within its set specification.

(c) That prior to the commencement of each search the NCSL's Magnetic Processor MP-01 and Frequency Translator FT-01 should be tested by following the instructions laid down for calibration in Report Number NCSL 247-75.

(d) That towing stability tests are made to measure the dynamic orientation of the sensor tow body. Tests should be conducted on both mag tow bodies (with sensors fitted) and ballast adjustments, if necessary, be made to ensure level flight under all tow conditions.

5.2.4 Cubic Autotape

As outlined in this report (Table 2-5), there are two areas in which navigational Interference occurred within the trial area. The error caused by this interference can result in the search vessel wandering off track by as much as 10 meters and is responsible for about 5% of the total off track time. It is possible that reflected signals are being received. The geometry of the search area to R_1 and R_2 is good so it would appear that some other problem exists. If the NAVEODTECHCEN is interested in resolutions of this problem they could request that a CUBIC engineer investigate the problem.

NOTE: This is a good example of the need for more than two shore stations in the navigation net.

5.2.5 H.P. Desk Top Computer 9825

The CDD boat programs should be revised to include the changes recommended within this report, i.e.:

a. Operating with depth information.
b. Operating with depth and slant range information
c. Calculations to determine magnetic anomaly position
d. Calculations to determine target position
c. Drawing track lines on the plot prior to the commencement of a search

Prior to any away deployment of the MSS, it is recommended that these programs should be debugged in the local area of the NAVEODTECHCEN.

5.2.6 NAVSCHOLEOD Search Vessel

On commencement of the next MSS trial either with the NAVSCHOLEOD search vessel or any other vessel it is advisable to calibrate engine revolutions for speed through the water. The trial should be conducted towing the CDD. Runs at a set RPM should be made in two directions, preferably with, then against the tide. The mean speed is calculated as the mid point between both runs. On completion RPM/Speed charts should be furnished to the search operator and helmsman.

5.3 Search-Operational Considerations

5.3.1 Optimum Search Altitude

A detailed analysis of the theoretical anomaly pattern of a dipole target (Chapter 3) was accomplished. Target strengths of 35K, 50K and 70K cgs were selected and footprints were produced for altitudes of 10, 15, 20, 25, 30 and 40 feet

(Figure 5-1). One object of the study was to select the optimum altitude at which to fly a magnetometer sensor to have the greatest probability of detecting a target. The footprint patterns were for gamma iso-intensity lines which approximated 1, 3 and 10 gammas and an earths field inclination of 68° North. Maximum target width in a West/East direction, maximum gamma track length in a North/South direction and area of the enclosed gamma intensity were measured. Table 5-1 contains an example of this information for a 50K cgs di-pole. It can be seen from the data that positive gamma influence width changes very little over the 10 to 20 feet altitude range, and that negative gamma influence rapidly falls off as altitude is increased. The actual area of influence is greatest at 20-feet with 793 square meters for the area enclosed by the 1 gamma iso-intensity line. If maximum signal strength is the major criterion for determining the height of the sensor, then an altitude of 10 feet would have to be selected. To take advantage, however, of the entire footprint width, length and area, a height of approximately 15 feet would be selected as the optimum altitude of the sensor.

It must be born in mind that the above figures refer to perfect di-poles that have a single magnetic moment. Actual targets will have two longitudinally displaced magnetic moments and the area of influence will be skewed left or right of the North/South line depending upon their orientation. This has the advantage of increasing the total width of influence of the target. Field tests also prove that the anomaly width is in fact greater at 15 and 20 feet than at 10 feet.

Data obtained from the trials of 12 and 18 April 1984 were also studied to assess optimum altitude.

Figure 5-1

50K cgs Target Depicting 10 to 40 ft Altitude Changes for the 1 Gamma Intensity Lines

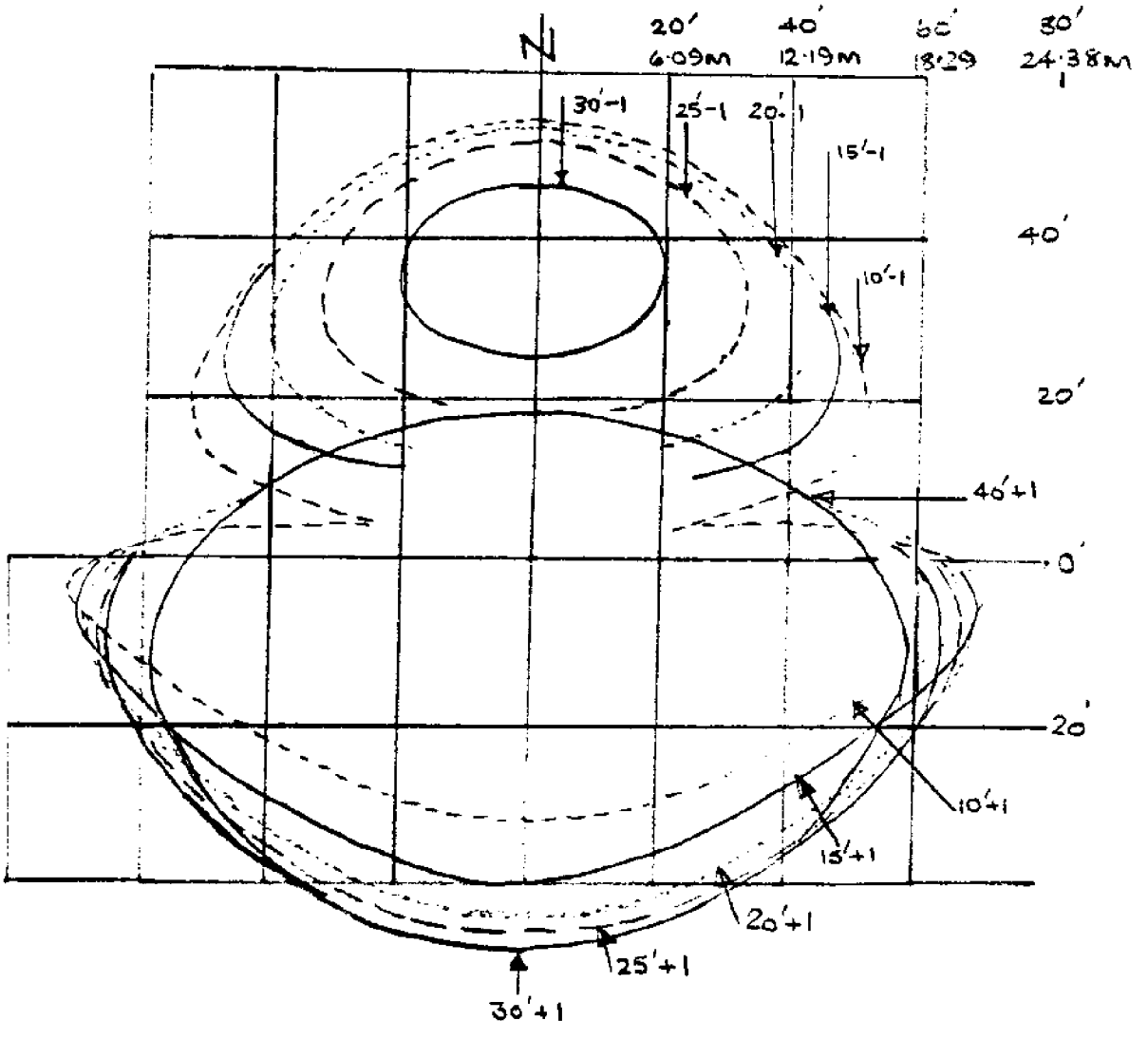

Figure 5-1

50K cgs Target Depicting 10 to 40 ft Altitude Changes for the 1 Gamma Intensity Lines

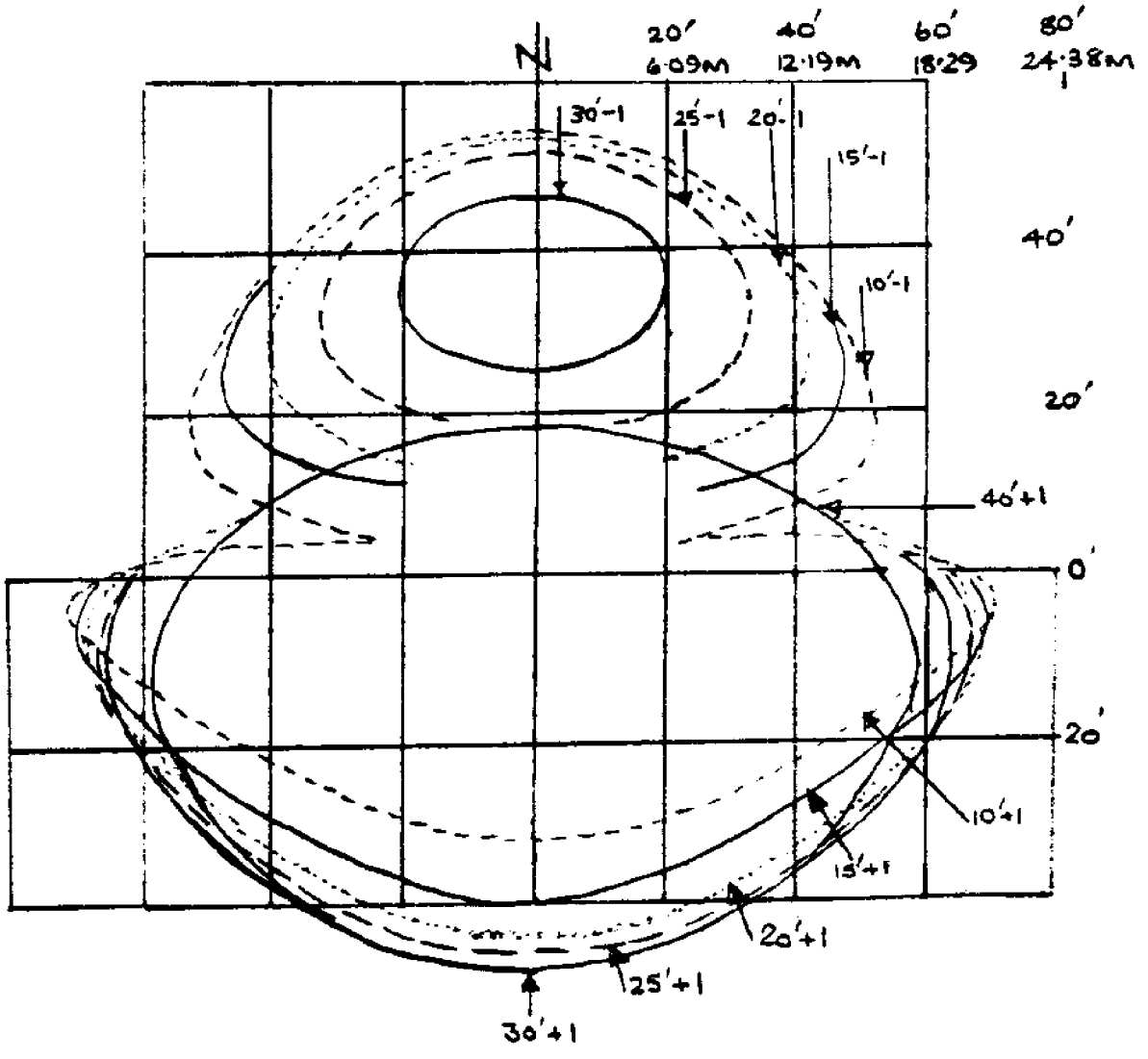

Table 6-1 Theoretical Magnetic Footprint Widths of a 50K cgs Di-pole to Determine Optimum Sensor Altitude

Key: (○) Most favorable within 3 meters

Width Gamma / Altitude Feet	Width(m) -1 gamma	Width(m) +1 gamma	Width(m) -3 gamma	Width(m) +3 gamma	Width(m) -10 gamma	Width(m) +10 gamma	1 gamma Total area of influence sq.m	3 gamma Length of signal north to south	3 gamma Total area of influence sq.m
10	31.5	42.45	19.92	28.9	11.15	18.61	684	19.3	288.1
15	28.5	42.6	16.4	28.7	2.72	17.4	730	20.5	400.7
20	24.92	41.96	10.07	27.2	NIL	15.78	793	20.0	329.2
25	19.92	40.6	NIL	25.9	NIL	12.62	643	13.9	294 Positive Only
30	12.1	39.1	NIL	23.73	NIL	7.4	633	13.8	286 Positive Only
40	NIL	35.37	NIL	16.32	NIL	NIL	528	10.7	145.1 Positive Only

It was concluded (2.3.2.2c) that when the sensor approached to within 10 feet or less altitude, the background noise due to proximity of the sea bed surface and small magnetic anomalies distorts the clean gradient. The resultant signal masks target anomalies.

Data has shown (2.3.2.1) that although the CDD has excellent flying characteristics it cannot be expected to fly at an exact height above the sea bed. Very seldom does it climb above the set point altitude, its normal tendency is to fly 2 to 4 feet below the set point with occasional excursions to 6 feet.

Therefore, this report concludes that the optimum altitude to fly the sensor is the range of depths from 15 to 20 feet.

Study of the altitude strip chart data concludes that to achieve this range of depths the ideal set point will be 19 feet.

5.3.2 Optimum Track Widths

(a) Target. Determination of optimum track widths is dependent upon the maximum range at which it can be expected that the sensor will find a target. It will be assumed that at least a 3 gamma signal is required for the operator to distinguish the target from the background noise. From the theoretical study of the di-pole for an average target (Table 5-1), it can be seen that the sensor at 20' altitude should be capable of locating a target at 27.2 meters. Since actual target measurement data concludes that this range is a conservative estimate, it can be assumed that average to small targets will be seen at 27.2 meters.

(b) Navigation. Chapter 4 discusses the positional error factors and how they can be calculated. It is known that the method of interpolating sensor position actually reduced the helmsman error to 2 meters. However, let us assume that this error is still present and that a 10^{o} crab angle and a 0.4 knot cross current increase the error by another 2 meters. The method to determine the average error is to take its root mean square:

$$2^2 + 2^2 = \sqrt{8} = 2.828 \text{ rounded to 3 meters}$$

(c) Calculation. Using the following formulae, a table can be produced to indicate the coverage of lane widths, assuming a navigation error of 3 meters, a target width of 27.2 meters and an altitude of 20 feet. The calculations determine the probability of at least two hits on the target.

e.g., for 20 meter lane widths

$$\text{Mean} = \frac{\text{Footprint Width - Lane Width}}{\text{Lane Width}} \quad \frac{27.2 - 20}{20}$$

$$\text{Maximum} = \frac{\text{Footprint Width - Max Error}}{\text{Max Error}} \quad \frac{27.2 - 26}{26}$$

$$\text{Minimum} = \frac{\text{Footprint Width - Min Error}}{\text{Min Error}} \quad \frac{27.2 - 14}{14}$$

Table 5-2 Lane Coverage
Probability of at Least Two Hits

Lane Width(m)	Mean	Max	Min
25	0.09	0.13	0.42
20	0.36	0.05	0.94
15	0.81	0.29	0.99
13.6	0.99	0.39	0.99
10.0	0.99	0.7	0.99

The average detection rate (2 hits) for the 12 April trial was 70% at 10m lane spacing this is encouraging considering the magnetometer had a down time of 53%. If the sensor downtime can be considerably reduced then track widths of 15 meters should be feasible with a search effectiveness comparable with the APSS, i.e., 80% probability at an 80% confidence level for locating average magnetic target anomalies.

5.3.3 CDD

Trials should be conducted to ascertain those environmental conditions, equipment malfunctions or maneuvers that induce the CDD to oscillate. If possible, the trial crew should try to recreate conditions similar to when the CDD oscillated on the 12 April trial. If the oscillations can be re-created the CDD should be fully monitored on the strip chart to allow wing angle, pitch and roll, set point information and altimeter to be read along with hand notations of different loop gain settings. Alternative methods of recovery to level flight should also be attempted, e.g., switching to depth control, switching to manual control or altering loop gain. On completion of the trial the conditions that cause the oscillations and the quickest way to recover the CDD to level flight should be identified.

5.3.4 Magnetometer

Each search track will experience an area gradient either positive or negative. If possible this gradient should be measured during the preparation period before the actual search commences. Prior knowledge of the gradient will allow the operator to set the strip chart stylus in the correct position at track start. e.g., In the trial area the average gradient is + 38 gamma, therefore, on the 50 gamma full scale the, stylus should be set at a position 6 small divisions in from the edge of the chart. If the operator has to adjust the stylus during a search run he should ensure that it is not done during an anomaly reading.

If during the search, the strip chart operator notices that the CDD either starts to porpoise or moves outside the altitude limit of 14 to 21 feet he should inform the Computer/Plotter operator to note that, during this period, an incomplete search has been made.

5.3.5 Trial Area

Consideration should be given to re-evaluating actual target and other anomaly positions each time the trial area is visited. The suggested way, which has proven to be the most accurate in the past, is to tie on to the target or anomaly from a light skiff. The light skiff should then take range/-range readings to be converted to XY coordinates at a later time.

5.3.6 Speed and Maneuvering

(a) The CDD design speed of 7 knots has been proved. However, conducting search runs at an "over the ground" speed of 6 knots ensures that the design

speed is not exceeded. Consideration should be given to controlling the search vessels speed to 6 knots "over the ground" in Normal and Reverse runs. This will give:

(i) Allowance for a maximum of 1 knot current
(ii) Good steerage way for the helmsman
(iii) Records of even length
(vi) Records of even gradient

NOTE: To ease the problem of uneven records, the Techcen could consider the purchase of a strip chart recorder whose paper speed is controlled by boat speed.

(b) It can be seen from para 2.3.2.5 that conducting turns with the CDD submerged does not give satisfactory results (Figure 5-2). It not only allows the CDD to loose depth and speed during the turn but greatly increases the strain upon the CDD during the turn recovery phase. Consideration should be given to making turns in accordance with "Memorandum for the Record", 505/BJ:mbs dated 7 March 83. If the turns are completed at slow speeds with the CDD on the surface it is not only safer but very much easier to control. Sufficient stand-off is required to enable the CDD to resume operating depth before entering the search area.

(c) Consideration should be given to making recoveries of the CDD and sensor at minimum ahead speed on one shaft. The CDD should be surfaced and the search vessel should be maneuvered to head into the current. One person should be in charge aft. The person in charge should not aid in the recovery but

Figure 5-2

CDD Maneuvers During a Turn

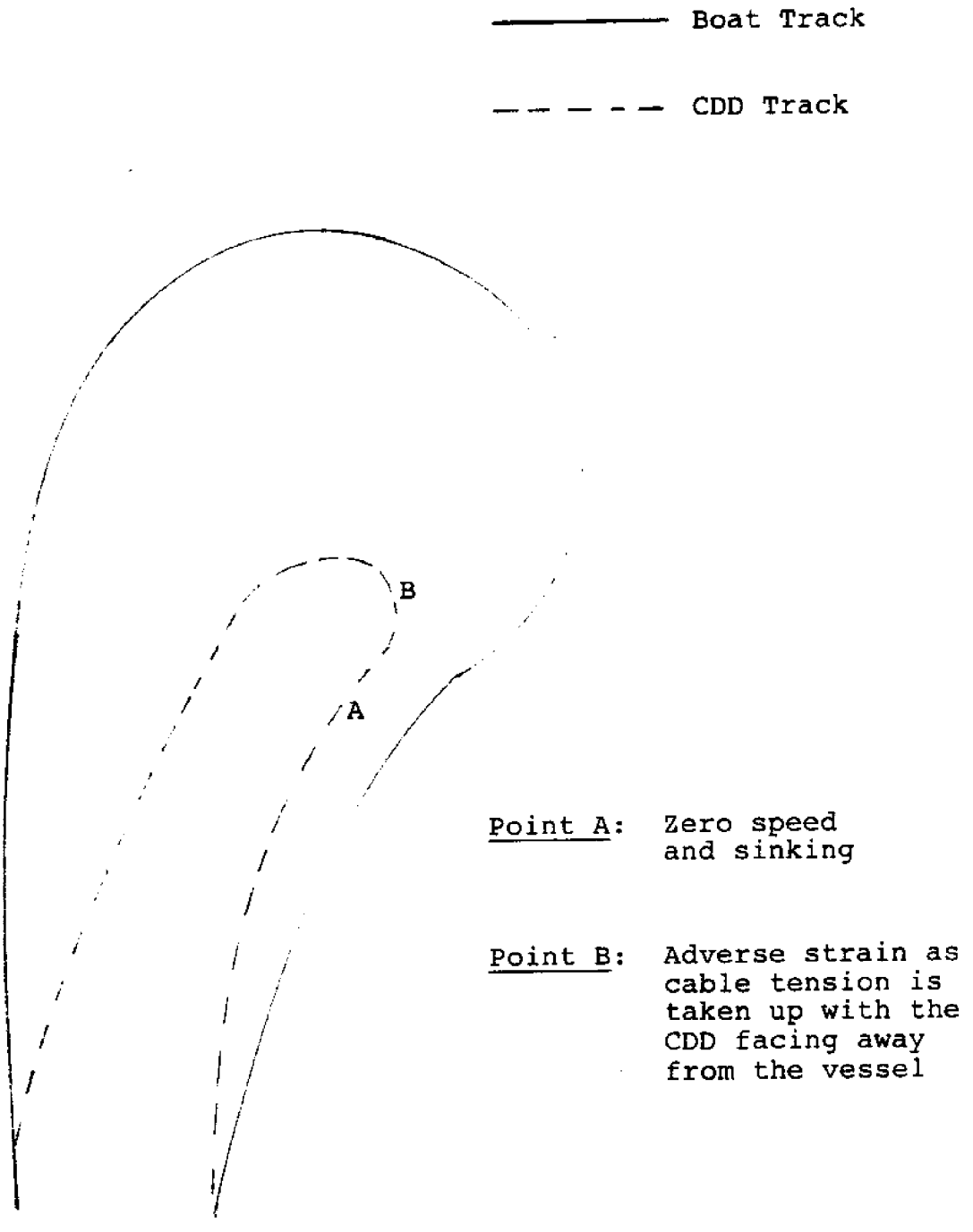

direct operations from a position where both the recovery crew and the helmsman can hear his commands.

5.3.7 Navigation and Tracking

(a) To assist in identifying holidays in the search due to navigation and tracking, consideration should be given to altering the HP 9825 program to allow the plotter to draw the expected track courses as well as the actual. Operators could then make real-time comparisons of actual to expected track and immediately identify excessive track wander.

(b) It is suggested that gaps in the search not be re-searched until after completion of the entire search. Very often adjacent tracks inadvertently cover the area missed by the previous track. Leaving the re-search until last, also ensures that it is planned and covered in the most efficient manner.

(c) Control of "end of track" turns should be given to the computer/plotter operator instead of the helmsman. This would entail making the plot of the area longer in the X coordinate to allow monitoring of the stand off distance. If this is considered undesirable, the laying of marker buoys at track end and track start could be considered. This would give the helmsman a visual indication of where to commence track start.

5.3.8 Scope

(a) In Section 2.2 it was determined that with a cable scope of approximately 300 feet and a set altitude of 20 feet, the CDD remained in stable flight throughout a depth range of 45 to 80 feet. Beyond 80 feet, the CDD tended to "fight" the cable for greater depth as depicted in Figure 2-8 Assuming that the ratio of scope to depth is approximately linear, the following constant scope vs depth range table will aid the operators in future trials at 6 knots.

Length of cable (scope) = 300 feet
Depth of water = 80 feet
Ratio = 300/80 or 3.75 : 1

Table 5-3 Scope vs Usable Depth Guide

Depth (feet)	Scope (feet)
20 - 50	250
50 - 80	300
80 - 100	375
100 - 125	470
125 - 150	560
150 - 175	655
175 - 200	750
200 - 250	940
250 - 300	1125

NOTE: Slower speeds than 6 knots may require a slight reduction of cable length.

(b) Consideration should be given to operating with a minimum scope length of 250 feet for the following reasons:

(i) The CDD tends to fight the cable on short tethers trying to assume a too acute down angle.

(ii) Trail distances will vary less using a longer cable scope length.

(iii) Cable scope lengths of less than 250' increase the chances of the CDD being outside of the slant range transducers 15° conical field of view.

Using the formula, $\text{Sine } \theta = \frac{\text{Depth}}{\text{Scope}}$,

The following table shows the optimum transducer angle from the horizontal plane and the range of operating depth for a fixed cable scope.

Table 5-4 Slant Range Operating Depths

Scope(feet)	Transducer Angle °	Depth Range(feet)
250	9	6 - 71
300	13	33 - 105
375	13	42 - 131
470	13	53 - 167
560	13	63 - 196
655	13	74 - 230
750	14	84 - 262
940	12	90 - 313
1125	13	127 - 393

5.3.9 Trail Calculations

The CDD boat program should be revised to determine trail for two different modes of operation, namely "operating with depth information" or "operating with depth and slant range information". It is not suggested that these programs attempt to calculate the sensor position in real time, only that the information should be displayed on the print out for use in post data analysis, e.g., with Depth and Slant range operating the printer would display:

Event # Boat XY, Depth and Slant Range

Obviously if slant range is not available then it will be omitted from the print out.

a. With Slant Range Sonar Operable: When the slant range sonar is operating properly, the trail can be computed using the following equation from Chapter 4 (Figure 4-5).

$$T = x1 + x2 + X$$

where $X = \sqrt{r_s^2 - d_s^2}$ yields:

$$T = x1 + x2 + \sqrt{r_s^2 - d^2}$$

where T = trail distance from radio antenna to towfish
x1 = distance from antenna to slant range sonar on the boat
x2 = distance from CDD to towfish
r_s = slant range from CDD to slant range sonar

d = CDD depth
X = horizontal (x) distance from sonar to CDD

b. Without Slant Range Sonar. If the CDD slant range equipment continues to be inoperative, the importance of time spent at the beginning of a search operation in calculating an accurate trail, cannot be over emphasized. It is recommended that consideration be given to executing trail calibration runs (Section 2.2) for three depths. Depending upon the range of water depths in the search area, runs should be made in the deepest depth, the mean depth and the shallowest depth. This information can then be put into the HP 9825 to enable a more accurate trail distance to be interpolated at various depths within the area.

For example, if the trails calculated for the three depths are as follows:

d1 (shallow) = T_1

d2 (mid) = T_2

d3 (deep) = T_3

where d = depth
T = trail distance

See Figure 5-3.

If we linearly interpolate between points, we can determine a trail value for any depth d between d1 and d2 using the equation:

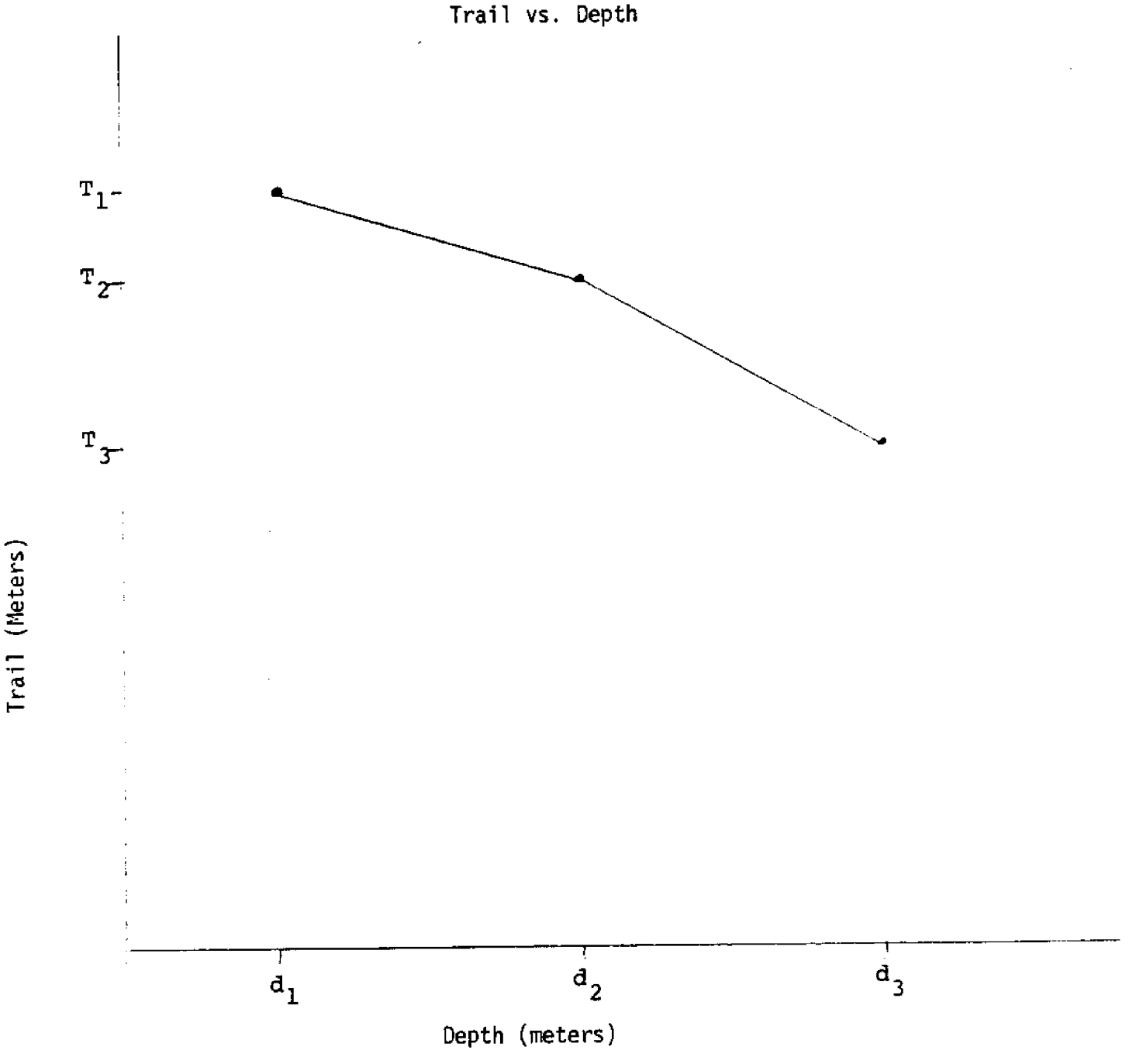

FIGURE 5-3 Trail Versus Depth Interpolation

$$T = T_1 - \frac{(d - d1)}{(d2 - d1)} (T_1 - T_2)$$

and similarly for a depth d between d2 and d3 the expression is:

$$T = T_2 - \frac{(d - d2)}{(d3 - d2)} (T_2 - T_3)$$

If it is found that the variation in trail is sufficiently linear with depth that only a shallow and deep trail calculation is required (i.e. T_1 and T_3 only) then the expression would be:

$$T = T_1 - \frac{(d - d1)}{(d3 - d1)} (T_1 - T_3)$$

It would also seem that if accurate records were kept regarding length of cable versus trail for various depths, that this information could be stored in the computer and used in subsequent searches without the need to repeat the same trail procedures over and over.

5.4 Data Reduction

5.4.1 Strip Chart Analysis

The strip chart analysis outlined below will derive a satisfactory target position from peak positive gamma strength positions within the test area. This method should not be used when searching in areas where the angle of inclination is more than 78° or less than 58°. This section is written on

the assumption that the recommendation that search operations be conducted at a constant over the ground speed is implemented. The first step is to lay out the strip charts and study the overall picture. The speed over the ground should be checked between event marks , where speeds are not constant the chart should be annotated. The next parameter to be studied is the CDD altimeter trace, the depths should vary evenly from 14 to 21 feet. Where oscillations or rapid changes occur the chart should once again be marked. the operator should now take a ruler and draw a mean gradient line through the entire length of each gamma signal if the speed has remained constant. Where large anomalies (e.g., the submarine) occur the line should continue to be extended (Figure 5-4) through the anomaly. This will highlight the extent of the magnetic influence of this large object and indicate to the operator that readings cannot be taken in this area. The next task will be aided by studying the magnetic footprints for the search altitude in Section 3.2. Figure 3-3 depicts the appearance of an average target when viewed from a search vessel passing directly over the target on a North/South course. Figures 3-6 through 3-12 show the magnetic footprints of a target with a magnetic moment of 50K cgs. The magnetic moments of actual targets will range from about 35K cgs to 120K cgs, therefore, the diagrams can be adjusted as in Section 3.2 to represent the target strengths expected in the search area. Actual targets will not be lying in an exact North/South orientation, therefore, their signatures will be skewed slightly in an East/West direction extending the negative response either to the West or East of the target. [The planned magnetic signature analysis work in the next phase of the program will result in a set of typical anomaly patterns for various dipole orientations and for monopoles. These and composites from the NCSL 1952 report (Ref. 5) can be furnished to the analysts to aid in interpreting the meaning of each anomaly data set.] When this occurs, it is possible that the operator will only see a negative response. Another

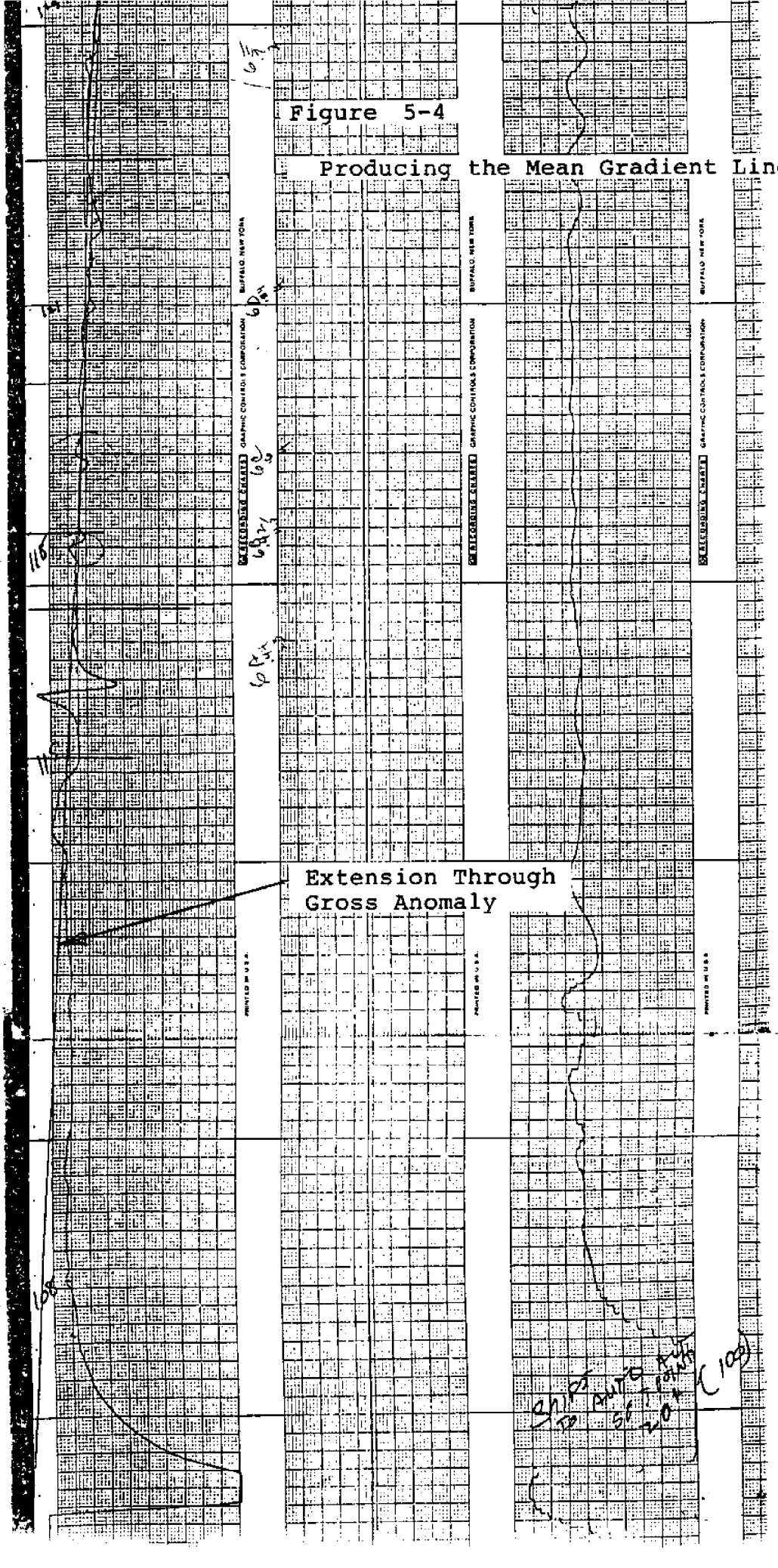

Figure 5-4

Producing the Mean Gradient Line

change that occurs due to varying the targets orientation is to produce small areas of negative gamma response to the South of the main positive gamma response. However, if a target produces a positive and a negative response then the main positive response will always occur to the South, followed by a weaker negative response to the North. The length of the average target response in the North/South direction from gradient level through anomaly and back to gradient level is about 40 meters. The width of the average target response in the West/East direction from +3 gamma through the anomaly and back to +3 gamma is approximately 30 meters. Therefore, if search lanes continue to be run at 10 meter intervals in a North/South direction it could be possible to witness four hits on one target and there is a very high probability of at least seeing the target twice.

The algorithm incorporated in Section 3.2 calculates the targets position using the XY position of the peak positive gamma response of the signal. Therefore, it is suggested that future target information be input to the HP 9825 in the following manner:

TITLE	EXAMPLE
Name	1A (Track 1,first contact)
Amplitude	7 (Peak positive gamma reading)
Altitude	15 (height in feet of CDD above sea bed)
Fraction	0.66 (fraction between 1st and 2nd XY)
X_1Y_1	1309 875
Depth	80 (depth in feet of CDD)
Slant Range*	140 (boat transducer to CDD receiver in meters
X_2Y_2	1431 875
Depth	82
Slant Range*	141

*NOTE: If slant range is not available it is suggested that a code e.g., "N" be input at this time to allow the computer to select the correct algorithm to be used (5.3.16).

Assuming that fixed offsets have already been input, the computer using the algorithms in Section 3.2 will now print out:

XY (position of the peak gamma response)

The computer will then look for other gamma responses in the vicinity of that XY position. If they are present it will calculate the XY position and magnetic moment for the suspected target. It will then print out:

XY,T	(Targets position)
Amplitude,T	(Magnetic Moment of the target)

When all peak positive gamma anomaly responses have been input they can then be displayed on the plotter. It is suggested that anomaly position crosses and names are allocated different colors (as with the present system) 0 to 3, 3 to 5, 5 to 10, 10 to 15 and 15 to infinity. The final plotter color pen should be allocated to marking the position and magnetic moment of the target.

On completion of plotting of all the contacts the tracks should be laid along side each other to see if gamma responses not plotted coincide with those that have been plotted in adjacent tracks. This process will highlight anomalies of low level intensity that may have been missed.

CHAPTER 6

FUTURE IMPROVEMENTS

6.0 Conclusions and Recommendations for Future Improvements

6.1 Introduction

The previous Chapter addressed those MSS equipment and procedural improvements that could be quickly implemented by the NAVEODTECHCEN staff. They will meet the immediate needs in taking the MSS through its OPEVAL. This Chapter discusses some post-OPEVAL modifications that will significantly improve the operational capability of the MSS.

A primary conclusion is that the single magnetometer MSS, as currently configured, requires an inordinate amount of time and effort to measure and chart sensed ferrous objects, particularly under complex magnetic background situations. The recommended improvements presented in this Chapter will accomplish the following operational improvements.

A. Provide a real-time analysis, measurement and charting capability.

B. When the Inshore Pilot is available, enable real-time comparison of current magnetic search contacts to the cumulative contact/gradient history in the area.

C. Provide a capability for real-time merging (overlay) of sonar search data in the area.

These operational improvements will be accomplished by our principle recommendation that the MSS be converted, in total, to a microcomputer based system capable of analyzing and charting the results of the search operation in real-time. The system implementation recommended herein can be ready for sea trials in approximately 15 months from program authorization.

6.2 Automated MSS Hardware Configuration

Machine processing of the magnetic anomaly data during the search operation is almost a mandatory next step in the development of the MSS. The technical approach outlined herein, will also complete the very limited degree of automated navigation data logging in the present system to fully automate the charting process. There are two distinct components in this system upgrade program. The first is to automate the acquisition analysis and interpretation of magnetometer data. This includes machine analysis and interpretation of sensed anomaly patterns utilizing algorithms of the type developed in Chapter Three.

The second component is to fully automate the process of determining and logging sensor position in the precision radio navigation grid system. This involves real-time solution of the equations developed in Chapter Three utilizing direct sensor input to the MSS microprocessor. Each of these two components are discussed separately. They will be implemented in a single microprocessor.

6.2.1 Magnetometer Signal Analysis and Interpretation

The simplified block diagram of the magnetometer processor is shown in Figure 6-1. The cesium vapor sensor, frequency translator (NCSL FT-101), precision discriminator (NCSL-MP-101) and strip chart recorder (MFE-1600) will remain essentially as in the current MSS system. The separate Frequency Synthesizer, shown in Figure 1-2, can be either the current manually set unit or replaced by a computer controlled unit such as one of the Hewlett-Packard family of digital frequency synthesizers. The current components of the MSS system that would be retained are shown above the dashed line in Figure 6-1. Below the line are the new components the key

Figure 6-1

SIMPLIFIED BLOCK DIAGRAM - AUTOMATED MSS

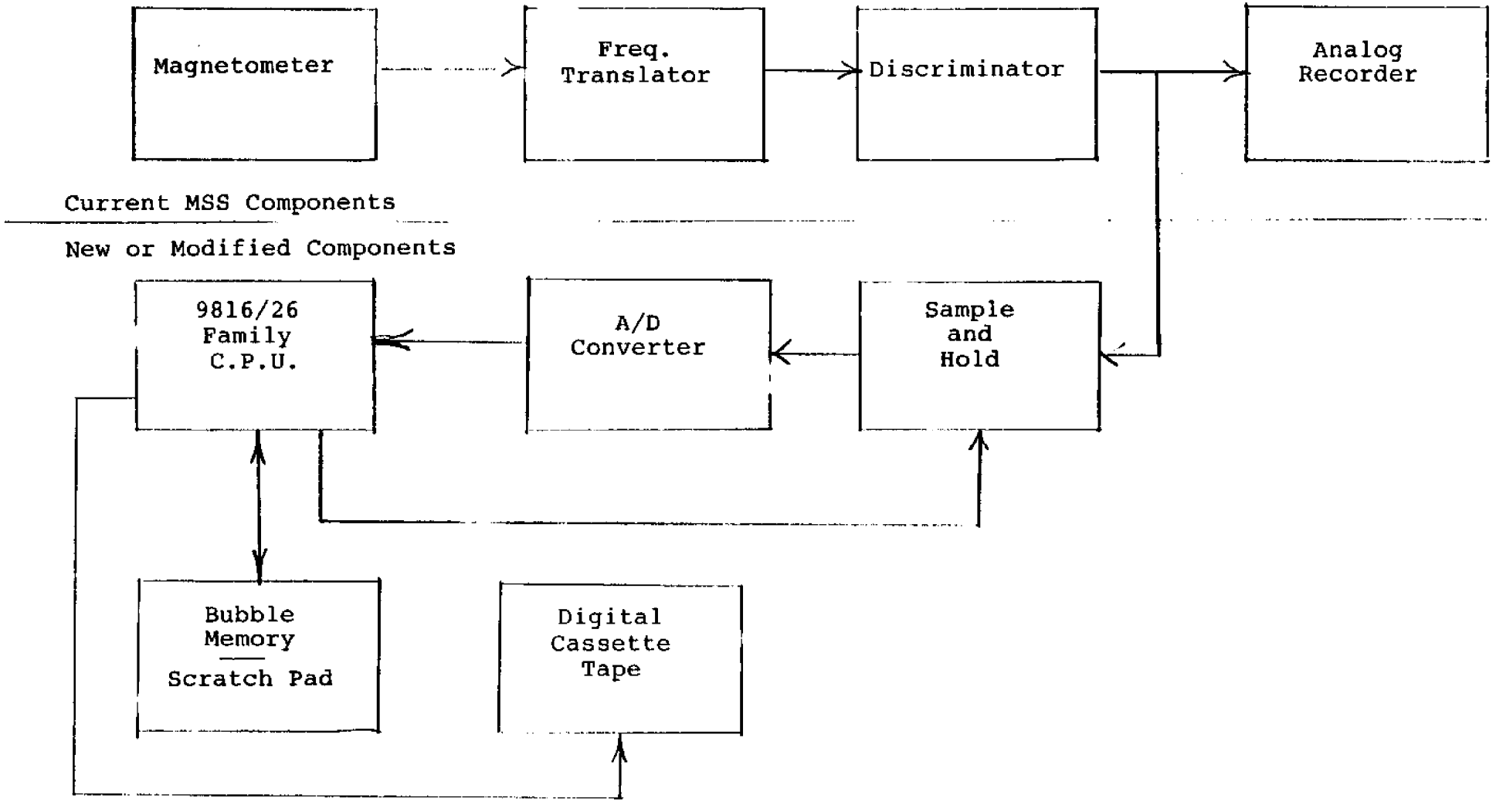

unit being a modern microprocessor such as the HP 9826. This is an advanced desk top unit that essentially replaces the HP 9825 now used in the MSS. The analog output from the NCSL MP-101 is the input to the digital processor. The sample and hold and A/D converter are synchronized by the CPU to sample and digitize the Larmor frequency analog at a rate proportional to tow vessel speed over ground. Sampling at a rate not less than one reading per meter of travel, provides a direct measurement of total field gradient as the sensor transits through the contours of a magnetic anomaly. The CPU will then compare sequential readings to measure peak excursion and slope between positive and negative peaks (when they occur).

Since at least two transits (hits) through the anomaly pattern are necessary to compute the magnetic moment and location of ferrous objects, a scratch pad storage is necessary in the CPU. Since the storage interval may be quite long and the small boat environment is not appropriate for hard or floppy disks, we recommend the use of a moderate size bubble memory. A 500 kByte or larger bubble memory would be capable of storing all the magnetometer and navigational reference data for a full days search operation. This is an inexpensive and reliable form of non-volatile memory. A DC-300 type digital cassette recorder is added to record the data on all magnetic objects encountered during a search operation. Unless the area is a magnetic mess, this cassette recorder will be lightly utilized. It could also serve as the historical file tape when the MSS is utilized for magnetic channel conditioning.

6.2.2 Sensor Position Calculations

The second function accomplished in the digital processor is determination of sensor position as a function of time. The equations for these calculations were discussed in Chapter Three. The on-board inputs to these calculations include:

A. Slant range measurement (sonar)
B. Tow body depth
C. Boat heading relative to track heading (crab angle)
D. Radio positioning system output
E. Drag and cross-current hydrodynamic characteristics of the tow bodies and cables

When the Inshore Pilot data base is available, current patterns in the water column will be available for the calculation of cross-track offset of the tow body (sensor relative to the boat). The preferred approach is a short base line acoustic position measurement system added to the slant range sonar to directly measure sensor offset from the boat track.

6.2.3 Interpretation of Magnetic Anomaly Data

A time and position correlated history of magnetic field variations in the search area, are the necessary inputs to the interpretation algorithms. The illustrative examples in Chapter Two are for some of the simpler aspects of a computer-based interpretation system. There are significant variations from these simple algorithms caused by dipole orientation, monopole targets, search track orientation and earths' field orientation. The continued research in the next phase of the magnetic search sensor program will develop a series of signature analysis and interpretation algorithms that are adaptable to a wide range of MSS configurations. They will be usable for implementing the machine interpretation of data from a single magnetometer search system. The MSS single sensor system would become a single axis temporal

gradiometer with good resolution along the track. Its resolution as a spatial gradiometer in a horizontal or vertical plane would be much less useful. There would still be a requirement for at least two transits (hits) (N-S track) through an anomaly to measure magnetic mass and location. E-W tracks may be more difficult to analyze.

6.3 Rationale for Improvement

The full automation of the single sensor MSS will not increase the sensitivity of the system or materially decrease the time required to search a given area. If the recommended changes presented in the previous Chapter are implemented, the analog/manually interpreted system search rate and sensitivity will reach limits set by the intrinsic nature of the single sensor system. However the laborious post search analysis and manual interpretation (with its computer aided charting) will be eliminated by the automation recommended herein. The magnetic moment and location of ferrous objects will be determined and printed out (charted) within seconds of the second hit on the target. With appropriate communications, suspicious objects can be designated to follow-up inspection and neutralization teams.

If the automated MSS is utilized for magnetic channel conditioning, any "new" ferrous masses can be immediately designated as a "probable" based upon their recent appearance in the channel. A second equally significant feature in an automated MSS is the capability to overlay magnetic search data with side scan sonar search data taken in the channel. With the planned configuration control in the Integrated Search and Inshore Pilot systems, overlay and storage of multiple sensor search data is easily accomplished.

It is our recommendation that the program to develop and demonstrate the automated MSS be initiated immediately. The system can be demonstrated in approximately 15 months utilizing commercial class ADP equipment. Program documentation would include the necessary data and specifications for the competitive procurement of production systems by the EODTC.

The single sensor system is viewed as an interim pending the development of a ganged sensor system capable of covering a much wide search track. The signature processing algorithm development in the next phase of this program will lay the basis for the evaluation of a multi-sensor MSS using temporal and precision spatial gradiometric processing to achieve a four fold or greater improvement in MSS search rates. It is conveivable that MSS search rates could approach those achievable with high resolution side scan sonar systems.

REFERENCES

References

1.

2. S. Breiner "Applications Manual for Portable Magnetometers" Geometrics, 1973.

3. Murphy L. Dalton, Jr. "Searching with 1 and 2 Sensor-Location Magnetometers. Copyright 1982 by Murphy L. Dalton Jr.

4. R.K. Jobison, G.I. Allen "Ganged Magnetic Sensor System" NCSL 247-75, June 1975.

APPENDIX A

TARGET LOCATION CODE IMPLEMENTATION

Tue May 22 13:17:35 1984 /x/sigr.c Page 1

```
#include <stdio.h>
#define MLOW     25.0 e 006
#define MHIGH    70.0 e 006
#define METERSI  100.0
#define METERSO  0.01
#define FEETI    30.0
#define FEETO    0.0333333
#define INNER    1.0
#define NHITS    2

double  in[3] = {METERSI, FEETI, INNER};
double out[3] = {METERSO, FEETO, INNER};
double  yplus[0,0], yminus[0,0], xtarg[0,0], ytar[0,0], z[2][0,0];
unsigned short units[0];
main()
{
double  xhit[2], yhit[2], t[2], xtarg[NHITS], ypls[NHITS], ymin[NHITS],
        msize;
double  sqrt(), sqr(), ln(), exp(), calc(), cabs(), decide(), compute(),
        size();
unsigned char   n, targnum;

write(STDERR,"I/O units: 0 = meters, 1 = feet, 2 = feet * 3\n",47);
getfmt("%s",&units);

targnum = 100;
while(targnum++)
    {
    putfmt("Data for Target # %i\n",targnum);
    write(STDERR,"\n",1);
    for(n = 0; n < NHITS; n++)
        {
        write(STDERR,"input hit x, y, z, t:\n",22);
        getfmt("%d %d %d %d",&xhit[n],&yhit[n],&z[n],&t[n]);
        putfmt("xhit = %6.1f    yhit = %6.1f    zhit = %6.1f    t = %4.1f\n",
            xhit[n], yhit[n], z[n], t[n]);
        xhit[n] *= in[units];   yhit[n] *= in[units];
        z[n] *= FEETI;
        xtarg[n] = calc(xhit[n], yhit[n], z[n], t[n]);
        ypls[n]  = yplus;
        ymin[n] = yminus;
        }
    ytar = decide(ypls[0], ymin[0], ypls[1], ymin[1]);
    msize = (size(yhit[0], z[0], t[0]) + size(yhit[1], z[1], t[1]))/2.0;
    putfmt("xtar=%8.1f      ytar=%6.1f      msize=%5.0f\n\n\n",
        out[units]*(xtarg[0] + xtarg[1])/2.0, out[units] * ytar,
        msize * 1.0 e-08);
    }
}

double calc(xhit,yhit,z,t)
double xhit, yhit, *z, t;
{
double klow, khigh, val1, val2, yplus1, yplus2, yminus1, yminus2;

    /* identify states a to the x = end's + n(a)       */
```

```
    klow    = exp(0.66667 * ln((2.0 * MLOW) / t));
    khigh   = exp(0.66667 * ln((2.0 * MHIGH) / t));

    val1 = compute(z, klow);
    val2 = compute(z, khigh);
    yplus1 = yhit + val1;
    yplus2 = yhit + val2;
    yminus1 = yhit - val1;
    yminus2 = yhit - val2;

    yplus = (yplus1 + yplus2)/2.0;
    yminus = (yminus1 + yminus2)/2.0;

    xtar = (xhit - 0.41 * *z);

/*
    putfmt("xtar=%6.1f    y+=%6.1f    y-=%6.1f\r",
        xtar*out[units], yplus*out[units], yminus*out[units]);
*/
return(xtar);
}

double compute(z, k)
double  *z, k;
{

if(*z > sqrt(k/1.168))
    {
    *z = sqrt(k/1.168);
    putfmt("error flag:  new z = %6.1f\r",*z * FEETO);
    return(0.0);
    }
else
    return(sqrt(k - 1.168 * sqr(*z)));
}

double decide(yplus1, yminus1, yplus, yminus)
double yplus1, yminus1, yplus, yminus;
{
double dif[4];
unsigned char min1, min2, min0;

dif[0] = dabs(yplus1 - yplus);
dif[1] = dabs(yplus1 - yminus);
dif[2] = dabs(yminus1 - yplus);
dif[3] = dabs(yminus1 - yminus);

if(dif[0] < dif[1])
    min1 = 0;
else
    min1 = 1;
if(dif[2] < dif[3])
    min2 = 2;
else
    min2 = 3;
```

```
if(diff[min1] < diff[min2])
    min0 = min1;
else
    min0 = min2;

switch(min0)
    {
    case 0: ytar = (yplus1 + yplus) / 2.0;
            break;
    case 1: ytar = (yplus1 + yminus) / 2.0;
            break;
    case 2: ytar = (yminus1 + yplus) / 2.0;
            break;
    case 3: ytar = (yminus1 + yminus) / 2.0;
    }

return(ytar);
}

double  size(yhit, z, t)
double  yhit, z, t;
{
double val;

val = exp(1.5 * ln(sqr(ytar - yhit) + 1.165 * sqr(z)));
return((t/2.0) * val);
}
```

APPENDIX B
ANOMALY HITS GROUPING,CODE IMPLEMENTATION

file: groupC.alg
disk: mag2 rot.

Algorithm to Group C

This algorithm correlates a list of hits into groups.

loop [read in data: name, frac, trail, amp, x1, y1, x2, y2
      calculate sensor x, y
      count # records

Sort list with respect to x position largest first.

Filter x data by applying x threshold to data set. All consecutive entries which are less than the threshold form a group.

Sort and filter data in each of the existing groups. Delete any entry or group which does not pass the y threshold.

Output remaining groups.

```
/*  Correlate magnetometer data from file  magdat" into targets */

#include <stdio.h>
#define XTHRESH 7.0
#define YTHRESH 41.0

typedef struct {
unsigned char start;
unsigned char size;
}   GROUPBLK;

GROUPBLK    group[201];        /* allows 20 groups */
double  x[65],0.0), y[65](0.0), amp[65](0.0);
unsigned char ix[63](0), iy[10](0), name[65][3](0);
unsigned char entry(0), numrecs(0), numgroups(0);
double ydif();

main()
{
double dum, frac, x1, y1, x2, y2, trail;
unsigned short i, index, k;
FIO pfio;

fopen(&pfio,"magdat",READ);
i = 0;
while(name[i][0] != 'E')          /* read until END */
    {
    ++i;
    getf(&pfio,"%b%d%d%d%d%d%d%d\n",
        &name[i][0], &dum, &frac, &trail, &amp[i], &x1, &y1, &x2, &y2);
        /* read into dum because a wierd b_g I couldn't find */

    /* Sensor position calculations */
    if(x2 > x1)
        x[i] = x1 + (x2 - x1) * frac - trail * 12.0;
    else
        x[i] = x1 - (x1 - x2) * frac + trail * 12.0;
    y[i] = (y1 + y2)/2.0;
    }

numrecs = i - 1;
sort(x, ix, numrecs);              /* does x sort into ix array */
prt_xsort();                    /* print input */
make_groups();                  /* Organize sorted data into groups */
prt_results();                  /* Print output grouping */
}


sort(list, ia, numentries)
double *list;                   /* pointer to variables to be sorted */
unsigned char *ia;              /* list sorted by shifting pointers */
unsigned short numentries;      /* number of entries to be sorted */
{

ia[1] = 1;                      /* set first entry to biggest */
for(entry = 2; entry <= numentries; entry++)
```

```
    {
    if(list[entry] > list[ia[i]])
        {
        push(list, ia, i);      /* move other entries down 1 place */
        ia[i] = entry;          /* new largest */
        }
    else
        find(list, ia);         /* find where new entry should go */
    }
}


find(list, ia)
double *list;                   /* pointer to current list */
unsigned char *ia;              /* array of sorted pointers */
{
unsigned short k;

k = 1;
while(list[entry] < list[ia[k++]]);     /* find insert location */
k -= 1;                         /* back up 1 */
push(list, ia, k);              /* push other elements down */
ia[k] = entry;                  /* pointer to new = current entry */
}


push(list, ia, i)               /* pushes list down 1 location */
double *list;                   /* pointer to working list */
unsigned char *ia;              /* pointer to current index array */
unsigned short i;               /* start index in sorted list */
{
unsigned short k;

for(k = entry; k > i; k--)
    ia[k] = ia[k - 1];          /* move down by 1 location */
}


make_groups()                   /* correlate data into groups */
{
numgroups = 0;
xfilter();
yfilter();
}


xfilter()                       /* filter x data */
{
unsigned short i, k;
double xmax;

i = 0;
k = 0;
while(++i <= n_mrecs)           /* do all records */
    {
    if(x[ix[i]] - x[ix[i + 1]] < XTHRESH)
```

```
        /* Search for beginning of new group in sorted list */

        ++numgroups;            /* increment # of groups */
        group[++k].size = 2;    /* new group started */
        group[k].start = i;     /* pointer to first group element */
        xmax = x[ix[i]];        /* remember first element */
        i += i;                 /* step past second element */

        /* find other elements in group */
        while((xmax - x[ix[++i]]) < XTHRESH)
            group[k].size++;
        --i;                    /* back up to first non-group member */
        }
    }
}


yfilter()                       /* correlate data on y variable */
{
double ydat[6];                 /* local pointer array for y sort */
unsigned short i, k, index;

for(i = 0; i < 6; i += 1)
    ydat[i] = 0;                /* clear small ydata array */

for(i = 1; i <= numgroups; i += 1)
    {
    index = group[i].start; /* index of first group element */
    for(k = 1; k <= group[i].size; k += 1)
        ydat[k] = y[ix[index++]];

    if(ydiff(ydat, group[i].size) > YTHRESH)
        /* if threshold exceeded remove offending element or group */
        delete(ydat, i);
    }
}


double ydiff(ydat, size)        /* sorts and returns span of y elements */
double *ydat;                   /* pointer to input list of data */
unsigned short size;            /* size of input list */
{
double yspan;
unsigned char i, k;

for(i = 1; i <= size; i++)
    iy[i] = 0;                  /* zero index array */

sort(ydat, iy, size);           /* sort y data into iy index array */

yspan = ydat[iy[1]] - ydat[iy[size]];   /* largest - smallest */
return(yspan);
}


delete(ydat, grpnum)            /* Find threshold violation and delete */
```

```
double *ydat;                   /* pointer to y input list */
unsigned short grpnum;          /* working group # */
{

if(group[grpnum].size == 2) /* if violation in size = 2; delete group */
    delete_group(grpnum);

else
    {
    findbad(ydat, grpnum);  /* find /lo string element and delete element */
    if(group[grpnum].size < 2)
        delete_group(grpnum);   /* can't have a group of 1 */
    }
}

delete_group(grpnum)            /* Deletes group from record */
unsigned short grpnum;          /* Group to be deleted */
{
unsigned short i;

/* Deletes group by pushing data structure up one element */
for(i = grpnum; i <= numgroups; i += 1)
    {
    group[i].size = group[i + 1].size;
    group[i].start = group[i + 1].start;
    }
--numgroups;                    /* decrement # of groups */
}


findbad(ydat, grpnum)           /* Find /lo string element */
double *ydat;                   /* pointer to y data set */
unsigned short grpnum;          /* working group # */
{
unsigned short index, i;

/* This currently works only for group sizes of 2 and 3 elements; it must
    be enhanced to properly handle larger groups                    */
i = 0;
index = group[grpnum].start;

if(ydat[iy[1]] - ydat[iy[2]] < (THRESH))
    i = iy[3];                  /* sorted element 3 out of range */

if(ydat[iy[2]] - ydat[iy[3]]) > (THRESH))
    i = iy[1];                  /* sorted element 1 out of range */

if(i == 1)
    {
    /* Skip over first element and reduce group size */
    --group[grpnum].size;
    group[grpnum].start = ix[index + 1];
    }

else if(i == 2)
    {
```

```
    /* This section remains unwritten. When the second record in a group
       causes the violation it must be removed from the sortec x list.*/
    }

else if(i == 3)
    {
    /* Shorten group size and thereby eliminate element 3 */\
    --group[grpnum].size;
    }

else
    delete_group(grpnum);    /* both 1 and 3 out of range */
}


prt_results()                /* output results of data correlation */
{
unsigned short i, k, index;

for(i = 1; i <= numgroups; i += 1)
    {
    index = group[i].start; /* index for start of group */
    for(k = 0; k < group[i].size; k -= 1)
        {
        putfmt("%b  %4.1f    %4.1f    %4.1f\n",
        &name[ix[index]][0], 3, x[ix[index]], y[ix[index]], amp[ix[index]]);
        ++index;
        }
    putfmt("\n");
    }
}

prt_xsort()
{
/*
unsigned short i;

for(i = 1; i <= numrecs; i++)
    putfmt("%b  %4.1f    %4.1f    %3.1f\n",&name[ix[i]][0],3,x[ix[i]],y[ix[i]],
    amp[ix[i]]);
*/
}
```